SUPPLEMENTO
AL VOLUME III, SERIE X, DEL
NUOVO CIMENTO
A CURA DELLA SOCIETÀ ITALIANA DI FISICA

1956 1° Semestre N. 1

ARTICOLI
SCRITTI DA FISICI RUSSI

ARTICLES
DE PHYSICIENS RUSSES

PAPERS
BY RUSSIAN PHYSICISTS

PRESENTAZIONE

DI

G. POLVANI

Presidente della Società Italiana di Fisica
e Direttore del Nuovo Cimento

Quando quattro anni fa, per autorevole proposta del prof. MOTT, Presidente dell'Unione Internazionale di Fisica pura ed applicata, e per l'efficace suo stimolo, ci proponemmo di presentare ai lettori del *Nuovo Cimento* rassegne che illustrassero i lavori di Fisica pubblicati in Europa orientale e particolarmente in Russia, pensammo che non solo ai fisici dell'Occidente avremmo dovuto chiedere di compilare tali rassegne, ma anche agli stessi fisici russi.

Ne interessai pertanto l'Accademia delle Scienze dell'URSS per via diretta e per via diplomatica; e, sia pure con un certo ritardo, date le difficoltà che allora incontravano le relazioni epistolari con l'URSS, ne ebbi risposta affermativa, confermata poi, l'estate passata, dall'arrivo al giornale di un certo numero di articoli, dei quali alcuni hanno carattere di pura rassegna, ed altri anche quello di lavoro originale. Ne pubblichiamo qui circa un terzo.

La favorevole accoglienza fatta alla nostra proposta dall'Accademia delle Scienze dell'URSS, ci rende ben lieti di porgere ad essa, al suo illustre Presi-

dente, il prof. A. N. Nesmejanov, e a tutti gli autori il nostro più vivo ringraziamento, al quale aggiungiamo, sicuri di non sbagliare, quello dei molti lettori del *Nuovo Cimento*.

Gli articoli di rassegna, qui presentati, hanno un carattere diverso dalle precedenti rassegne sui lavori di fisica sovietici già pubblicate nel *Supplemento*. La differenza proviene dal fatto che quasi tutti i compilatori russi parlano, soprattutto e specialmente, dei propri lavori, e quindi la loro parola spesso acquista, inevitabilmente, un calore che la scarna presentazione scientifica non sempre riesce a celare. Inoltre il compilatore, in quanto autore, prende sovente occasione dalla stessa rassegna per aggiungere un qualcosa di nuovo: una notizia, un'osservazione, un dato, una tabella, una precisazione, un altro modo di presentare o risolvere una questione....

Avremmo molto desiderato pubblicare prima questi articoli: ma varie circostanze — il trasferimento e l'ampliamento della tipografia del giornale, un certo affollamento di lavori, la revisione della traslitterazione dal russo secondo le norme della International Standard Organization (I.S.O.), e, infine e soprattutto, il dover provvedere coi soli mezzi della Redazione alla completa correzione delle bozze (e gli autori e i lettori vorranno scusarci se qualche svista è sfuggita) — ci hanno impedito purtroppo di corrispondere al nostro stesso desiderio: ce ne rammarichiamo e speriamo di potere provvedere con sollecitudine alla pubblicazione dei restanti articoli.

In merito alla questione della traslitterazione dei caratteri cirillici, vorrei prendere occasione per richiamare l'attenzione di tutti gli scienziati sulla confusione che attualmente regna in proposito. Dati il carattere e il valore internazionale delle norme fissate dalla I.S.O., *Il Nuovo Cimento* si attiene ad esse; ma molti ed autorevoli giornali seguono norme proprie diverse da quelle. La confusione è tale che in alcuni casi si stenta a riconoscere, sotto traslitterazioni diverse, un medesimo autore russo. Per evitare questo inconveniente siamo stati tentati, quasi quasi, di presentare in questo fascicolo i nomi russi in caratteri cirillici, aggiungendo tra parentesi la traslitterazione: forse questa potrebbe essere la soluzione generale migliore.

Comunque qui vorrei rinnovare l'augurio, che già ebbi occasione di formulare in seno alla Commissione delle Pubblicazioni dell'UIPPA, quando la Commissione stessa fu ospite, l'anno passato, della nostra Società a Varenna, che presto cioè si addivenga, in questa questione, ad una intesa comune.

Chiudendo queste brevi parole di presentazione, desidero esprimere alla signorina dott. Luisa Basilico un particolare elogio e un particolare ringraziamento per tutto il lavoro da lei svolto per la preparazione di questo fascicolo; e desidero anche ringraziare il prof. F. Fumi e i dott. G. F. Dell'Antonio, F. Duimio, R. Fieschi, R. Girelli, P. Gulmanelli, G. M. Prosperi, A. Scotti, M. Tosi, per l'aiuto dato nella sistemazione di alcune parti degli articoli.

INDICE DEGLI SCRITTI

A. Baldin – On a Rule for the Interaction of the Electromagnetic Field with Nucleonic and Mesonic Fields . . . . . pag. 4

S. Z. Belen'kij and L. D. Landau – Hydrodynamic Theory of Multiple Production of Particles . . . . . » 15

A. Belousov, A. Kutcenko and E. Tamm – Photoproduction of π^0-Mesons on Deuterium . . . . . » 32

V. Ginzburg – The Nature of Cosmic Radio Emission and the Origin of Cosmic Rays . . . . . » 38

B. S. Dželepov and Ju. V. Hol'nov – An Electron Recoil Study of the Gamma Spectra of ^{124}Sb, ^{59}Fe, ^{110}Ag, ^{64}Cu, ^{192}Ir, ^{140}La and ^{198}Au . . » 49

B. S. Dželepov and S. A. Šestopalova – The RaC γ-Ray Spectrum . . . » 54

V. P. Dželepov, U. M. Kazarinov, B. M. Golovin, V. B. Fljagin and V. I. Satarov – Experimental Investigation of Neutron-Nucleon and Neutron-Deuteron Interaction in the Energy Region 380 ÷ 590 MeV » 61

L. Landau, U. Abrikosov and I. Halatnikov – On the Quantum Theory of Fields . . . . . » 80

E. Lejkin, R. Osokina and B. Ratner – Investigation of Photoprotons from Copper and Nickel . . . . . » 105

M. G. Meščerjakov, N. P. Bogačev and B. S. Neganov – Investigations of the Proton-Proton Interaction at High Energies . . . . . » 119

N.B. – Nella traslitterazione delle parole russe, sono state seguite le norme fissate dalla I.S.O. con la « Recommendation n. 9 » del Settembre 1954, qui riportate a pag. 133, per comodità del lettore.

SUPPLEMENTO AL VOLUME III, SERIE X
DEL NUOVO CIMENTO

N. 1, 1956
1° Semestre

On a Rule for the Interaction of the Electromagnetic Field with Nucleonic and Mesonic Fields (*).

A. BALDIN

Institute of Physics of the Academy of Sciences of the USSR - Moscow

CONTENTS. — **1.** Introduction. – **2.** Formulation of a rule for the relation between matrix elements describing the processes of interaction of the electromagnetic field with nucleonic and mesonic fields. – **3.** Test of the validity of the rule in the study of some well known experimental effects. – **4.** Study of the reactions of photoproduction of π^0-mesons by d, ^{4}He, ^{12}C, in which the application of the rule gives a direct proof of the hypothesis of isotopic invariance for the π^0-meson field. – **5.** Application to the photoproduction of meson pairs. – **6.** Application to the photodisintegration of nuclei.

1. – Introduction.

In the first papers on the photoproduction of mesons [1] it has been already noted that meson current plays a most important role in the interaction of electromagnetic field with nucleonic and mesonic fields. This result was obtained on the basis of the perturbation theory and its meaning is very simple, viz: the mesons being less heavy, have a greater mobility and interact more vigorously with the electromagnetic field than the heavy nucleons. This result however has a more general character and may be formulated rigorously without use of any calculation schemes in the wave fields theory. Furthermore, it may be shown, without postulating the validity of isotopic invariance and the concrete aspect of the meson theory, that the operators of the mesonic and

(*) The results discussed in this paper were for the most part obtained in collaboration with V. V. MIHAJLOV and published over the period 1951-53. (See references in text).

nucleonic currents have different transformation properties in the isotopic space. This enables us to formulate a rule [2, 3] for the relation between matrix elements, describing various interaction processes between electromagnetic field and nucleonic and mesonic fields.

This rule is based on a wealth of experimental facts and may be further confirmed by a number of arguments based on meson theories.

Owing to the general character of this rule it has consequences for different processes, among which the most important is the direct test of the validity of the hypothesis of isotopic invariance for the π^0-meson field.

2. Formulation of a Rule for the Relation between Matrix Elements Describing the Process of Interaction of the Electromagnetic Field with Nucleonic and Mesonic Fields.

Let

$$i\frac{\partial \Omega}{\partial t} = H_0 \Omega \tag{1}$$

describe the interacting nucleonic and mesonic fields, and Ω the rigorous solution of the equation (1).

In reference to H_0 we assume only:

$$[H_0, P_{180}] = 0\,, \tag{2}$$

where P_{180} is the rotation operator for 180° in the isotopic space, in other words we assume charge independence.

Now let us take into account the interaction with the electromagnetic field. In order to do this let us substitute in H_0:

$$\begin{cases} \dfrac{\partial}{\partial X_j} \to \dfrac{\partial}{\partial X_j} + i\,e\dfrac{1+\tau_3}{2}\mathcal{A}_j, \\ \dfrac{\partial}{\partial x_j} \to \dfrac{\partial}{\partial x_j} + i\,eL_3\mathcal{A}_j\,, \end{cases} \tag{3}$$

X_j, x_j are the nucleonic and mesonic coordinate respectively,

$(1+\tau_3)/2$ the charge operator of the nucleonic field,

L_3 the charge operator of the mesonic field having eigenvalues ± 1 and 0 respectively for $\pi^{\pm}$ and π^0 mesons.

Let us expand the hamiltonian into series of e and limit ourselves to the

first term

$$i\frac{\partial\Omega}{\partial t} = (H_0 + H_e)\Omega\,. \tag{4}$$

We assume the interaction with the electromagnetic field to be weak and consider H_e as a weak perturbation, inducing the transformations in the mesonic and nucleonic field systems. The matrix elements representing interaction processes of the electromagnetic field with mesons and nucleons have the form

$$(\Omega_f^*,\, H_e\Omega_i)\,. \tag{5}$$

As seen from (2) and (3), H_e is composed of two parts

$$H_e = S + V\,; \qquad [S,\, P_{180}] = 0\,; \qquad [P_{180},\, V] = 2P_{180}V\,. \tag{6}$$

The possibility on such splitting of the transformation matrix was pointed out by WATSON [4], assuming the validity of isotopic invariance and pseudoscalar meson theory. As appears from the above formulae, (6) has a more general character and may be extended to the case of charge symmetry. This is important for the conclusions which will be developed below.

Now let us consider the consequence of the rule to be discussed, and which may be formulated as follows:

$$(\Omega_f^*\,,\, S\Omega_i) \sim \frac{\mu}{M}\,(\Omega_f^*\,,\, V\Omega_i)\,, \tag{7}$$

where $\mu/M = 0.15$ is the ratio of meson to nucleon mass.

It follows from (3) that S, according to definition, is a part of the operator of nucleonic current and affects only nucleonic variables in Ω if Ω is considered as a wave function with an indefinite number of particles (Fock functional). Hence, on all theories with fixed nucleon S is simply equal to zero.

The rule (7) follows also from the calculations of meson photoproduction effect in the various approximations of the weak coupling theory (perturbation theory, theory of radiation damping).

The rule (7) is, furthermore, based on a great amount of experimental facts. In order to make possible the comparison between theory and experiment and to derive certain consequences from (7) the following theorem I will be used: the magnitude of the matrix elements is not affected by any unitary transformation U in the configuration space.

This statement follows from the obvious fact that the matrix element,

according to its definition, is a scalar product:

$$(\psi_f^*, Q\psi_i) \equiv (\psi_f^* U^{-1} U Q U^{-1} U \psi_i) = (\psi_{f_1}^*, Q_1 \psi_{i_1}) ,$$

where the subscript 1 denotes transformed operators and functions.

For the derivation of different relations we will use this theorem in relation to transformation of the P_{180} rotation about 180° in the isotopic space.

3. – Test of the Validity of the Rule in the Study of Some Well Known Experimental Effects.

Let us test the validity of the rule (7) in a number of well studied experimental effects.

Consider the proton and neutron magnetic moments.

The magnetic moment may be determined as the mean value of the magnitude $\boldsymbol{\mu}$, which is involved in the hamiltonian in the form $(\boldsymbol{\mu}\cdot\mathcal{H})$ in presence of the static magnetic field $\mathcal{H}$:

$$H_e = S + V = \int (\boldsymbol{j}\cdot\boldsymbol{A})\,\mathrm{d}v , \qquad \boldsymbol{A} = \tfrac{1}{2}[\boldsymbol{r}, \mathcal{H}]$$

hence

$$(\boldsymbol{\mu}\cdot\mathcal{H}) = S + V \quad \text{where} \quad \mathcal{H}\,\text{const}, \quad \boldsymbol{\mu} = \tfrac{1}{2}\int [\boldsymbol{j}, \boldsymbol{r}]\,\mathrm{d}v .$$

The mean value of $\boldsymbol{\mu}_p$, the magnetic moment of the proton, takes the form:

$$\mu_p = 2.78\gamma_0 = \langle \Omega_p^* | S + V | \Omega_p \rangle , \tag{8}$$

where γ_0 is the nuclear magneton, Ω_p the wave function of the proton.

The value of the magnetic moment of the neutron may be written, using the theorem I:

$$\mu_n = -1.91 = \langle \Omega_n | S + V | \Omega_n \rangle = \langle \Omega_p | S - V | \Omega \rangle . \tag{9}$$

Solving eq. (8) and (9) we obtain

$$\langle S \rangle = 0.18 \langle V \rangle .$$

By means of an analogous treatment of magnetic moments of ^{3}H and ^{3}He we obtain

$$\langle S \rangle = 0.17 \langle V \rangle .$$

Now let us apply the theorem I to the photoproduction of π^0-mesons from protons and neutrons. The cross-section ratios for these processes may be written in the form

$$\frac{\sigma_n}{\sigma_p} = \frac{(\Omega_{\pi^0}, \Omega_n | S + V | \Omega_n)^2}{(\Omega_{\pi^0}, \Omega_p | S + V | \Omega_p)^2} = \frac{(\langle S \rangle - \langle V \rangle)^2}{(\langle S \rangle + \langle V \rangle)^2} . \tag{10}$$

Experimental values of this ratio may be derived from data on the production of π^0-mesons from deuterium [5]. It appears to be ~ 0.8 for various angles and for γ-ray energies up to 500 MeV [6].

From (10) we obtain:

$$\mathrm{Re}\, \langle S \rangle^* \langle V \rangle = 0.06 |\langle V \rangle|^2 .$$

The analogous analysis of experimental data on the photoproduction of π^+ and π^- mesons from deuterium, carbon, and helium [7] gives nearly similar results.

4. – Study of the Reactions of Photoproduction of π^0-Mesons by d, ^{4}He, ^{12}C in which the Application of the Rule gives a Direct Proof of the Hypothesis of Isotopic Invariance for the π^0-Meson Field.

As is well known, the hypothesis of isotopic invariance is widely accepted, since it is supported by quite a number of indications derived from experiments on the interaction between mesons and nucleons and nuclei. However all the evidence in support of this hypothesis (even the most conclusive) [8] are based merely on a test of its consequences. A proper test of the validity of the principle of isotopic invariance must be based on the study of effects, which would rule out other symmetry types, not contradicting already studied experimental facts.

Let us show that the analysis of the reactions:

$$\gamma + \mathrm{d} \rightarrow \mathrm{d} + \pi^0 \tag{11a}$$

$$\gamma + {}^4\mathrm{He} \rightarrow {}^4\mathrm{He} + \pi^0 \tag{11b}$$

$$\gamma + {}^{12}\mathrm{C} \rightarrow {}^{12}\mathrm{C} + \pi^0 \tag{11c}$$

provides such a test of the validity of the isotopic invariance hypothesis for the π^0-mesonic field.

The following variants of the π^0-mesonic field are not in contradiction both with the condition of charge symmetry and the already known experimental

facts:

1) The transformation P_{1s0} does not affect the sign of the π^0-mesonic field φ_0 (it is a scalar in the isotopic space) . This case corresponds to the hamiltonian of interaction of the π^0-mesonic and nucleonic fields of the form (not considering nonrelevant factors):

$$g\varphi_0 \,.$$

The coupling constants of the π^0-mesonic field with the protons and neutrons are equal and have the same sign $g_n = g_p$.

2) The π_0-mesonic field φ_3 changes its sign in the transformation P_{1s0} (is the third component of the vector). This case corresponds to the hamiltonian of interaction of the π^0-mesonic and nucleonic fields of the form

$$g\tau_3\varphi_3 \,.$$

The coupling constants are equal and have opposite signs $g_n = -g_p$.

The second variant conforms with isotopic invariance whereas the first does not. It will be shown that the experimental data on the reactions (11) are not compatible with the first variant.

Let us write down the matrix element describing the first reaction (11a) and apply the theorem I:

$$(12) \qquad (\pi^0 d \,|\, S+V \,|\, d) = \begin{cases} +(\pi^0 d \,|\, S-V \,|\, d) = \langle S \rangle & \text{for the first variant,} \\ -(\pi^0 d \,|\, S-V \,|\, d) = \langle V \rangle & \text{for the second variant.} \end{cases}$$

Here π^0, d are the wave functions of the π^0-meson and the deuton respectively.

Hence, taking into account the rule (7), it becomes apparent that the cross-sections of the reactions (11) essentially depends on the symmetry variant of the π^0-mesonic field in the isotopic space. Consider, for instance, the cross-section of the photoproduction from a free proton

$$(13) \qquad \gamma + \mathrm{p} \to \mathrm{p} + \pi^0 \,.$$

If the first variant were realised in nature the cross-section for the reaction (13) would be $(M/\mu)^2 \sim 40$ times that for the reaction (11a). This follows from the fact that the cross-section for the reaction (13) is described by the matrix element $\langle S \rangle$ as well as by $\langle V \rangle$, whereas the cross-section of reaction (11a) is described only by $\langle S \rangle$.

The experiments carried out with reactions (11) [9, 10] show the cross-

sections of the reactions (11) to be of the same order of magnitude as that of reaction (13). Consequently the first symmetry variant (φ a scalar and $g_p = g_n$) is in contradiction with experimental facts. The suggestion that an answer to the problem of the sign of the coupling constants g_p and g_n may be found in the study of the reaction (11*a*) was simultaneously obtained in the works [11]. In these papers, however, the perturbation theory was applied to the meson-nucleon interaction, anomalous magnetic moments (*) were phenomenologically introduced and other assumptions were made. Such a treatment naturally could not serve as a base for the demonstration of so important a relation as $g_p = -g_n$ or the more general relation $P_{180}\varphi_3 = -\varphi_3$.

The approach suggested in this paper is based only on the rule (7) which has a quite simple physical meaning and is based on a great amount of experimental facts.

The cross-section relations of processes (11) and (13) assume a more explicit form if the rule (7) is interpreted as describing the electromagnetic properties of individual nucleons. Such a treatment follows from the theory of impulse approximation and from quite conclusive evidence according to which photoproduction of mesons from nuclei is due to the contribution of individual nucleons [12]. This means that the scattering matrix may be written as a sum of the scattering matrices of individual nucleons,

$$M = \sum_i M_i = \sum_i (S_i + V_i)\,, \tag{14}$$

where $\sum_i$ is the sum over all the nucleons within the nucleus. Consequently relation (7) takes the form

$$\langle S_i \rangle \sim \frac{\mu}{M} \langle V_i \rangle\,. \tag{7'}$$

The cross-section of (11) is proportional to $|\langle \sum S_i \rangle|^2$ (in the case when π^0 is scalar in isotopic space) whereas the cross-section of reaction (13) is $|\langle S_i + V_i \rangle|^2$.

The effect of the nucleon binding which has been evaluated by a variety of methods for different processes of meson-nucleon interaction introduces corrections to cross-section of the order of the cross-section itself or less, whereas by using (7') we obtain (in the first variant) the ratio of cross-sections of the processes (13) and (11) of the order 10 or more. In order to illustrate this let us consider the cross-section processes for the reactions (11) and (13)

(*) The photoproduction cross-sections has been calculated incorporating a Pauli type term (representing the interaction of the photon with anomalous magnetic moments) by A. M. Baldin and V. V. Mihajlov: *Žu. Eksper. Teor. Fiz.*, **21**, 562 (1951) somewhat earlier than by M. F. Kaplon: *Phys. Rev.*, **83**, 712 (1951).

on the theory of impulse approximation. The scattering matrix has the form [13, 14]

$$M = \sum_j [(\boldsymbol{\sigma}^j \cdot \boldsymbol{K}^j) + L_j] \exp [i(\boldsymbol{\varkappa} - \boldsymbol{k}) \cdot \boldsymbol{z}_j],$$

where $\boldsymbol{\varkappa}$ and $\boldsymbol{k}$ are the moments of the photon and the meson respectively. According to (6) and (7),

$$(6'') \qquad \begin{cases} \boldsymbol{K} = \boldsymbol{K}_s + \boldsymbol{K}_v\,, & [P_{180}, \boldsymbol{K}_s] = [P_{180}, L_s] = 0\,, \\ L = L_s + L_v, & [P_{180}, \boldsymbol{K}_v] = 2P_{180}\boldsymbol{K}_v, \qquad [P_{180}, L_v] = 2P_{180}L_v\,, \end{cases}$$

$$(7'') \qquad \langle \boldsymbol{K}_s \rangle \sim \frac{\mu}{M} \langle \boldsymbol{K}_v \rangle\,, \qquad L_s \sim \frac{\mu}{M} \langle L_v \rangle\,.$$

The cross-section for the process (13) has the form

$$(16) \quad \mathrm{d}\sigma_{pp} = \{|\langle \boldsymbol{K}_s \rangle + \langle \boldsymbol{K}_v \rangle^{\,2} + |\langle L_s \rangle + \langle L_v \rangle|^2\} \frac{\mathrm{d}\boldsymbol{k}}{(2\pi)^2} \int \mathrm{d}\boldsymbol{p}\, \delta(\boldsymbol{p} - \boldsymbol{\varkappa} + \boldsymbol{k})\, \delta(E_f - E_0)\,,$$

where $\boldsymbol{p}$ is the moment of the recoil nucleon.

The cross-section for the process (11a) may be easily obtained for example, from (14) using eq. (6″) and the theorem I.

For the first symmetry variant we obtain

$$(17) \qquad \mathrm{d}\sigma_{dd} = \left\{\frac{2}{3} |2\langle \boldsymbol{K}_s \rangle|^2 + |2\langle L_s \rangle|^2\right\} I^2 \frac{\mathrm{d}\boldsymbol{k}}{(2\pi)^2} \int \mathrm{d}\boldsymbol{p}\, \delta(\boldsymbol{p} - \boldsymbol{\varkappa} + \boldsymbol{k})\, \delta(E_f - E_i)\,,$$

and for the second

$$(18) \qquad \mathrm{d}\sigma_{\bar{d}\bar{d}} = \left\{\frac{2}{3} |2\langle \boldsymbol{K}_v \rangle|^2 + |2\langle L_v \rangle|^2\right\} I^2 \frac{\mathrm{d}\boldsymbol{k}}{(2\pi)^2} \int \mathrm{d}\boldsymbol{p}\, \delta(\boldsymbol{p} - \boldsymbol{\varkappa} + \boldsymbol{k})\, \delta(E_f - E_i)\,,$$

where

$$I = \int \psi_d^2 \exp\left[i(\boldsymbol{\varkappa} - \boldsymbol{k}) \cdot \frac{\boldsymbol{r}}{2}\right] \mathrm{d}\boldsymbol{r}\,,$$

ψ_d is the wave function of the deuteron,
$\boldsymbol{p}$ the moment of the recoil deuton.

For small angles of the outgoing meson, where $I^2 \approx 1$ and is independent from the form of the deuteron wave function, the comparison between cross-sections reduces to a comparison between the squares of matrix elements $\langle S_i \rangle$ and $\langle V_i \rangle$.

As seen from the formulas, however, the difference in the magnitude values

of the matrix elements is so great that the factor I^2 cannot sensibly affect the relation under consideration even at different angles. Moreover, it can only decrease the cross section while experimental data show the cross-sections of the reactions (13) and (11) to be of the same order of magnitude.

In case of photoproduction of π^0-mesons from nuclei at sufficiently high $\varkappa$ and sufficiently small angles θ when $|\varkappa - k| a \ll 1$ (a dimension of the nucleus) the treatment is very simple and leads to results analogous to (17) and (18): the cross-sections, as in (17) and (18), are proportional to the square of matrix elements involved in (16), it being proportional to the square of the number of nucleons within the nucleus as in (17) and (18) (*).

This conclusion is in good agreement with the results of experimental work on reactions (11) [15]. It follows from these results as well as from experiments on the (11a) reactions that the first symmetry variant must be discarded.

5. – Application to the Photoproduction of Meson Pairs.

The region of applicability of the rule (7) is at present uncertain, but all available experimental facts relating to the proton energy range of $0 \neq 500$ MeV seem to support (7).

It may therefore be expected to be valid likewise in case of meson pair production. Since the wave function of the π^0-meson pair does not change its sign under P_{180} transformation, it follows from (7) and theorem I, in analogy with the above, that the elastic cross-section for the photoproduction of meson pairs from D, ^{4}He, ^{12}C nuclei must be very small. If (7) is valid over a large energy range the above conclusion must apply to any even number of mesons. The elastic photoproduction of (π^+, π^-) meson pairs on the same nuclei will occur essentially on in isotopic odd states (the wave function of the meson pair under P_{180} transformation changes its sign). Since the π-mesons are bosons their coordination function must likewise change sign when the substitution of $\begin{Bmatrix}\pi^-\\ \pi^+\end{Bmatrix}$ for $\begin{Bmatrix}\pi^+\\ \pi^-\end{Bmatrix}$ is made. It follows therefore that mesons elastically created on D, ^{4}He, ^{12}C nuclei will have states with odd relative orbital momentum. Notably the S state will be strongly suppressed. As pointed out by BRUECKNER and WATSON [16], the interaction between mesons in the S-state must strongly affect the correlation of their respective motions. It follows that the absence of such a correlation in case of elastic photoproduction of (π^+, π^-) pairs on D, ^{4}He, ^{12}C nuclei and their presence in case of inelastic photoproduction might

(*) The existence of quadratic dependence of the scattering cross-sections from the number of nucleons at small angles has been already pointed out by E. L. FEINBERG: *J. of Phys. USSR*, **5**, 177 (1941).

be considered as direct evidence for the interaction between mesons in states with odd orbital moments.

6. – Application to the Photodisintegration of Nuclei.

It must likewise be noted that since the effects forbidden according to rule (7) are due to S current only, the interaction between the electromagnetic and mesonic fields completely disappears. This becomes immediately evident if we express Ω in form of wave functions with an indefinite number of particles (in a Fock representation).

S affects only the nucleonic variables in these functions and the process proceedes as if the proton and neutron had the same charge and interacted only with the neutral mesonic field, as exemplified by such effects as the magnetic moments of nuclei with $Z=N$, and photodisintegration of nuclei of the type

$$\gamma + {}^4\mathrm{He} \to 2\mathrm{d}\,, \quad \text{etc.} \tag{19}$$

The latter consideration is of special interest since the reaction of nuclear photodisintegration is known to exhibit a considerable rise near the threshold of photoproduction of mesons. It is only natural to link this effect with meson currents. The reactions (19) proceed at the expense of the interaction between electromagnetic field and nucleon currents. In this connection we may expect a considerable difference in the magnitude of cross-sections and the characteristics of the reactions:

$$\gamma + {}^4\mathrm{He} \to \begin{cases} \mathrm{d} + \mathrm{d} \\ \mathrm{d} + \mathrm{d} + \pi^0 \\ \mathrm{d} + \mathrm{p} + \mathrm{n} \end{cases}$$

In the last two reactions, in contrast to the first, the contribution of meson currents is not forbidden.

* * *

In conclusion I wish to express my gratitude to Prof. M. Markov for many stimulating discussions.

REFERENCES

[1] A. M. Baldin and V. V. Mihajlov: *Usp. Fiz. Nauk*, **44**, 20 (1951).
[2] A. M. Baldin and V. V. Mihajlov: *Dokl. Akad. Nauk SSSR*, **91**, 479 (1953).
[3] A. M. Baldin: *Dokl. Akad. Nauk SSSR*, **94**, 947 (1954).
[4] K. M. Watson: *Phys. Rev.*, **85**, 852 (1952).
[5] G. Cocconi and A. Silverman: *Phys. Rev.*, **88**, 1230 (1952).
[6] H. H. Bingham, J. C. Keck and A. V. Tollestrupp: *Bull. Am. Phys. Soc.*, **30**, No. 1, 48 (1955).
[7] M. Sands, J. Teasdale and R. L. Walker: *Phys. Rev.*, **95**, 592 (1954); R. S. White, M. J. Jacobson and A. G. Schulz: *Phys. Rev.*, **88**, 836 (1952); R. M. Littauer and D. Walker: *Phys. Rev.*, **86**, 838 (1952).
[8] R. H. Hildebrand: *Phys. Rev.*, **89**, 1090 (1953); R. A. Schluter: *Bull. Am. Phys. Soc.*, **29**, N. 4, 51 (1954).
[9] A. Belousov, A. Kucenko and E. Tamm: in this issue, pag. 32.
[10] J. W. DeWire, A. Silverman and B. Wolfe: *Phys. Rev.*, **92**, 520 (1953).
[11] N. C. Francis and R. E. Marshak: *Phys. Rev.*, **85**, 496 (1952); W. Heckrotte, L. R. Henrich and J. V. Lepore: *Phys. Rev.*, **85**, 490 (1952); V. V. Mihajlov and A. M. Baldin: *Dokl. Akad. Nauk SSSR*, **84**, 47 (1952).
[12] I. Gorevskaja and N. Panova: in press.
[13] M. Lax and H. Feshbach: *Phys. Rev.*, **81**, 189 (1951).
[14] G. F. Chew and H. W. Lewis: *Phys. Rev.*, **84**, 779 (1951).
[15] G. DeSaussure and L. S. Osborne: *Bull. Am. Phys. Soc.*, **29**, No. 1, 19 (1954).
[16] K. A. Brueckner and K. M. Watson: *Phys. Rev.*, **87**, 621 (1952).

SUPPLEMENTO AL VOLUME III, SERIE X
DEL NUOVO CIMENTO

N. 1, 1956
1° Semestre

Hydrodynamic Theory of Multiple Production of Particles.

S. Z. Belen'kji and L. D. Landau

Institute of Physical Problems of the Academy of Sciences of the USSR - Moscow
Institute of Physics of the Academy of Sciences of the USSR - Moscow

Contents. — **1.** Introduction. – **2.** Termodynamic relationships in the break-up. – **3.** Total number of particles. – **4.** Energy and angular distribution of particles. – **5.** Collisions of particles of different masses.

1. – Introduction.

It is known experimentally that in the collision of very fast particles, a large number of new particles is created (nuclear events). Fermi [1,2] advanced the idea of using thermodynamic methods in investigating the process of very high-energy collision. The basic postulates of his theory are the following.

1) When two very fast nucleons collide the energy, in the center of mass system, is released in a very small volume V. As the nuclear interaction is very great and the volume small, the energy distribution will be determined by statistical laws. This permits to examine the collision of high-energy particles without using any particular theory of nuclear interaction.

2) The volume V in which the energy is released is determined by the dimensions of the nucleon meson cloud, whose radius is of the order $\hbar/\mu c$, where μ is the pion (π-meson) mass. But since the nucleons move at high velocity, the meson cloud surrounding them undergoes Lorentz contraction in the direction of the nucleon's motion. Thus, the volume will be of the order of magnitude

$$V = \frac{4\pi}{3}\left(\frac{\hbar}{\mu c}\right)^3 \frac{2Mc^2}{E'}, \tag{1}$$

where M is the nucleons mass, and E' is the total energy of the two colliding nucleons in the center of mass system.

3) The particles are created in the volume V at the initial moment of collision, according to the laws of statistical equilibrium and, assuming that they no longer interact with each other, they escape from the volume in a « frozen » state.

4) FERMI examined both close collisions, which according to his calculations lead to isotropic angular distribution, and distant collisions. In the latter case, his statistical calculations took into account both energy conservation and angular momentum conservation. Distant collisions produce non-isotropic angular distribution in the center of mass system.

FERMI's basic idea regarding the application of statistical methods in investigating collision processes is, undoubtedly, very fruitful. Some of his assumptions and quantitative computations, however, are not convincing [3,4]. Thus, his assertion that the number of particles in a nuclear star is determined by the number of particles created in the volume V at the moment of collision is unfounded. Owing to high density of the particles and to strong interaction between them, one cannot really speak of their number at that moment. Actually, the system expands and the number of particles becomes definite only when the interaction between them becomes small. Then the particles escape freely. This has been pointed out by I. POMERANČUK [3]. FERMI [2] further incorrectly computed the distant collisions and, consequently, also the angular and energy distribution of particles based on that computation. It must be noted that this consideration is hardly compatible with the theory of relativity. According to FERMI, in an essentially distant collision, during the time of a collision, of the order $(\hbar/\mu c)(Mc^2/E')(1/c)$, the interaction extends over the entire volume of the meson cloud, i.e., over a distance of the order $\hbar/\mu c$. This means that the perturbation has to spread at a velocity substantially exceeding that of light. The defects of Fermi's theory are basically due to his incorrect point of view on the expansion of the compound system. As LANDAU [5] has shown, the expansion of the system can be examined on the basis of relativistic hydrodynamics, the use of which in this case is just as warranted as the use of thermodynamics, since the range of their application coincides.

From the qualitative aspect the collision process is as follows [5]:

1) In the collision of two nucleons a compound system arises and energy is released in a small volume V, Lorentz-contracted in the transverse direction. At the moment of collision, a large number of « particles » is created, the « collision mean free path » in the created system is small compared with its dimensions, and a statistical equilibrium is established in the system.

2) The second stage of the collision consists in the expansion of the system. This stage should be examined hydrodynamically considering the ex-

pansion as motion of an ideal (non-viscous and non-heat-conducting) fluid. In the process of expansion the mean free path remains small compared with the dimensions of the system, which precisely justifies the application of hydrodynamics. As the velocities in the system are comparable with the velocity of light, relativistic rather than usual hydrodynamics should be used. During the first and second collision stages, owing to high energy density and strong interaction between the parts of the system, particles are continually created and absorbed in it. Hence the system can hardly be characterized by the number of particles.

3) With the expansion of the system, interaction decreases and the mean free path increases. The number of particles, as a physical characteristics, appears when the interaction is sufficiently small. When the mean free path becomes comparable with the linear dimensions of the system, the latter disintegrates into separate particles. We call this stage the break-up. It takes place at a temperature $T \approx \mu c^2$, where μ is the pion mass. (The temperature is here in all cases given in energy units).

2. – Thermodynamic Relationships in the Break-up.

In examining the break-up of the system, we may neglect the interaction between particles, and therefore we will obtain a number of simple relationships (see [6]). Let us consider a certain section of the system at the break-up temperature T_k. Pion equilibrium density is described by the following expression:

$$n_\pi = \frac{\bar{g}_\pi}{2\pi^2}\left(\frac{T_k}{\hbar c}\right)^3 F(z_\pi) \qquad \text{where } z_\pi = \frac{\mu c^2}{T_k}. \tag{2}$$

Here g_π is the number of the possible states of the particle, in our case (corresponding to the presence of π^+, π^-, π^0-mesons) $g_\pi = 3$. The function $F(z)$ may be represented in the following form:

$$F(z_\pi) = z_\pi^2 \sum_{m=0}^{\infty} \frac{K_2[z_\pi(1+m)]}{(1+m)}, \tag{3}$$

where $K_2(z)$ is a modified Bessel function of the second order (see [6, 7]). The series (3) rapidly converges. The pion energy density ε_π is described by the following expression:

$$\varepsilon_\pi = T_k\left(\frac{\bar{g}_\pi}{2\pi^2}\right)\left(\frac{T_k}{\hbar c}\right)^3 \Phi(z_\pi) \tag{4}$$

where

$$\Phi(z_\pi) = z_\pi^2 \sum_{m=0}^{\infty} \frac{3K_2[z_\pi(1+m)] + z_\pi(1+m)K_1[z_\pi(1+m)]}{(1+m)^2}. \tag{5}$$

Here $K_1(z)$ is a modified Bessel function of the first order. We now have the following expression for the entropy density of pions (in absolute units):

$$s_\pi = \left(\frac{T_k}{\hbar c}\right)^3 \left(\frac{\bar{g}_\pi}{2\pi^2}\right) g(z_\pi), \tag{6}$$

where

$$g(z_\pi) = z_\pi^2 \sum_{m=0}^{\infty} \frac{4K_2[z_\pi(1+m)] + z_\pi(1+m)K_1[z_\pi(1+m)]}{(1+m)^2}. \tag{7}$$

Also the presence of nucleons in the system should be considered. Since in high-energy collisions there are several nucleons (not less than two) already before collision, nuclear charge conservation should likewise be noted (see [7]). The chemical potential μ_0, which is determined by the condition of nuclear charge conservation, should be introduced in the distribution function of the number of nucleons. As a result, we obtain the following expression for the density of nucleons $n_{\text{НН}}$ and of anti-nucleons $n_{\text{АН}}$:

$$n_{\text{НН}} = \frac{\bar{g}_\text{Н}}{2\pi^2}\left(\frac{T_k}{\hbar c}\right)^3 F_0(z_\text{Н}) e^{y}\ ; \quad n_{\text{АН}} = \frac{\bar{g}_\text{Н}}{2\pi^2}\left(\frac{T_k}{c\hbar}\right)^3 F_0(z_\text{Н}) e^{-y}, \tag{8}$$

where $g_\text{Н}$ is the number of the possible states of the particle with the given momentum. For nucleons $\bar{g}_\text{Н} = 4$, $z_\text{Н} = Mc^2/T_k$, M is the nucleon mass, $y = \mu_0/T_k$, μ_0 the chemical potential. The index 0 denotes that we take the first term in the series of the type (3). For the energy density of nucleons and anti-nucleons ($\varepsilon_{\text{НН}}$ and $\varepsilon_{\text{АН}}$) and for the entropy densities ($S_{\text{НН}}$ and $S_{\text{АН}}$) we have:

$$\varepsilon_{\text{НН}} = T_k\left(\frac{\bar{g}_\text{Н}}{2\pi^2}\right)\left(\frac{T_k}{\hbar c}\right)^3 \Phi_0(z_\text{Н}) e^{y}; \quad \varepsilon_{\text{АН}} = T_k\left(\frac{\bar{g}_\text{Н}}{2\pi^2}\right)\left(\frac{T_k}{\hbar c}\right)^3 \Phi_0(z_\text{Н}) e^{-y} \tag{9}$$

$$S_{\text{НН}} = \left(\frac{T_k}{\hbar c}\right)^3 \left(\frac{\bar{g}_\text{Н}}{2\pi^2}\right)[g_0(z_\text{Н}) - yF_0(z_\text{Н})] e^{y}\ ;$$

$$S_{\text{АН}} = \left(\frac{T_k}{\hbar c}\right)^3 \left(\frac{\bar{g}_\text{Н}}{2\pi^2}\right)[g_0(z_\text{Н}) + yF_0(z_\text{Н})] e^{-y}. \tag{10}$$

We shall use formulae (2-10) for computing certain quantities. Let us first evaluate the break-up temperature T_k. Since pion density is much greater than nucleon density, this quantity is determined mainly by the pion density. In order that the break-up of the system might be possible at the temperature T_k, the collision mean free path l of the particles must be, at T_k, of the order of the characteristic dimensions of the system L. A more detailed hydrodynamic calculation shows that L may approximately be written thus: $L \approx (\hbar/\mu c)(E/Mc^2)^{1/2}$, where E is the energy of the initial nucleon and M its mass. The mean free

path is $l \approx 1/n\sigma$, where σ is the cross-section for pion interaction. Assuming, for a first evaluation, that the order of magnitude of σ is $\sigma = \pi(\hbar/\mu c)^2$, and taking for n the expression determined by formula (2), we obtain

$$\frac{l}{L} = \frac{2\pi}{3} \frac{z_\pi^3}{F(z_\pi)} \left(\frac{Mc^2}{E}\right)^{\frac{1}{12}} \tag{11}$$

If $E = 10^{12}$ eV and $T_k/\mu c^2 = 0.5$, $l/L = 9$; if $T_k/\mu c^2 = 1$, $l/L = 0.7$; if $T_k/\mu c^2 = 2$, $l/L = 0.07$. It should be noted that the uncertainty of our computation, due to the fact that both σ and L are taken only in the order of magnitude, does not permit to determine theoretically the break-up temperature T_k. The dependence of T_k on l/L is rather small: while the value of l/L changes in the ratio 100 : 1, the value of T_k changes only in the ratio 4:1. On the other hand, as l/L depends very little on the initial energy, T_k depends on it even less. Thus the introduction of the quantity T_k, which practically does not depend on the properties of the system (i.e. on the initial energy) has a physical meaning.

We shall now proceed to compute the number of antinucleons. Assuming that each section of the system disintegrates at the same temperature T_k, though the moments of disintegration for the various sections may, of course, not coincide, the ratio of the total number of nucleons in the system to the total number of pions will equal the ratio of their densities. From formulae (2) and (8) it is easy to obtain:

$$\frac{N_{\text{н}}}{N_\pi} = \sqrt{\left(\frac{N_{\text{н}}^0}{N_\pi^0}\right)^2 + \left(\frac{N_0}{N_\pi}\right)^2}\,, \tag{12}$$

where N_π^0 and $N_{\text{н}}^0$ are the number of pions and nucleons (nucleons and anti-nucleons) in the system, provided there are no initial nucleons: N_0 is the number of initial nucleons, N_π, $N_{\text{н}}$ the total number of π-mesons and nucleons (nucleons and anti-nucleons) with the presence of initial nucleons. Similarly, we obtain the ratio of the total energy density of the nucleons and anti-nucleons $\varepsilon_{\text{н}}$ to the pion energy density ε_π

$$\frac{\varepsilon_{\text{н}}}{\varepsilon_\pi} = \sqrt{1 + \left(\frac{N_\pi^0}{N_{\text{н}}^0}\right)^2 \left(\frac{N_0}{N_\pi}\right)^2 \cdot \left(\frac{\varepsilon_{\text{н}}^0}{\varepsilon_\pi^0}\right)}\,, \tag{13}$$

where $\varepsilon_{\text{н}}^0$ and ε_π^0 are the densities of the energies of the nucleons and π-mesons when the number of initial nucleons $N_0 = 0$. It can be proved that the ratio $\varepsilon_{\text{н}}/\varepsilon_\pi$ does not depend on the frame of reference in which the collision process is examined. The ratios $N_{\text{н}}^0/N_\pi^0$ and $\varepsilon_{\text{н}}^0\,\varepsilon_\pi^0$ are derived from formulae (2), (4), (8) and (9), if $y = 0$ is put in the formulae (10) and (12). The respective numerical values are given in [6]. Thus at $T_k = 1.5\mu c^2$, $N_{\text{н}}^0/N_\pi^0 = 0.27$.

Assuming that $N_0/N_\pi = 0.15$ (which corresponds to 3 initial nucleons and 20 mesons) then it follows from formula (12) that $N_H/N_\pi = 0.3$. The formula (8) gives the ratio of energy carried off by the nucleons to the energy carried off by the pions. Let $T_k = 1.2\mu c^2$: then $\varepsilon_H^0/\varepsilon_\pi^0 = 0.3$, $N_H^0/N_\pi^2 = 0.13$. If $N_0/N_\pi = 0.15$, $\varepsilon_H^0/\varepsilon_\pi^0 = 0.42$. If, however, $N_0/N_\pi \approx 1$, then $\varepsilon_H^0/\varepsilon_\pi^0 = 2.3$, i.e. the nucleons carry off about 70 per cent of the total energy. It should be stressed however that with $N_0 = N_\pi$, the number of the created particles is small and the theory is roughly approximate. It must be noted that the number of antinucleons can be determined also at a higher temperature than that of the break-up. One may introduce a quantity that does not depend on N_0/N_π and is determined only by the system's break-up temperature T_k, even when the number of nucleons is fixed also at a higher temperature. It is easy to see that the ratio of energy per one nucleon to the energy per one pion depends only on the break-up temperature T_k, and an experimental determination of this ratio would, apparently, be the best way to determine the break-up temperature. It must be noted that this ratio does not depend on the frame of reference. The values of this ratio are given in Table I.

Table I.

$T_\pi/\mu c^2$	$a = \frac{\varepsilon_H}{\varepsilon_\pi}\frac{n_H}{n_\pi}$
$T_k \gg \mu c^2$	6.8
0.5	3.76
1	2.65
1.5	2.16
2	1.83

It is essential to find the relation between the entropy and the number of particles. The expansion of the system, (the second stage of collision) it must be remembered, is regarded as the motion of an ideal fluid and therefore is adiabatic. This adiabatic motion can be violated by shock waves, but they do not appear in the process of expansion. Therefore the entropy of the system and of its several parts changes only in the first collision stage and remains unchanged during the entire hydrodynamical expansion stage down to the break-up. From equations (2), (6), (8), (10) we obtain the following expression for the system's entropy:

$$S = \left\{\frac{g_0(z_H)}{F_0(z_H)} - y\,\mathrm{tgh}\,y\right\} N_H + \frac{g(z_\pi)}{F(z_\pi)} H_\pi. \tag{14}$$

Let $N_0 = 0$, then $y = 0$ and formula (14) reduces to the following:

$$N^* = \alpha(T_k) S\,, \tag{15}$$

where $N^* = N_{\text{H}} + N_\pi$, i.e. N^* equals the total number of the created particles (nucleons and pions), and the coefficient α is:

$$\alpha = \frac{8F_0(z_{\text{H}}) + 3F(z_\pi)}{8g_0(z_{\text{H}}) + 3g(z_\pi)} . \tag{16}$$

The function α is given in Table II.

TABLE II.

$T_k/\mu c^2$	α
0.17	0.113
0.5	0.198
1	0.223
2	0.213
$T_k/\mu c^2 \gg 1$	0.25

As it follows from this table, the function α depends to a small degree on the break-up temperature T_k. Passing on to the case when the initial number of nucleons is important, the nuclear charge conservation should be used. From equations (2)-(14) we have found the ratio N/N_0 as function N^*/N_0, where N is the total number of nucleons and pions in the system, N^* the number of particles created at $N_0 = 0$, N_0 the initial number of nucleons. It appears that with $N^*/N_0 > 2$ we have the formula

$$N = \alpha S , \tag{17}$$

with N denoting the *total number* of particles created in the collision, and the initial nucleons. With $N^*/N_0 < 2$ the number of created particles decreases, and with $N^*/N_0 < 1$, $N/N_0 \to 1$.

3. – Total Number of Particles.

For a hydrodynamical examination of the system, in the first two stages of collision, an equation of state is required. We take the following equation of state (see [5]) for highly compressed medium at temperatures $T \gg \mu c^2$

$$p = \frac{\varepsilon}{3} , \tag{18}$$

where p is the pressure, and ε the energy density. Though we have no precise proof, the choice of the equation of state in the form of (18) is quite plausible.

As the number of particles in the system is not given, and the number itself is determined from the statistical equilibrium, the chemical potential vanishes. Hence $\varepsilon - Ts + p = 0$, where s is the specific entropy. Using the equation of state we obtain

$$s \approx \varepsilon^{\frac{3}{4}}, \qquad T \approx \varepsilon^{\frac{1}{4}}. \tag{19}$$

The relationships (19) coincide with those for « black body radiation », which, of course, should have been expected.

We have already observed that the entropy of the system remains constant during the hydrodynamic stage of expansion and changes only in the first stage, in the first moment of collision. On the other hand the number of particles in the star is connected with the entropy by the relationship (17). Hence, to determine the total number of particles it is necessary to compute the entropy in the first moment of collision. This entropy is most easily calculated in the case of collision of two like particles, such as two nucleons, for instance. Let E' be the nucleon energy in the center of mass system. Owing to symmetry, the substance in the center of mass system is at rest at the moment directly following the collision. The total entropy of the system is proportional to $\varepsilon^{\frac{3}{4}} V_1$, where ε is the energy density, and V_1 the volume in which the energy is concentrated. Therefore $\varepsilon = E'/V_1$ when the entropy and, consequently, the number of particles, is proportional to $E'^{\frac{3}{4}} V_1^{\frac{1}{4}}$. Since the volume V_1, due to Lorentz contraction, is inversely proportional to E', and the energy E in the laboratory system is proportional to E'^2, we finally obtain

$$N \approx E^{\frac{1}{4}}, \tag{20}$$

where E is the energy in the laboratory system. From dimensional considerations formula (20) may be written as follows:

$$N = K\left(\frac{E}{2Mc^2}\right)^{\frac{1}{4}}, \tag{20'}$$

where K is a constant of the order of 1. From experimental data it follows that $K \approx 2$. The relationship (20) coincides with that obtained by FERMI, which is natural, as in deducing it we proceeded from the equation of state for the « black body radiation », as FERMI did, and from the relationship $N \approx S$ which is valid at any break-up temperature of the system. According to FERMI, the disintegration temperature is determined in the first moment after collision. This assumption which, as it has been proved [3], is contradictory in itself, does not, however, influence the correctness of the relationship (20).

We have examined close collisions, in which particles pass at distances comparable to their radius of interaction. Now let us take up the distant collisions, where the impact parameter is great compared with the radius of the forces of both particles. At first glance it may seem that the average number of created particles must rapidly decrease with the increase of the impact parameter, due to the fact that the energy of the meson field of colliding nucleons concentrated in each section would seem (in the frame of reference of this section) to decrease rapidly with increasing distance from their centers. This viewpoint is stated in the works of HEISENBERG [8] and BHABHA [9] on high-energy multiple production, but it contradicts the uncertainty relation, and is therefore erroneous (see [5] and also [10]). Indeed, if the energy of the system's section would decrease, it would very soon become small compared with the uncertainty $\Delta E \approx \hbar c/l$, where l is the section's thickness, compressed due to the Lorentz contraction. Hence, it is not the true total energy of the system, but its mathematical expectation that is small. In other words, it is not the total energy of the system and the total number of particles that decreases, but only the probability that such a collision may occur at all. A detailed examination of distant collisions requires a quantum approach, as the classical one is not suitable owing to violation of the uncertainty relation. The effective cross-sections of the collisions are determined, in their order of magnitude, by the nucleon «radius» $\hbar/\mu c$ (*).

Nucleon-nuclei and nuclei-nuclei collisions will be examined in Section 5.

4. – Energy and Angular Distribution of Particles.

The following equations of relativistic hydrodynamics [11] should be used in investigating the system expansion:

$$\frac{\partial T_{ik}}{\partial x_k} = 0 \,, \tag{21}$$

$$T_{ik} = \omega u_i u_k + p g_{ik} \,, \tag{22}$$

where $\omega = \varepsilon + p$ is the specific enthalpy, u_i the four-velocity. Below we shall use $c = 1$, $g_{11} = g_{22} = g_{33} = 1$, $g_{44} = -1$, $x_i = x_1, x_2, x_3, it$.

At the moment of collision the system in the center-of-mass frame has the form ot a very flat disc, whose transverse dimensions $a = \hbar/\mu c$ are $E'/2M$ times

(*) Due to incorrect consideration of distant collisions HEISENBERG [8] draws the erroneous conclusion that the collision cross-section grows logarithmically with energy. (See [10]).

greater than its thickness Δ. This form holds during a large part of the expansion stage, when the motion of the substance may be regarded as one-dimensional. A solution for the one-dimensional as well as for the subsequent three-dimensional stage of expansion was first obtained by LANDAU [5]. A more exact solution for the one-dimensional stage was later obtained by HALATNIKOV [12] from an investigation of the general one-dimensional problem in relativistic hydrodynamics. In the one-dimensional case one may apply the Legendre transform (see [10]) to equation (21) and then the problem is reduced to solving the following equation for the potential χ:

$$\frac{\partial^2\chi}{\partial\alpha^2} - c_0^2\frac{\partial^2\chi}{\partial y^2} + (c_0^2 - 1)\frac{\partial\chi}{\partial y} = 0\,, \tag{23}$$

where $\alpha = \operatorname{Arch} 1/\sqrt{1-v^2}$, v is the usual velocity, $y = \ln T$ the temperature, c_0 the sound speed in the medium. Since the equation of state is $p = \varepsilon/3$, then $c_0^2 = \frac{1}{3}$, and consequently:

$$3\frac{\partial^2\chi}{\partial\alpha^2} - \frac{\partial^2\chi}{\partial y^2} - 2\frac{\partial\chi}{\partial y} = 0\,. \tag{23'}$$

The transition from the potential χ to the variables x and t occurs according to the following formulae:

$$\begin{cases} t = e^{-y}\left(\dfrac{\partial\chi}{\partial y}\operatorname{ch}\alpha - \dfrac{\partial\chi}{\partial\alpha}\operatorname{sh}\alpha\right), \\ x = e^{-y}\left(\dfrac{\partial\chi}{\partial y}\operatorname{sh}\alpha - \dfrac{\partial\alpha}{\partial\chi}\operatorname{ch}\alpha\right). \end{cases} \tag{24}$$

Let us now take up our problem of the expansion of the flat disc whose initial thickness equals Δ. In the center of mass system the disc expands both ways symmetrically. It is therefore sufficient to examine the expansion only in one way. Let $x = 0$, so that the expansion is symmetrical in relation to the plane $x_1 = -l$ where $l = \Delta/2$. The boundary conditions are as follows. In the plane $x_1 = -l$ the medium must be at rest, and this means that $\alpha = 0$; using equation (24) this condition is described by

$$\left(\frac{\partial\chi}{\partial\alpha}\right)_{\alpha=0} = le^{-y}\,. \tag{25}$$

At the outside edge the solution must go over into a simple (Riemann) wave. It can be proved (see [11]) that in the simple wave the quantities α and y are connected by the relationship: $\alpha = -y/c_0$. From the condition of linking

the general solution with the simple wave it follows that

$$\chi = 0 \quad \text{when} \quad \alpha = -\frac{y}{c_0}. \tag{25'}$$

And further the solution is derived by Laplace's transform [12].

Finally, the potential χ which satisfies the boundary conditions has the following form:

$$\chi = l\sqrt{3}\, e^{y} \int_{\alpha/\sqrt{3}}^{y} e^{2y'} I_0\left(\sqrt{y'^2 - \frac{\alpha^2}{3}}\right) \mathrm{d}y' . \tag{26}$$

By the relationships (24) we can now find the dependence of y (i.e. T) and α (i.e. v) on x and t, and thus fully solve the problem.

For the later stage of the one-dimensional expansion ($t \gg \Delta$) when y and α are large, using for I_0 the asymptotical expression

$$I_0\left(\sqrt{y^2 - \frac{\alpha^2}{3}}\right) \approx \exp\left[\sqrt{y^2 - \frac{\alpha^2}{3}}\right], \tag{27}$$

the potential χ will be of the order

$$\chi \approx \Delta \exp\left[-y + \sqrt{y^2 - \frac{\alpha^2}{3}}\right]. \tag{28}$$

If we restrict ourselves to logarithmic precision, using (24) it is easy to obtain

$$\alpha = \frac{1}{2}\ln\frac{t+x}{t-x}\,; \quad y = -\frac{1}{3}\left[\ln\frac{t+x}{\Delta} + \ln\frac{t-x}{\Delta} - \sqrt{\ln\frac{t+x}{\Delta}\ln\frac{t-x}{\Delta}}\right]. \tag{29}$$

We then introduce the following expressions: $\ln\left((t+x)/\Delta\right) = \tau$, $\ln\left((t-x)/\Delta\right) = \eta$. Since $y = \ln T$ and the energy density is $\varepsilon \approx T^4$, the second equation (29) may be written:

$$\varepsilon = \varepsilon_0 \exp\left[-\tfrac{4}{3}(\eta + \tau - \sqrt{\eta\tau})\right]. \tag{30}$$

Further, with $\alpha > 1$, $\alpha = \operatorname{Arch} u \approx \ln 2u$ where $u = 1/\sqrt{1 - v^2}$, the first of the equations (29) then yields:

$$\frac{1}{1 - v^2} = u^2 \approx \frac{t+x}{t-x}. \tag{31}$$

The equations (30) and (31) coincide with the equations (16) and (24) derived firstly by LANDAU in his work [5].

The following formulae are obtained for the distribution of the energy density and entropy density along the layer thickness (see [5]):

$$(32) \qquad dE \approx \varepsilon a^2 u^2 \, d(t-x) \approx \exp\left[-\tfrac{1}{3}(\sqrt{\tau}-2\sqrt{\eta})^2\right] d\eta ,$$

$$(33) \qquad dS \approx s a^2 u \, d(t-x) \approx \exp\left[-\tfrac{1}{2}(\sqrt{\tau}-\sqrt{\eta})^2\right] d\eta .$$

This shows that the energy is concentrated in a narrow layer $t-x \approx \sqrt[4]{t\Delta^3}$ close to the boundary of the region and the entropy is mainly in the region $t-x \approx t$.

Let us now examine the three-dimensional expansion stage [5].

The solution obtained above holds until the motion may be regarded as one-dimensional. For this it is necessary that the distance covered by the given element in the transverse direction should be smaller than the dimensions of the system a. This condition may be written:

$$(34) \qquad t\vartheta \ll a ,$$

where ϑ is the angle formed with the axis x by the path of the given element. For evaluating the angle ϑ we apply the transverse component of equation (21), and get: $\partial T_{42}/\partial t \approx \partial T_{22}/\partial y$, or in the order of magnitude $T_{42}/t \approx T_{22}/a$. But $T_{42} \approx \varepsilon u^2 \vartheta$ and $T_{22} \approx \varepsilon$, hence $u^2\vartheta \approx t/a$. Since according to (31) $u^2 \approx t/\delta$, where $\delta = t-x$, then $\vartheta \approx \delta/a$, and from the formula (34) it follows:

$$(35) \qquad t \ll \frac{a^2}{\delta} ,$$

which determines the condition for the application of the one-dimensional solution. Beginning with the moment $t_1 = a^2/\delta$, side deviation is essential. The motion arising may be examined only approximately. Qualitatively it can be characterized as conical expansion. In the second stage, which is three-dimensional, the quantity L becomes practically constant for every element of the substance, as the speed is very nearly that of light. Besides that, it may be proved that all derivatives of the hydrodynamic quantities both in the direction δ and in the transverse direction may be neglected. This means that the side forces are small and we have radial expansion. From here it follows that both the flow of energy and the flow of entropy that are transferred inside any cone with a given angle ϑ must remain constant. Since $\delta = t-x \ll t$, the area of the cone cross-section is $\sim t^2$ and the constancy of the energy and entropy flow

means that

$$\varepsilon u^2 t^2 = \text{const}\,, \qquad s u t^2 \approx \varepsilon^{\frac{3}{4}} u t^2 \approx \text{const}\,. \tag{36}$$

Hence

$$u \approx t\,, \qquad \varepsilon \approx \frac{1}{t^4}\,. \tag{37}$$

These relationships determine the change with time of the quantities ε and u in the conical expansion. The region of transition from the first to the second stage is quite complex and is not examined in detail. Instead, the solution derived for the second stage is linked with the one-dimensional solution at the point where the latter becomes unsuitable, i.e., at the point $t_1 = a^2/\delta$.

For S we obtain the following formula, with $t = t_1$,

$$\mathrm{d}S \approx \exp\left[\sqrt{L^2 - \lambda^2}\right] \mathrm{d}\lambda$$

where we have introduced the notations:

$$\frac{t - x}{a} = \frac{\delta}{a} = e^{-\lambda}\,; \qquad \frac{\Delta}{a} = e^{-L}\,. \tag{38}$$

It will be remembered that

$$\frac{\Delta}{a} = \frac{M}{E'} = \sqrt{\frac{2M}{E}}\,, \quad \text{hence} \quad L = \tfrac{1}{2} \ln \frac{E}{2M}$$

where E' is the energy in the centre of mass system, and E the energy in the laboratory system. Since each element further shifts from $\delta = \text{const}$ and the entropy of the elements of the substance, due to adiabatic motion, remains constant, the formula holds until the system disintegrates into several parts. But we know that the number of particles is proportional to the entropy. Consequently, for the distribution of particles we have

$$\mathrm{d}N \approx \exp\left[\sqrt{L^2 - \lambda^2}\right] \mathrm{d}\lambda\,, \tag{39}$$

$$\vartheta \approx \frac{\delta}{a} = e^{-\lambda}\,. \tag{40}$$

The angle ϑ remains constant, together with δ, for each particle. Formulae (39) and (40) determine parametrically the angular distribution of the particles in the center of mass system. Most of the particles are created at $\delta = t$, as the maximum entropy is in this region. The angle of escape of these particles is theretore ≈ 1. A smaller number of particles is formed at small angles, but they possess greater energy. From (39) and (40) it follows that in close collisions the angular distribution in the center of mass system is by no

means isotropic, as FERMI assumed [1]. Note that the highest value of the quantity λ which still has some meaning, is determined from the condition $\int_{\lambda}^{L} \mathrm{d}N \approx 1$. Hence one may deduce that

$$\lambda_{\max} = \frac{\sqrt{3}}{2} L . \tag{41}$$

To determine the distribution of the particles among the energies, it is first of all necessary to link the values u and ε with $t = t_1$. Free escape of the particles begins at the moment t_k when the temperature of the section of the system becomes equal to the «critical» temperature T_k. It can be proved that the quantity u_k is related to t_k by the formula

$$u_k \approx \frac{t_k}{a} . \tag{42}$$

On the other hand in a simple way the quantity u_k is connected with the energy of the escaping particles. If the energy of the particle in the frame of reference where the given element of the substance is at rest is E_0, then in the center of mass system it is $E_0 u_k$. Using the expression for the energy density one can prove that $t_k \approx \text{const} \cdot \exp\left[\lambda + \frac{1}{3}\sqrt{L^2 - \lambda^2}\right]$. The constant in this relationship is determined by $\int E_0 u_k \, \mathrm{d}N = E'$. Hence, we obtain the following formula for the energy $\mathcal{E} = E_0 u_k$ of the particle:

$$\mathcal{E} \approx M \exp\left[-\frac{L}{6} + \lambda + \tfrac{1}{3}\sqrt{L^2 - \lambda^2}\right]. \tag{43}$$

The equations (39) and (43) give the parametric distribution of the particles among the energies. If particles with different masses are created or the energy carried off by the nucleons plays an essential part, then this fact must be considered on the basis of the discussions in section 2. Most of the particles (λ=0) possess relatively small energy. The particles, however, which come at small angles possess a substantially high energy. Thus there is a concentrated flow of energy at small angles.

We shall now pass on from the center-of-mass system to the initiall aboratory system. Neglecting the details of the transformation, which has been described in [5], we give here the final formulae:

$$\mathrm{d}N = \frac{K}{\sqrt{2\pi L}} \exp\left[-\frac{L}{2} + \sqrt{L^2 - \lambda^2}\,\mathrm{d}\lambda\right], \tag{44}$$

$$\mathcal{E} = \frac{5\sqrt{5}}{2\sqrt{3}} \frac{M}{K} \exp\left[\frac{5L}{6} + \lambda + \frac{1}{3}\sqrt{L^2 - \lambda^2}\right]. \tag{45}$$

The coefficients in the (44) and (45) are deduced from the conditions:

$$\int \mathrm{d}N = N\,, \qquad \int \varepsilon \mathrm{d}N = E\,.$$

Fig. 1 shows the distribution of particles computed by these formulae. A significant characteristic of the collision is the angle in which half the energy is radiated. For the energy of 10^{14} eV, for example, this angle, according to the theory in question, is 0.1 ($1.3 \cdot 10^{-4}$ in the laboratory system), whereas according to Fermi's theory [2], in which the distant collisions are not consistently taken into account, it is 0.31 ($6.7 \cdot 10^{-4}$ in the laboratory system) (see [13]).

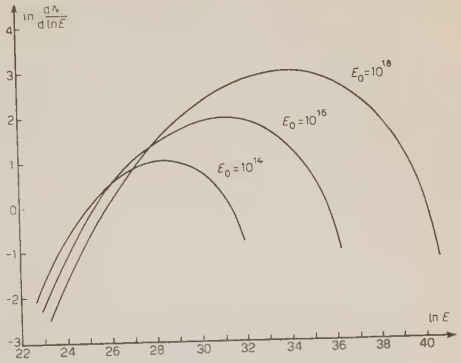

Fig. 1. – Differential spectra of the energy of secondary particles created in high-energy nuclear interaction. E_0 is the energy of the initial particle in the laboratory system.

5. – Collisions of Particles of Different Masses.

Until now we have been examining only collisions of nucleons with nucleons. In the experiment, however, one observes frequently, at high energies, collisions of nucleons with nuclei, and of nuclei with nuclei. It would be wrong to consider the collision nucleon-nucleus, or nucleus-nucleus, as a series of collisions of nuclear protons and neutrons. Since the distance between the particles in the nucleus is of the order of the radius of nuclear forces, and several new particles are created in each collision, the collision must lead to a process of simultaneous creation of particles in the whole range through which the nucleon passes in the nucleus, or the smaller nucleus in the larger. The nucleon, for example, will here interact not with the whole nucleus but only with a part of the nucleus, i.e. it will cut a « tube » in the nucleus (see [13]). The number of particles created in the collision will be connected with the entropy by the relationship (17), with N denoting the total number of created particles and nucleons participating in the collision. The close collision of two like nuclei of atomic weight A is most simply examined. Applying the discussions that have led us to (20), we obtain the following formula:

$$N = KA^{\frac{3}{4}} \left(\frac{E}{2Mc^2} \right)^{\frac{1}{4}}. \tag{46}$$

Considerably more complicated is the calculation of the collision nucleon-nucleus, or of nuclei of different atomic weights. In the case of nucleon-nucleus collision (see [14]), the calculation of the number of particles created is reduced to the calculation of the entropy in the first stage of collision, as in the star the entropy does not change during the process of hydrodynamic expansion.

Let us extend our conception of the nuclear substance as a continuous medium to the examination of the first stage of collision, the compression of nuclear substance. Such examination is, of course, highly approximate and is used only for orientation. One cannot strictly speak of a shock wave or of an expansion wave « travelling » over the nucleon. We shall select a frame of reference in which nucleon and nucleus have equal velocity, but in opposite directions. Due to Lorentz contraction the nucleon and the nucleus, in this system, are two very thin discs, owing to which the problem at the beginning of the collision may be regarded as one-dimensional. The collision of the nucleon with the nucleus is thus a collision of the nucleon with the tube cut from the nucleus, the cross-section of the tube equalling that of the nucleon, and its length changing from the diameter of the nucleus to the « diameter » of the nucleon. When nucleon and tube come close to each other, the « shock waves » travel in both directions over the substance of the tube and the substance of the nucleon. The substance between the shock waves will, in our system, be at rest. The shock wave which travels over the lighter particle will reach the edge sooner than the one travelling over the tube. When the wave reaches the edge, the substance will begin to flow out from the edge, and the rarefaction wave will travel over the nuclear substance with speed equal to that of sound in the medium. The shock wave which has not yet reached the edge will at the same time travel in the same direction. The computation of entropy will vary depending on whether the rarefaction wave will catch up with the shock wave before the shock wave reaches the edge and the contraction process ends. Since we proceed from the equation of state $p = \varepsilon/3$, the velocity of sound is $c_0 = 1/\sqrt{3}$, and the velocity of the shock wave is $D = \frac{1}{3}$. Hence it is not hard to prove that the length of the tube over which the rarefaction wave will catch up with the shock wave equals $l_k/d = 3.7$, d beeing the « length » of the nucleon. When the length of the tube is $l < l_k$ the entropy change can be simply computed, an we obtain the following formula,

$$\frac{S}{S_0} = \left(\frac{1}{2}\frac{l}{d} + 1\right), \tag{47}$$

where S_0 is the entropy change in the collision nucleon-nucleon. The inexactness of this formula is due to the uncertainty in the nucleon form. It becomes more exact in the collision of a light nucleus with a heavy one. In this case d denotes the size ot the light nucleus.

The solution becomes more complex when the tube length exceeds $l_k = 3.7d$. In this case the expansion wave will catch up with the shock wave but will not be able to pass through the shock wave and will be reflected from it. There will appear a region bounded by the shock wave on the right and by the expansion wave on the left. The equations (23) and (23′) for the arbitrary one-dimensional motion of the relativistic gas should be used to describe the motion of the medium in this region. By rather complex computation, given in detail in [14], we obtain

$$\frac{S}{S_0} = 0.92\left(\frac{l}{d} - \frac{1}{4}\right)^{\frac{1}{4}}, \tag{48}$$

where S_0 is the entropy in nucleon-nucleon collision, and S the total entropy in the collision of the nucleon with the tube. If the formulae (47) and (48) are averaged over all possible collisions in the nucleus, from close collision to collision with the distant nucleon, the result obtained may be described by the following formula, up to a precision of about 5%,

$$\frac{S}{S_0} = A^{0.19}, \qquad \frac{N}{N^{\mathrm{H}}} = A^{0.19}. \tag{49}$$

Here A is the atomic weight, N^{H} the number of particles created in the nucleon-nucleon collision. In agreement with experiment (see [13]), the multiplicity does not depend very much on atomic weight. Thus, according to this formula, the multiplicity in lead ($A = 207$) differs only 1.7 times from that in nitrogen ($A = 14$).

REFERENCES

[1] E. Fermi: *Prog. Theor. Phys.*, **5**, 570, (1950).
[2] E. Fermi: *Phys. Rev.*, **81**, 689 (1951).
[3] I. Ja. Pomerančuk: *Dokl. Akad. Nauk SSSR*, **78**, 889 (1951).
[4] E. L. Feinberg and D. S. Černavskij: *Dokl. Akad. Nauk SSSR*, **81**, 795 (1951).
[5] L. D. Landau: *Izv. Akad. Nauk SSSR, Ser. Fiz.*, **17**, 51 (1953).
[6] S. Z. Belen′kij: *Dokl. Akad. Nauk SSSR*, **99**, 523 (1594).
[7] S. Z. belen′kij: *Žu. Èksper. Teor. Fiz. SSSR*, **28**, 111 (1955).
[8] W. Heisenberg: *Zeits. f. Phys.*, **133**, 65 (1952).
[9] H. J. Bhabha: *Proc. Roy. Soc.*, A **219**, 293 (1953).
[10] E. L. Feinberg and D. S. Černavskij: *Dokl. Akad. Nauk SSSR*, **91**, 511 (1953).
[11] L. Landau and E. Lifšic: *Mehanika splošnyh sred* (*Mechanics of Continuous Media*), 2nd Edition (Moscow-Leningrad, 1953).
[12] I. M. Halatnikov: *Žu. Èksper. Teor. Fiz.*, **27**, 529 (1954).
[13] I. L. Rozental′ and D. S. Černavskij: *Usp. Fiz. Nauk*, **52**, 185 (1954).
[14] S. Z. Belen′kij and G. A. Milehin: *Žu. Èksper. Teor. Fiz.*, **29**, 20 (1955).

SUPPLEMENTO AL VOLUME III, SERIE X
DEL NUOVO CIMENTO

N. 1, 1956
1° Semestre

Photoproduction of π^0-Mesons from Deuterium

A. BELOUSOV, A. KUCENKO and E. TAMM

Institute of Physics of the Academy of Sciences of the USSR-Moscow

CONTENTS. — 1. Introduction. – 2. Experimental arrangement. – 3. Results.

1. – Introduction.

One of the main aims of investigations devoted to the study of the interaction between mesons and nucleons is to verify experimentally the validity of the hypothesis of isotopic invariance. Until recently, the experimental confirmation of this hypothesis consisted in a verification of some of the conclusions which follow from it; thus a particular type of symmetry is predicted which leads to invariance with respect to rotation of 180° about an axis in the (x, y) plane and with respect to substitution of all neutrons by protons and all protons by neutrons and also of $\left.\begin{matrix}\pi^+\\ \pi^-\end{matrix}\right\}$ mesons by $\left.\begin{matrix}\pi^-\\ \pi^+\end{matrix}\right\}$ mesons.

In order to prove the validity of isotopic invariance and to exclude more specific types of symmetry one may investigate, for example, the neutral π-meson field functions. According to the hypothesis of isotopic invariance the π^0-meson field wave function should be expressed in terms of the third component of a vector in isotopic space; thus the coupling constants of protons and neutrons with π^0-mesons (g_p and g_n) should have opposite signs. If, however, the π^0-meson field wave function is a scalar, then g_n and g_p should have the same sign.

Photoproduction of π^0-mesons from deuterium

$$\gamma + \mathrm{d} \rightarrow \begin{cases} \mathrm{d} + \pi^0 & \text{Process I} \\ \mathrm{p} + \mathrm{n} + \pi^0 & \text{Process II} \end{cases}$$

permits one to determine the relative signs of the interaction constants.

MIHAJLOV and BALDIN have shown that the cross-section for process I strongly depends on the relative signs of g_p and g_n [1]. The cross-sections for processes I and II were calculated from perturbation theory for pseudoscalar mesons with pseudovector coupling. The calculations were carried out in Pauli's approximation, with phenomenological introduction of anomalous nucleon magnetic moments. Similar calculations were carried out simultaneously by FRANCIS [2]. In both of these investigations a number of assumptions were made which reduced the generality of the results. Subsequently, BALDIN and MIHAJLOV obtained similar results by proceeding from some very general principles of quantum mechanics [3, 4, 5].

The Schrödinger equation for meson and nucleon fields interacting with electromagnetic radiation has the form

$$i\frac{\partial\psi}{\partial t} = (H_0 + H_e)\psi\,.$$

In [3] and [4] it is shown that for any photonuclear process in which a photon is emitted or absorbed

$$H_e = S + V_3\,,$$

where S is proportional to the nucleon current and V_3 is proportional to the meson as well as nucleon current. Here $S \sim (\mu/M)V_3$, where μ and M are respectively the meson and nucleon masses. It can be shown that if the π^0-meson wave function is expressed in terms of the third component of the vector ($g_p = -g_n$), then $\sigma_I \sim (V_3)^2$. If, on the contrary, the π^0-meson is described by a scalar ($g_p = g_n$), then $\sigma_I \sim (S)^2$. Thus, the ratio of the cross-sections for process I when $g_p = -g_n$ and $g_p = g_n$ will be

$$\frac{\sigma_I(g_p = -g_n)}{\sigma_I(g_p = g_n)} \sim \left(\frac{V_3}{S}\right)^2 \cong 40\,.$$

If process II takes place then $\sigma_{II} \sim (S+V_3)^2$ or, inasmuch $V_3 \gg S$:

$$\sigma_{II} \cong \sigma_I(g_p = -g_n)\,.$$

Thus an experimental estimation of the cross section of process I and a comparison of the cross-section for processes I and II permits one to determine the relative sign of g_p and g_n.

2. – Experimental Arrangement.

The γ-rays for studying processes I and II where obtained from the synchrotron of the Institute of Physics of the Academy of Sciences of the USSR. The targets, LiD and Li, were irradiated with a beam of γ-rays of 250 MeV max-

imum energy. The coincidence rate due to γ-rays from decaying π^0-mesons and to the recoil products (deutons or protons) was measured.

If the energy of the primary γ-rays is fixed, then from conservation laws it follows that the direction of emission of the π^0-meson uniquely defines the energy and angle of emission of the recoil deuton (process I).

Synchrotrons emit a continuous radiation spectrum and therefore even when the angle of emission of the π^0-meson is fixed the recoil deutons will be distributed in a broad interval of angle and energy. To record the π^0-mesons emerging from the target in a definite direction it is sufficient to use a telescope sensitive to the decay γ-rays and oriented in this direction. The reason for this is that the probability of emission of a γ-ray from a decaying π^0-meson within a solid angle $d\Omega$ at an angle θ with respect to the direction of the primary beam is expressed by the equation

$$P(\theta)\,d\Omega = \frac{d\Omega}{2\pi\gamma^2(1-\beta\cos\theta)}\,, \qquad \text{where } \gamma = (1-\beta^2)^{-\frac{1}{2}};$$

i.e. the angular distribution of the decay γ-rays has a maximum in the direction coinciding with the direction of motion of the π^0-meson.

γ-rays from decaying π^0-mesons were recorded in our apparatus at an angle of $90^\circ \pm 10^\circ$ with respect to the primary beam of γ-rays. As the upper limit of the bremsstrahlung spectrum from the synchrotron was 250 MeV, this means that the corresponding deutons had energies between 18 and 32 MeV and were confined to an angle interval from 0° to 47°. Protons in process II were also distributed in a broad interval of angle and energy.

Thus, in its essence, the experiment consisted in separating the deutons produced in process I from the protons of process II. This problem was solved by using a method suggested by V. I. VEKSLER. Use is made of the fact that the period of revolution T of a charged particle (charge e, mass m) in a homogeneous magnetic field H

$$T = \frac{2\pi mc}{eH}\,,$$

is independent of energy and proportional to the mass of the particle. Thus, if the target is placed in a magnetic field, the time of flight of the protons and deutons between target and detector (located on a circle of given radius) will differ by a factor of two. Separation of the particles can thus be carried out by measuring the delayed coincidences between the π^0-decay γ-ray telescope and the heavy particle counter. The coincidence rate as a function of delay in the channel connected to the γ-ray telescope should therefore exhibit two maxima corresponding to protons and deutons. The height of the peaks is a measure of the relative yields of processes I and II.

A scheme of the apparatus is shown in Fig. 1. In all experiments the strength of the magnetic field was $H = 8 \cdot 10^3$ oersted. Particles moving in a semi-circle of radius $\varrho = 35$ cm were recorded. The times of flight of the deuterons and protons between target and detector were respectively $8.2 \cdot 10^{-8} \pm \pm 1.6 \cdot 10^{-8}$ s and $4.1 \cdot 10^{-8} \pm 0.8 \cdot 10^{-8}$ s. Thanks to semi-circular focusing of the magnetic field, only those deutons and protons were recorded which emerged from the target in an angle interval between 13° and 37° measured in the plane perpendicular to the magnetic field and in an angle interval of $\pm 1.5°$ in the perpendicular plane. The respective particle energies were 2 ± 0.16 MeV and $4 \pm \pm 0.32$ MeV. It should be noted that the target thickness is greater than the range of the deutons produced in reaction I and therefore, in the angle interval under consideration, deutons emerging from the target will form a continuous spectrum between 0 and 32 MeV.

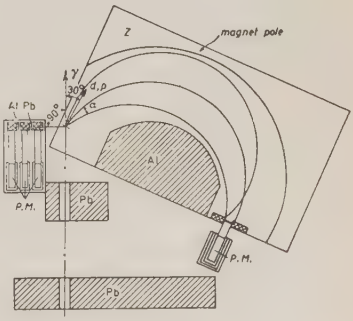

Fig. 1.

The telescope employed to detect the π^0-decay γ-rays consisted of three stilbene scintillation counters; coincidences between two of these counters and the heavy particle counter, and anticoincidences between the third counter and the heavy particle counter were recorded. A 5 mm thick lead converter was placed directly behind the anticoincidence crystal, and a 2 cm aluminium absorber was interposed between the coincidence crystals. This absorber raises the threshold of the γ-telescope to $E_\gamma = 30$ MeV.

A « FEU-19 » photomultiplier was used to detect the scintillations, a plexiglass light guide of 50 cm length being employed. The telescope was shielded from strong magnetic fields by covering each multiplier with two coaxial iron tubes.

A prevacuum chamber containing the target and the crystal of the heavy particle counter was placed between the magnet poles. The π^0-decay γ-rays emerged from the chamber through an aluminium window 100 μm thick. By means of special devices located in the chamber the target could be removed from the beam and the heavy particle detector could be covered by an absorber sufficient to stop the deutons and protons.

ZnS(Ag) phosphors were used to detect the protons and deutons. They were deposited as a thin layer on the end of the light guide used to transmit the scintillation light from the chamber to the photomultiplier. The proton and deuton multiplier was shielded from the magnetic field by four coaxial iron tubes.

Pulses from the photomultipliers were fed directly into a germanium diode coincidence circuit with resolving time $\tau = 1 \cdot 10^{-8}$ s. The circuit contained three identical channels each with a different delay interval.

Reliability of separation of deutons and protons was attained by sacrificing efficiency of detection of the heavy particles; the reason for this is that only protons and deutons confined to a narrow energy interval were recorded.

The low cross-section of the investigated processes and the large background due to γ-rays and to light charged particles significantly complicate the experiment. The background was lowered by collimating the synchrotron γ-ray beam by means of two collimators. By shielding the apparatus with 20 cm Pb and 5 cm Al the isotropic component of the background could be practically eliminated. The accidental coincidence rate was reduced by prolonging the duration of the synchrotron radiation pulse up to 3000 μs.

The γ-rays intensity was chosen in such a manner that the counting rate of the apparatus per unit intensity was independent of the counting rate of the monitor chamber. Accidental coincidences were estimated by carrying out the measurements with the heavy particle crystal unshielded and with this crystal covered by the heavy particle absorber. To check that the apparatus was recording effects due to mesons the maximum γ-ray energy was lowered to 150 MeV; the counting rate in this case was practically zero.

3. – Results.

The results of the measurements obtained with LiD and Li targets are presented in Fig. 2. The data in Fig. 2 show that within experimental errors the results obtained with the LiD target were identical with those one would expect to get with a pure deuterium target.

The absence of any deuton that may have been produced during the photodesintegration of Li with the formation of π^0-mesons is due to the fact that at least three particles are formed in the reaction. As a result, the particle trajectories are no longer coplanar and, due to bad focusing in the plane parallel to the magnetic field, the efficiency of measuring the process is much smaller. A similar effect also holds for protons produced in process II, but in this case the departure from coplanarity is insignificant because the proton-neutron binding energy is small. This difference in measurement

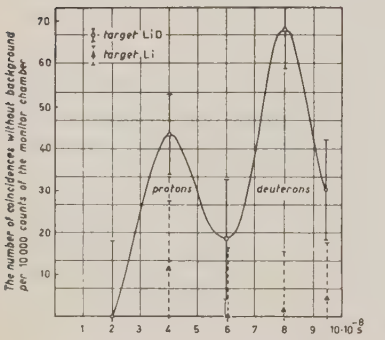

Fig. 2.

efficiency for processes I and II leads to a certain decrease in the number of recorded protons. Computations show that as a consequence of this efficiency difference, if $g_p = -g_n$, the proton maximum should be about four times smaller than the deuton peak.

If, on the contrary, $g_p = g_n$, then no deuton peak should be observed, as the efficiency of the apparatus is not sufficient to detect such small effects. The existence of a deuton peak (Fig. 2) and the fact that the magnitude of this peak is comparable with that of the protons, signifies that the cross-section of process I corresponds to the case when $g_p = -g_n$.

A similar result obtained by using a different technique was reported by DeWire, Silverman and Wolfe [6] who used γ-rays with maximum energy 320 MeV.

Thus, the results of the present investigation and of investigation [6] obtained by two different methods and for different energies of the primary γ-ray prove that the neutron and proton neutral meson field coupling constants have opposite signs. This fact confirms one of the most significant predictions of the isotopic invariance hypothesis.

* * *

In conclusion we consider it a pleasant duty to express our appreciation to V. I. Veksler and P. A. Čerenkov for interest in this work, and to A. M. Baldin for valuable suggestions. Thanks are also extended to the members of the accelerator operating staff.

REFERENCES

[1] V. V. Mihajlov and A. M. Baldin: *Dokl. Akad. Nauk SSSR*, **84**, 47 (1952).
[2] N. C. Francis: *Phys. Rev.*, **99**, 766 (1953).
[3] A. M. Baldin and V. V. Mihajlov: *Dokl. Akad. Nauk SSSR*, **91**, 479 (1953).
[4] A. M. Baldin: *Dokl. Akad. Nauk SSSR*, **96**, 949 (1954).
[5] A. M. Baldin: in this issue, p. 4.
[6] J. W. DeWire, A. Silverman and B. Wolfe: *Phys. Rev.*, **92**, 520 (1953).

SUPPLEMENTO AL VOLUME III, SERIE X
DEL NUOVO CIMENTO

N. 1, 1956
I° Semestre

The Nature of Cosmic Radio Emission and the Origin of Cosmic Rays.

V. L. GINZBURG

Academy of Sciences of the USSR - Moscow

CONTENTS. — **1. Introduction.** – 2. The magnetic bremsstrahlung nature of cosmic radio emission. – 3. The origin of cosmic rays.

1. – Introduction.

In order to formulate a theory of the origin of cosmic radation (c.r.) it is obviously necessary to have a certain amount of information on the composition, energy spectrum and spatial distribution of the c.r. outside the earth's atmosphere, in the solar system, in the Galaxy and between galaxies. However, up to very recent times only data (and very incomplete at that) on cosmic rays in the immediate vicinity of the earth (at top of atmosphere) have been available. As a result of this, various theories of origin of the cosmic rays were founded on rather arbitrary hypotheses and even the foundamental question concerning the sources and mechanism of acceleration of c.r. particles remained obscure. One of the main aims of the present paper is to demonstrate that with the development of radioastronomy this state of affairs has radically changed. Thus, if one interprets the non-thermal cosmic radio emission as being a type of magnetic bremsstrahlung (radiation from electrons accelerated in interstellar magnetic fields) then radioastronomical data permit one to determine the spectrum and concentration of relativistic electrons of the primary c.r. in the Galaxy and beyond it. Thus the theory of origin of c.r. can rest on a reliable foundation; it now becomes a branch of astrophysics based on empirical data. The nature of cosmic radio emission will be considered in the present paper and a theory of the origin of c.r. based on radio astronomical data will be described (a more detailed account of the theory is given in [1-3]).

2. – The Magnetic Bremsstrahlung Nature of Cosmic Radio Emission.

Cosmic radio waves emitted with a continuous spectrum consist of radiation from discrete sources and of « general » cosmic radio emission which varies relatively slowly with the galactic coordinates. The general radiation can in turn be resolved into metagalactic and galactic components. Finally the galactic radio emission may be divided into thermal and non-thermal components. The first of these is the thermal radio emission from interstellar gas and, similarly to the gas, it is located in the plane of the Galaxy. Naturally, the corresponding maximum effective temperature of the radiation, T_{eff}, cannot exceed the kinetic temperature of the gas and therefore cannot exceed $\sim 10\,000^{\circ}$. However, in the direction of the Galaxy anticenter and pole the optical thickness of the gas is small and even for waves in the meter band the thermal radio emission intensity is weak ($T_{\text{eff}} \lesssim 1000^{\circ}$); the same may also be said about the metagalactic radio emission. On the other hand the total intensity of cosmic radio emission of wave length say of 16.3 m travelling from the galactic pole corresponds to an effective temperature $T_{\text{eff}} \sim 50\,000^{\circ}$. This signifies that there exists some type of non-thermal general galactic radio emission which depends weakly on the galactic coordinates and which compared with thermal and metagalactic radiation is of decisive importance in the meter band. From an analysis of the cosmic radio emission isophotes it has been concluded [4] that the non-thermal galactic radio emission comes from a quasispherical sub-system, a sort of corona which surrounds the stellar Galaxy. The radius of this sub-system is $R \sim 3 \div 5 \cdot 10^{22}$ cm. Diffuse interstellar gas with a concentration of $n \lesssim 0.1$ cm^{-3} possesses about the same spatial distribution [5].

A convincing proof of the existence in the Galaxy of radio sources distributed in the manner described above is the discovery [6] of a similar « radio corona » around the nebula M31 in Andromeda which resembles our own Galaxy.

What is the nature of the non-thermal galactic radio emission? Even at the present time attempts are made to explain the radio emission as originating in a large number of hypothetical radio stars invisible in the optical range of the spectrum. This assumption, which for a number of reasons has always seemed to us to be improbable, becomes altogether untenable after the discovery that the discrete sources of cosmic radio waves are nebulae and not stars. There is therefore absolutely no justification in assuming the existence of an enormous number [4] of radio stars possessing some very queer properties and a very unusual spatial distribution. The « magnetic bremsstrahlung hypothesis » which associates non-thermal cosmic radio emission with the waves radiated by relativistic electrons moving in the interstellar magnetic field [7-9, 1-3]

seems to be much satisfactory in this respect. It will be shown in the following that not only this hypothesis can be made to agree with the probable values of the interstellar magnetic fields and with the concentration of relativistic electrons, but that it is very fruitful for radio astronomy as a whole and for the theory of origin of c.r.

As is well known, in a magnetic field H an electron moves along a helical path with a cyclic frequency

$$\omega_H = \frac{eH}{mc} \cdot \frac{mc^2}{E}, \tag{1}$$

where E is the total electron energy. In the ultra relativistic case, which is the only one of interest here, the electron radiates electromagnetic waves almost exclusively into a narrow cone whose angular aperture is $\theta \sim mc^2/E \ll 1$ in the direction of instantaneous velocity. Therefore, if the electron moves in circle, an observer at rest will «see» radiation pulses of duration

$$\Delta t \sim \frac{r\theta}{c}\left(\frac{mc^2}{E}\right)^2 \sim \left(\frac{mc}{eH}\right)\left(\frac{mc^2}{E}\right)^2,$$

where r is the radius of the orbit. If, however, the electron moves along a helix and the angle α between velocity and field is not too small (*) then $\Delta t \sim (mc/eH_\perp)(mc^2/E)^2$, where $H_\perp$ is the component of the magnetic field perpendicular to the direction of motion. The radiation spectrum will correspondingly consist of overtones of the frequency ω_H and practically may be considered as a continuous spectrum, the maximum being at a frequency $\omega_{\max} \sim 1/\Delta t \sim (eH_\perp/mc)(E/mc^2)^2$. Calculations show (see for example [10]) that the energy radiated by an electron per second in a frequency range $d\nu$ is $P(\nu, E)\,d\nu$, where

$$\begin{cases} P(\nu, E) = P(\nu) = 2\pi P(\omega) = 16\dfrac{e^3 H_\perp}{mc^2} p\left(\dfrac{\omega}{\omega_m}\right) = 16\ \dfrac{e^2}{c}\,\omega_{H\perp}\left(\dfrac{\omega}{2\omega_{H\perp}}\right)^{\frac{1}{3}} Y(u) \\ \omega_{H\perp} = \dfrac{eH_\perp}{mc}\cdot\dfrac{mc^2}{E}, \quad \omega_m = \dfrac{eH_\perp}{mc}\left(\dfrac{E}{mc^2}\right)^2, \quad u = \left(\dfrac{\omega}{2\omega_m}\right)^{\frac{2}{3}}, \quad Y(u) = \dfrac{p(2u^{\frac{3}{2}})}{u^{\frac{1}{2}}}. \end{cases} \tag{2}$$

Values of the function $Y(u)$ are given in the table; in the limiting cases

$$\frac{\omega}{\omega_m} \ll 1: \quad Y = 0.256, \qquad \frac{\omega}{\omega_m} \gg 1: \quad Y(u) = \frac{(2\pi)^{\frac{1}{2}}}{16} u^{\frac{1}{2}} \exp[-(4/3)u^{\frac{3}{2}}]. \tag{3}$$

(*) The radiation will be of a different nature if the angle $\alpha \lesssim \theta \sim mc^2/E$; this case is of interest for the theory of solar sporadic radio emission [11].

u	$Y(u)$	u	$Y(u)$
0.0	0.256	1.8	0.0085
0.2	0.204	2.0	0.0050
0.4	0.156	2.2	0.0028
0.6	0.115	2.4	0.0015
0.8	0.081	2.6	0.0008
1.0	0.055	2.8	0.0004
1.2	0.036	3.0	0.0002
1.4	0.023	3.5	0.00004
1.6	0.014	4.0	0.000006

The function $p(\omega/\omega_m)$ has a maximum at $\omega = 0.5\omega_m$, where it equals 0.1. Thus at the maximum

$$(4)\qquad \begin{cases} P(\nu_{\max}) = 1.6\dfrac{e^3 H_\perp}{mc^2} = 2.15\cdot 10^{-22} H_\perp \text{ erg/cycle} \\ \nu_{\max} = 0.5\dfrac{\omega_m}{2\pi} = 1.4\cdot 10^6 H_\perp \left(\dfrac{E}{mc^2}\right)^2 \text{ cycle/s}\,. \end{cases}$$

The intensity observed at the earth will be

$$(5)\qquad I_\nu = \frac{1}{4\pi}\int P(\nu, E) N_e(E, \boldsymbol{r})\,\mathrm{d}E\,\mathrm{d}r\,,$$

where $N_e(E, \boldsymbol{r})$ is the differential electron spectrum at the point $\boldsymbol{r}$. Integration is carried out along the ray of vision and it is assumed that, due to the random distribution of the field $\boldsymbol{H}$, the radiation on the average is isotropic (hence the factor $\frac{1}{4}\pi$ in (5)). This assumption means that the formulae are correct to a factor of the order of unity. Absorption and possible influence of the refraction index (which may be different from unity) have not been taken into account as they are of no consequence in the following exposition (see [1]).

If the electron spectrum does not change along a path R and has the form

$$(6)\qquad N_e(E) = KE^{-\gamma}$$

then

$$(7)\qquad I_\nu = \frac{R}{4\pi}\int_0^\infty P(\nu, E) N_e(E)\,\mathrm{d}E = \frac{3}{\pi}(2\pi)^{(1-\gamma)/2}\frac{e^3 H_\perp}{mc^2}\left[\frac{2eH_\perp}{m^3c^5}\right]^{(\gamma-1)/2} U(\gamma) K R \nu^{(1-\gamma)/2} \simeq$$

$$\simeq 1.3\cdot 10^{-22}(2.8\cdot 10^8)^{(\gamma-1)/2} U(\gamma) K R H_\perp^{(\gamma+1)/2} \lambda^{(\gamma-1)/2} \text{ erg/cm}^2 \text{ cycle steradian}\,,$$

where $U(\gamma) = \int_0^\infty Y(u) u^{(3\gamma-5)/4} \mathrm{d}u$ and, for example, for $\gamma = 1$, $5/3$, 2, 3 and 7 the function $U(\gamma)$ has the corresponding values 0.37, 0.163, 0.128, 0.087 and 0.153.

Data on non-thermal galactic radio emission in the band $1.5\ \mathrm{m} < \lambda < 17\ \mathrm{m}$ indicate that in a first approximation (*)

$$I_\nu \simeq a\frac{c}{\nu} = a\lambda, \qquad a \sim 5\cdot 10^{-21}\ \mathrm{erg/cm^3\ cycle\ steradian}\,. \tag{8}$$

From (7) and (8) we obtain

$$\gamma \cong 3, \qquad I_\nu \simeq 3.1\cdot 10^{-15} H_\perp^2 KR\lambda \simeq 5\cdot 10^{-21}\lambda \tag{9}$$

and hence $KH_\perp^2 R \sim 1.6\cdot 10^{-6}$. For the reasonably highest values of $R \sim 5\cdot 10^{22}$ cm and $H_\perp \sim 10^{-5}$ oersted one obtains a minimum value $K_{\min} \sim 3\cdot 10^{-19} \simeq$ $\simeq 10^{-5}\ (\mathrm{eV})^2/\mathrm{cm}^3$.

To be cautious we put $K \simeq 10^{-6}$ and thus arrive at the following electron spectrum

$$N_e(E) \simeq \frac{10^6}{E^3}(\mathrm{eV})^{-1}\,\mathrm{cm}^{-3}\,, \quad N_e(E > E_0) = \int_{E_0}^\infty N(E)\,\mathrm{d}E \simeq \frac{10^6}{2E_0^2}\,\mathrm{cm}^{-3}\,, \tag{10}$$

where E and E_0 are measured in eV. Hence $N_e\ (E > 10^9\ \mathrm{eV}) \simeq 5\cdot 10^{-13}$, which is not in contradiction with data on cosmic ray electrons near the earth (for more details see [9]). On the other hand $N_e\ (E > 10^8\ \mathrm{eV}) \simeq 5\cdot 10^{-11}$, which in order of magnitude equals the concentration of all primary cosmic ray particles incident on the earth (due to high latitude cut-off $cp \geqslant 10^9$ eV). Taking into consideration the form of the function $Y(u)$, it may be shown that the spectrum (10) should refer to the region $2\cdot 10^8 < E < 3\cdot 10^9$; uncertainties in the data permit one to lower the value $N_e\ (E > 10^9\ \mathrm{eV})$ by several times.

Therefore, as the magnitude of the interstellar magnetic field ($\sim 10^{-5}$ oersted) required by the hypothesis of the magnetic bremsstrahlung agrees with other estimates of this quantity and this hypothesis also yields a reasonable value for the electron concentration, one may conclude that the magnetic bremsstrahlung explanation of the non-thermal general galactic radiation is probably correct. Moreover, this hypothesis automatically explains the fact that not more than 1% of the primary c.r. with $E \geqslant 10^9$ eV incident on the earth consists of electrons. The reason of this is that electrons lose energy in magnetic bremsstrahlung (which is negligible for protons and nuclei). If one

(*) More accurately $I_\nu = a\nu^{-\alpha}$, where $\alpha = 0.8 \div 1.2$.

also assumes (and this seems quite natural) that electrons, protons and nuclei in the energy region $E \lesssim 10^{11}$ eV are generated by the primary c.r. sources with a spectrum of the same type of (6), with $\gamma = \gamma_0 \simeq 2$, then, due to deceleration of the electrons in the magnetic field, the electron spectrum will have the same form as (6), but with $\gamma = \gamma_0 + 1 \simeq 3$ (see [1-3, 9]). According to (10) this is just the type of spectrum one would expect on the basis of radio astronomical data (*).

The proposed magnetic bremsstrahlung mechanism may also be responsible for radio emission from powerful discrete sources [7, 8]. As a matter of fact in such sources as α Cassiopeiae, α Cygni, α Tauri, $T_{\text{eff}} \gtrsim 10^7$ degrees, whereas the electron kinetic temperature is much smaller. It is impossible to explain the radiation from such galactic sources as α Cassiopeiae or α Tauri as originating from hypothetical radio stars; the magnetic bremsstrahlung hypothesis, on the other hand, does not require any impossible assumption about the magnetic fields or the electron concentration in the sources.

If the electron spectrum and the magnetic field in the source are independent of the coordinates, then the radiation flux from the source will be

$$F_\nu = \int I_\nu \, d\Omega = \frac{V}{4\pi R^2} \int P(\nu, E) N_e(E) \, dE \,, \tag{11}$$

where V is the volume of the source and R is the distance from it. Under the optimum conditions (4)

$$F_\nu = 1.6 \, \frac{e^3 H_\perp}{mc^2} \cdot \frac{N_e V}{4\pi R^2} = 1.7 \cdot 10^{-23} H_\perp \frac{N_e V}{R^2} \text{ erg/cm}^2 \text{ cycle}, \tag{12}$$

where N_e is the concentration of electrons; it is considered that these possess an energy corresponding to the frequency $\nu = \nu_{\max}$ (see (4)). For α Tauri: $R \sim 5 \cdot 10^{21}$ cm, $V \simeq (4\pi r^3/3) \sim 10^{56}$ cm^3, while in the meter band

$$F_\nu \cong 2 \cdot 10^{-20} \text{ erg/cm}^2 \text{ cycle}$$

and is independent on the frequency. Putting $H_\perp \sim H \sim 10^{-4}$ which seems to be allowed [12] we obtain from (12) $N_e V \sim 10^{50}$ and $N_e \sim 10^{-6}$ cm^{-3}; obviously, these values are the minimal ones. By using formulae (7) and (10) one can determine the electron spectrum, and the energy in discrete sources can

---

(*) Wandering of protons and nuclei in interstellar space should not change their spectrum and therefore, near the earth, $\gamma = \gamma_0 \simeq 2$, which is the experimentally observed value for $E \sim 10^9 \div 10^{11}$ eV.

be obtained. For α Tauri (Crab nebula) $\gamma \simeq 1$, $N_e V \sim 10^{51}$ for $E > 2.5 \cdot 10^8$ eV, and the total energy of relativistic electrons with $E > 2.5 \cdot 10^8$ is approximately $W \sim 10^{47} \div 10^{49}$ erg (see [12] for further details). Compared with other powerful sources the source in Taurus should be considered exceptional (*) because in the majority of powerful sources (mostly extragalactic) $\gamma \simeq 3$; for Cassiopeia one also has $N_e \sim 10^{51}$ and $W \sim 10^{48}$ erg. The Crab nebula (α Tauri) is undoubtedly an expanding envelope of the supernova of 1054 A.D. According to [14] all other powerful galactic discrete sources are also envelopes of supernovae (thus Cassiopeia is a supernova of 369 A.D.).

We thus arrive at the conclusion that the total energy of relativistic electrons in the envelopes of supernovae is of the same magnitude as the energy of the optical radiation produced during the outburst. The radiation of powerful extragalactic discrete sources, according to the mass of collected data, should also be attributed to magnetic bremsstrahlung [15]. Thus, radio astronomy presents the possibility of detecting relativistic electrons in various parts of the universe. In particular, it is found that large amounts of electrons exist in the envelopes of supernovae and, possibly, of novae [12, 16, 17]. It seems difficult to overestimate the significance of this circumstance for the theory of the origin of c.r.

3. – The Origin of Cosmic Rays.

Data on the distribution of relativistic electrons in the Galaxy speak against the theory of solar origin of c.r. and also against the hypothesis of their metagalactic origin. One must therefore conclude that the main part of c.r. is generated somewhere in our Galaxy; these rays fill the Galaxy and form a quasi spherical system (mentioned in § 1) with $R \lesssim 5 \cdot 10^{22}$ cm. It is furthermore natural to suppose that the primary c.r. sources are supernovae and novae [1-3; 12, 17] the envelopes of which contain fast electrons and probably protons and nuclei. As time passes (in about $1000 \div 3000$ years) the supernovae envelopes smear out and the c.r. which previously diffused from the envelope become completely distributed throughout interstellar space. Now the particles wander through interstellar magnetic fields, diffuse towards the periphery of the Galaxy and simultaneously lose energy in nuclear collisions and, later on, in ionization collisions. Instead of nuclear collisions, electrons undergo bremsstrahlung collisions with the nuclei and with the electrons of the interstellar gas.

(*) The large amount of high energy electrons in α Tauri makes it probable that the magnetic bremsstrahlung mechanism is also responsible for the continuous optical radiation of the nebula [13].

The electrons also lose energy in magnetic-bremsstrahlung processes discussed in § 1. For a number of reasons, the acceleration of c.r. particles in the interstellar space [18] does not seem to be an effective process and even at very high energies ($E \gtrsim 10^{13}$ eV/nucleon) it probably is of no significance (see [1]). This conclusion [2] is not affected by attempts, which seem very inconvincing to us, to retain the theory of interstellar acceleration by assuming that the life time of the particles in the Galaxy is determined by their rate of exit from it [19, 20]. On the other hand Fermi's statistical acceleration mechanism [18] should be very effective [21] in turbulent envelopes of supernovae, where it is probably the main acceleration mechanism. Such is the picture one can draw of the origin of c.r. using radio astronomy data. It is impossible for us in this paper to consider the theory in detail (see [1-3]) and we will therefore discuss some of the more important points of the problem.

A most important condition which any theory of origin of c.r. must satisfy follows from energy considerations. If the cross-section for energy transfers between protons colliding in interstellar space is $\sigma \simeq 2.5 \cdot 10^{-26}$ cm^2, then on the average the life time of fast protons in the Galaxy should be $T \sim 4.10^8$ years$\sim$ $\sim 10^{16}$ s (the concentration of interstellar hydrogen is taken to be on the average $n \sim 0.1$ cm^{-3}). The energy density of cosmic rays is $w \sim 1$ eV/cm^3, the total energy being $W \sim wV \sim 10^{68}$ eV, as the volume of the Galaxy $V \sim$ $\sim (4\pi/3)R^3 \sim 10^{68}$ cm^3 for $R \sim 3 \cdot 10^{22}$ cm. It is thus clear that the power of the sources of primary c.r. should be $W/T \sim 10^{52}$ eV/s $\simeq 10^{40}$ erg/s. This value is probably too high by one or two orders of magnitude, as most likely the accepted values of W and R are too high). Thus

$$W/T \sim 10^{38} \div 10^{40} \text{ erg/s} . \tag{13}$$

Assuming that during supernova outbursts, say, 10^{48} erg appear as c.r. (see above) one finds that average power of the source should be $\lesssim 10^{38}$ erg/s as on the average supernovae outbursts take place at least once in 300 years $\sim$ $\sim 10^{10}$ s. It is likely that supernovae outbursts occur much more often, but because of absorption they remain invisible (this argument belongs to I. S. Šklovskij). Furthermore, according to the estimates in [1, 2], the contribution from novae may reach $3 \cdot 10^{40}$ erg/s. Thus supernovae and novae can satisfactorily provide the energy balance. It should be noted that energy considerations suggesting supernovae as possible sources of c.r. were proposed previously [22]. However, these arguments acquire new significance when one associates them with radio astronomical data which confirm the generation of c.r. in the envelopes of supernovae. It should also be noted that on the average the power of the c.r. generated by the Sun is of $\sim 10^{21}$ erg/s and therefore even 10^{11} stars of the solar type would yield only 10^{32} erg/s, which is by 6-8 orders lower then the required value (see [13]).

It has already been mentioned that in envelopes of supernovae and novae the particles are mainly accelerated by a statistical mechanism. This mechanism is capable of accelerating protons and light nuclei (*) to the highest energies observed in cosmic rays, i.e. up to $E \sim 10^{18}$ eV [1, 21]. At the same time it should be emphasized that many details of the acceleration mechanism in expanding turbulent envelopes are still obscure. For this reason a reliable theoretical prediction of the spectrum of generated particles cannot be given; moreover for different sources the spectra are different (for details see [1]). The spectra of electrons, protons and nuclei generated in the envelopes are probably of the same form and on the average, for energies $E \lesssim 10^{11}$, $\gamma \simeq 2$. Magnetic bremsstrahlung losses in interstellar space result in a softening of the electron spectrum (and therefore $\gamma \simeq 3$; see above).

The proton and nuclear spectra will remain unchanged (even when nuclear collisions are taken into account) if the energy of the secondary products (i.e. energy after the collision)

$$E_2 = \delta E_1 , \tag{14}$$

where δ is independent or depends only slightly on the primary particle energy E_1. The explanation of this is that relation (14) is a scale transformation, and collisions of this type do not lead to changes in the power exponent in spectra of the type (6). There are data which support this point of view [2, 23]. Furthermore, according to the theory outlined here, one should expect that in a first approximation a stationary state should exist in the Galaxy, i.e. that the concentration of the various particles should be independent of time. On the other hand, the primary c.r. sources form a plane subsystem, lying in the plane of the Galaxy (this is exactly the way novae and probably supernovae are distributed). This leads us to the result that an approximate equilibrium number of Li, Be and B nuclei should be present in the c.r. incident on the earth; thus the concentration of these nuclei should be about four tenths the concentration of all other nuclei [3]. This is exactly the value which the latest available data yield [24]. Furthermore, according to our point of view, the high latitude cut-off in the c.r. spectrum cannot be explained by ionization losses and is probably due to the existence of a magnetic moment of the solar system[9]. This conclusion is in accord with data [25] indicating that the high-latitude cut off is of a magnetic nature.

Finally, special attention should be paid to secondary electrons and positrons produced in the Galaxy during nuclear collisions between cosmic protons and nuclei. Thus, basing on the data of [23], it should be expected that in

(*) In the simplest case of statistical acceleration a particle of energy Mc^2 acquires, when accelerated for a time t, energy $E = Mc^2 \exp[\varkappa t]$ that is, the energy is proportional to the rest mass.

each collision about 5% of the energy of the primary particles should be given to electrons and positrons [2, 3].

It can be shown [2] that in the absence of interstellar magnetic fields the amount of primary c.r. electrons and positrons with $E > 10^9$ eV should be comprised within $\sim 1 \div 5\%$, even if these particles were produced exclusively in nuclear collisions. This value becomes about 10 times smaller if magnetic bremsstrahlung energy losses are taken into account. However there are reasons to believe that electrons are also produced in the primary sources (see § 1), their number being larger than that of the secondary electrons. Similar considerations and also the computations carried out in § 1 indicate (if no other factors must be taken into account) that the number of primary c.r. electrons near the earth with $E \geqslant 10^9$ eV should be about $0.1 \div 0.5\%$ of the number of primary protons with $E \geqslant 10^9$ eV. Some of these electrons are secondary and can be separated from the primaries, as the number of secondary electrons and positrons should be about equal, while in supernovae envelopes one should expect that only electrons be accelerated. Accordingly, a study of the primary electron-positron component near the earth seems to be of special importance. Other possible means of checking the ideas outlined in this paper are discussed in [3]. Therefore, in conclusion we confine ourselves to the statement that, as the previous discussion seems to indicate, the present data and conceptions support the picture of the origin of c.r. proposed in this paper and, at any rate, do not contradict it.

REFERENCES

[1] V. L. Ginzburg: *Usp. Fiz. Nauk*, **51**, 343 (1953); *Fortschritte der Physik* (Berlin), **1**, 659, (1954).
[2] V. L. Ginzburg: *Dokl. Akad. Nauk SSSR*, **99**, 703 (1954).
[3] V. L. Ginzburg: *Proceedings of 5th Conference on Cosmogony* (Moscow, 1955).
[4] I. S. Šklovskij: *Astron. Žu. SSSR*, **29**, 418 (1952).
[5] S. B. Pikel'ner: *Dokl. Akad. Nauk SSSR*, **88**, 229 (1953).
[6] J. E. Baldwin: *Nature*, **174**, 320 (1954).
[7] H. Alfvén and N. Herlofson: *Phys. Rev.*, **78**, 616 (1950); K. O. Kiepenheuer: **79**, 738 (1950).
[8] V. L. Ginzburg: *Dokl. Akad. Nauk SSSR*, **76**, 377 (1951); G. G. Getmancev: *Dokl. Akad. Nauk SSSR*, **83**, 557 (1952).
[9] V. L. Ginzburg, G. G. Getmancev and M. I. Fradkin: *Proceedings of 3th Conference on Cosmogony*, p. 149 (Moscow, 1954).
[10] V. V. Vladimirskij: *Žu. Éksper. Teor. Fiz.*, **18**, 393 (1948).
[11] G. G. Getmancev and V. L. Ginzburg: *Dokl. Akad. Nauk SSSR*, **87**, 187 (1952).
[12] V. L. Ginzburg: *Dokl. Akad. Nauk SSSR*, **92**, 1133 (1953).
[13] I. S. Šklovskij: *Dokl. Akad. Nauk SSSR*, **90**, 983 (1953).
[14] I. S. Šklovskij: *Astron. Žu. SSSR*, **30**, 15 (1953).

[15] I. S. Šklovskij: *Dokl. Akad. Nauk SSSR*, **98**, 353 (1953).
[16] J. G. Bolton, G. J. Stanley and O. B. Slee: *Austral. J. of Phys.*, **7**, 110 (1954).
[17] I. S. Šklovskij: *Dokl. Akad. Nauk SSSR*, **91**, 475 (1953).
[18] E. Fermi: *Phys. Rev.*, **75**, 1169 (1949).
[19] E. Fermi: *Astrophys. Journ.*, **119**, 1 (1954).
[20] P. Morrison, S. Olbert and B. Rossi: *Phys. Rev.*, **94**, 440 (1954).
[21] V. L. Ginzburg: *Dokl. Akad. Nauk SSSR*, **92**, 727 (1953).
[22] D. ter Haar: *Rev. Mod. Phys.*, **22**, 119 (1950).
[23] S. N. Vernov, N. L. Grigorov, G. T. Zacepin and A. E. Čudakov: *Izv. Akad. Nauk SSSR, Ser. Fiz.*, **19**, 493 (1955).
[24] M. F. Kaplon, J. H. Noon and G. W. Racette: *Phys. Rev.*, **96**, 1408 (1954).
[25] R. A. Ellis, M. B. Gottlieb and J. A. Van Allen: *Phys. Rev.*, **95**, 147 (1954).

SUPPLEMENTO AL VOLUME III, SERIE X
DEL NUOVO CIMENTO

N. 1, 1956
1° Semestre

An Electron Recoil Study of the Gamma Spectra of ^{124}Sb, ^{59}Fe, ^{110}Ag, ^{64}Cu, ^{192}Ir, ^{140}La and ^{198}Au.

B. S. Dželepov and Ju. V. Hol'nov
Academy of Sciences of the USSR - Moscow

Contents. — **1.** Description of the apparatus and calculation of the spectral sensitivity. – **2.** γ-spectra of various radioactive substances, obtained in earlier experiments and in the recent ones.

1. – Description of the Apparatus and Calculation of the Spectral Sensivity.

In recent years the γ-ray spectra of various radioactive substances have been investigated by us; the apparatus (« ritron ») shown in Fig. 1 was used in the experiments.

A narrow beam of γ-rays selected by means of a long collimator 12 strikes a thin cellophane target 2 (diameter 220 mm, thickness 50 μ) and ejects Compton electrons.

The electrons are focused on a slit 4 (2 mm×32 mm) by means of a homogeneous magnetic field. A counter 6 with large cellophane covered windows (∼ 1 μ) is placed behind this slit. After passing through the counter the diverging electron beam is focused on a second slit 5 (2 mm×46 mm); a second counter 7 is located behind this slit. The dependence of the coincidence counting rate on the magnetic field was measured.

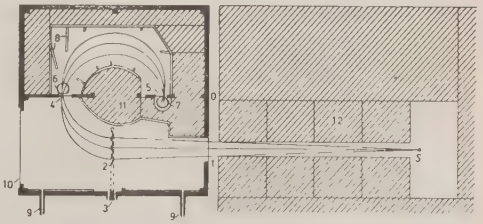

Fig. 1. – Ritron: schematic cross-section of the apparatus in a horizontal plane. *S*: γ-ray source. — 1. window; 2. target; 3. grounded joint; 4. and 5. main baffles (slits); 6 and 7. counters; 8. auxiliary baffles; 9. gas leads; 10. back wall of apparatus; 11. shields; 12. collimator.

Background measurements were carried out with the target removed.

The apparatus was filled with He (31 cm_{Hg}) and CH_4 (1.2 cm_{Hg}).

Each recorded γ-line formed a narrow peak. The shape of the lines can be deduced from the curves presented below; this is especially true for the ^{198}Au and ^{64}Cu spectra which possess well defined single lines.

The relative half-width of the lines depends on the energy (Fig. 2).

Energy calibration of the apparatus was carried out with γ-rays of accurately known energies (411.77 keV-^{198}Au, 510.98 keV-^{64}Cu, 1118 keV-^{65}Zn, 1171.5 and 1331.6 keV-^{60}Co, 2614.3 keV-ThC″, 2753.5 keV-^{24}Na).

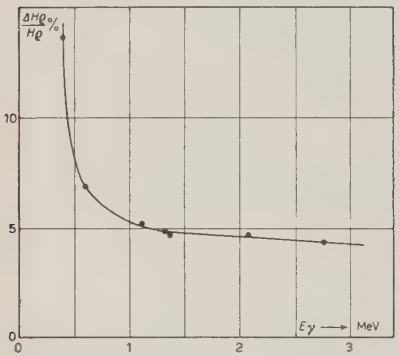

Fig. 2. – Dependence of $\Delta H\varrho/H\varrho$ of lines on γ-ray energy in 1955 experiments; $\Delta H\varrho$ being the lines half-width.

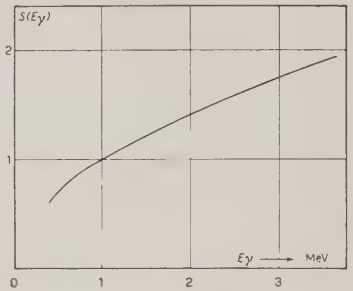

Fig. 3. – Calculated curve of the ritron spectral sensitivity for the Compton cut-off angle $\theta = 20°$.

Energies of the other γ-lines were determined with an accuracy of 1%.

In order to pass from the areas of the experimental peaks to relative γ-line intensities a knowledge of the spectral sensitivity of the apparatus was required. This was calculated and checked with the ^{24}Na lines (1.38 and 2.76 MeV). The following factors were taken into account in the computations: *a*) arrangement and dimensions of the target and slits, *b*) energy and angular distributions of the recoil electrons, *c*) multiple scattering of recoil electrons within the target, *d*) ionization energy losses.

The shapes of the lines for various $h\nu$ were calculated. The widths of the lines thus obtained were found to be smaller than the experimental values. Thus, for $h\nu = 2m_0c^2$ the calculated relative half-width was 3.2%, the experimental $\sim 5\%$. As the factors responsible for additional broadening of the lines have not been established, it was assumed that this broadening is not accompanied by a change of area.

On this assumption and also on the condition that a cut-off Compton angle of $\theta = 20°$ is applied for both the theoretical and experimental lines (a condition necessary for the application of Willams' theory of multiple scattering)

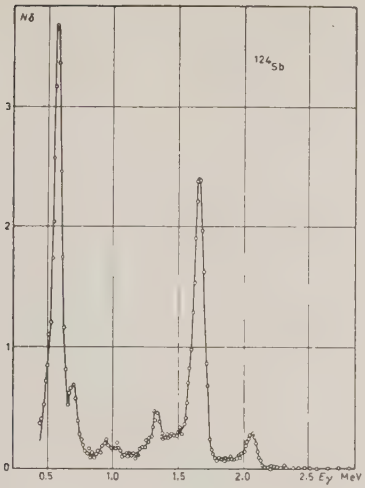

Fig. 4. – ^{124}Sb γ-spectrum.

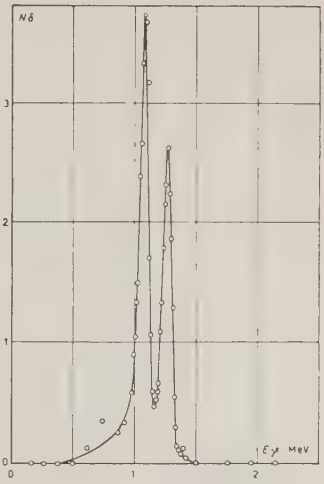

Fig. 5. – ^{59}Fe γ-spectrum.

one obtains a spectral sensitivity curve of the type shown in Fig. 3. The relative intensities of γ-lines could be obtained by dividing the area of the experimental peaks (after separation of the curves and cut-off at $\theta = 20°$) by the corresponding ordinates of Fig. 3. The ^{24}Na points used to check the results fall on the curve in a satisfactory manner.

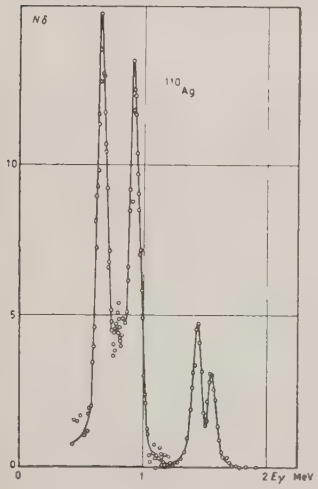

Fig. 6. – ^{110}Ag γ-spectrum.

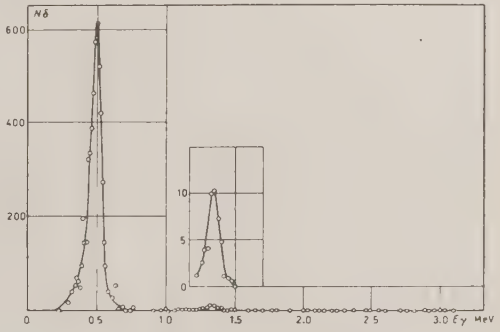

Fig. 7. – ^{64}Cu γ-spectrum.

It should be noted that the spectral sensitivity increases with the γ-ray energy.

Corrections for absorption of γ-rays in the sample and dependence of the

counter efficiency on electron energy have been included in the final results. If the assumption made above is correct, then for sufficiently resolved and intensive lines the uncertainties in our experimental value of the relative intensities should not exceed 3-5%.

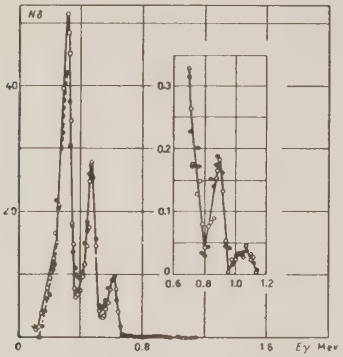

Fig. 8. – ^{192}Ir γ-spectrum. White points: spectrum obtained at gas pressure of 16 cm Hg gas in the apparatus; black points: 32 cm Hg. Gas pressure was varied in order to exclude Compton electron scattering effects.

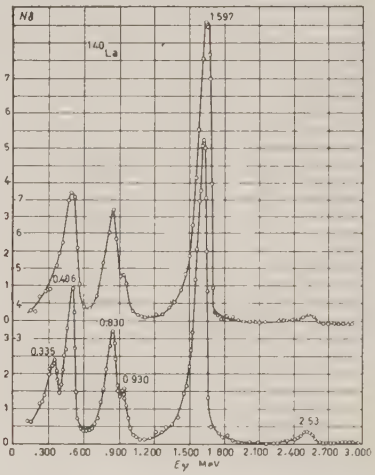

Fig. 9. – ^{140}La γ-spectrum. Upper curve: 1950-1952 experiments, lower curve: 1953 experiments (counter windows covered with thin ~ 1 μm cellophane).

2. – Spectra of various Radioactive Substances, obtained in Earlier Experiments and in the Recent Ones.

The γ-spectra of ^{124}Sb, ^{59}Fe, ^{110}Ag, ^{64}Cu, ^{192}Ir, ^{140}La and ^{198}Au are presented in Fig. 4-10.

The first four curves were obtained with the apparatus used in 1950-1952, the remaining curves with the modified apparatus used in 1953-1954 (17 μm cellophane windows were replaced by 1 μm windows and the construction of the baffles was somewhat changed). Fig. 2 and 3 correspond to the condition described above. The relative line intensities are given in Table I. More detailed information on the γ-spectra mentioned above may be found in papers [1-5]. A more precise evaluation of the spectral sensitivity of the apparatus explains the small discrepancy between the relative intensities obtained in the present investigation and

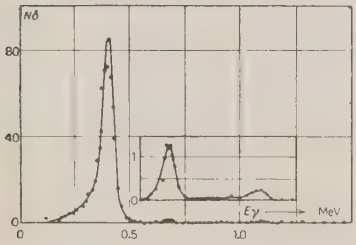

Fig. 10. – ^{198}Au γ-spectrum.

those of earlier studies. The γ-spectra of ^{60}Co, ^{134}Cs and ^{82}Br were also investigated with the 1951-1952 apparatus. The results are presented in papers [6-8].

TABLE I. – *Relative γ-line intensities.*

hν (MeV)	Relative intensity	*hν* (MeV)	Relative intensity
	^{124}Sb		^{192}Ir
0.603 + 0.650	127	0.296 + 0.308 + 0.316	445
0.714	25.9	0.4675	256
0.958 (*)	6.4	0.589 + 0.605 + 0.613	100
1.052 (*)	4.0	0.880	2.07
1.347 (*)	14.7	1.053 (*)	0.58
1.708	100		
2.062	13.0		^{140}La
	^{59}Fe	0.3286	15.9
1.100 (*)	100	0.4864	37
1.278 (*)	77	0.8156	35
		0.926	11.4
		1.597	100
		2.535 (*)	5.9
	^{110}Ag		^{198}Au
600 ÷ 750	100		
850 ÷ 1 000	87	0.41177	100
1,386	22.5	0.6765	1.11
1.480 + 1.506	14.6	1.0889	0.28
	^{64}Cu		^{24}Na
0.51098	100	1,3679	100
1.346	2.07	2.7535	102

(*) γ-ray energy determined in present investigation. The remaining γ-line energies are the most reliable of the published values; our values agree with them to within 1 %.

REFERENCES

[1] B. S. DŽLEPOV, N. N. ŽUKOVSKIJ and JU. V. HOL'NOV: *Izv. Akad. Nauk SSSR, Ser. Fiz.*, **18**, 599 (1954).

[2] K. JA. GROMOV, B. D. DŽELEPOV, N. N. ŽUKOVSKIJ, A. V. SILANT'EV and JU. V. HOL'NOV: *Dokl. Akad. Nauk SSSR*, **86**, 255 (1952).

[3] B. S. DŽELEPOV, N. N. ŽUKOVSKIJ and JU. V. HOL'NOV: *Dokl. Akad. Nauk SSSR*, **86**, 497 (1942).

[4] B. S. DŽELEPOV, N. N. ŽUKOVSKIJ and JU. V. HOL'NOV: *Dokl. Akad. Nauk SSSR*, **77**, 597 (1951).

[5] B. S. DŽELEPOV, N. N. ŽUKOVSKIJ, V. P. PRIHODCEVA and JU. V. HOL'NOV: *Izv. Akad. Nauk SSSR, Ser. Fiz.*, **17**, 511 (1953).

[6] B. S. DŽELEPOV, N. N. ŽUKOVSKIJ and JU. V. HOL'NOV: *Dokl. Akad. Nauk SSSR*, **77**, 233 (1951).

[7] K. JA. GROMOV and B. S. DŽELEPOV: *Dokl. Akad. Nauk SSSR*, **85**, 299 (1952).

[8] B. S. DŽELEPOV and A. V. SILANT'EV: *Dokl. Akad. Nauk SSSR*, **85**, 533 (1952).

SUPPLEMENTO AL VOLUME III, SERIE X
DEL NUOVO CIMENTO

N. 1, 1956
1° Semestre

The RaC γ-Ray Spectrum.

B. S. Dželepov and S. A. Šestopalova

Academy of Sciences of the USSR - Moscow

Contents. — **1.** Modifications made to the spectrometer (ritron), described in the preceding paper in order to reduce the half-width of the lines and to permit the separation of the spectrum into its components. – **2.** Description of the characteristics of the new spectrometer (elotron). – **3.** Experimental curve obtained for the RaC γ-spectrum and corrections brought to it. – **4.** Conclusions and discussion about a possible $0 \rightarrow 0$ transition existing at 1415.9 keV.

1. – Modifications Made to the Spectrometer (Ritron), Described in the Preceding Paper in Order to Reduce the Half-Width of the Lines and to Permit the Separation of the Spectrum into its Components.

By means of the γ-spectrometer (« ritron ») described in the preceding paper, spectral lines of relative half-width of about 5% can be obtained near $h\nu = 1$ MeV. If in the spectrum there is abundance of γ-rays this half-width may be not sufficient to permit separation of the observed spectrum into its components. We have consequently attempted to design a spectrometer in which the relative half-width of the lines would be still smaller [1].

In order to reduce the width of the lines it was necessary to improve the focusing properties of the instrument compared with those of the « ritron ». With this aim in mind two improvements were incorporated:

1) The plane target was substituted by a bent target; in this manner recoil electrons ejected in the forward direction from various points in the target could be focused on a line (first slit). The equation of the corresponding surface of the bent target may be found in [2].

2) In the second part of the instrument (located behind the first slit) the variation of magnetic field with rectangular coordinates was the same as

in spectrometers of the « ketron » type [3]. In this manner it was possible to obtain fine focusing of a plane recoil electron beam moving in the plane of symmetry of the instrument.

2. – Description of the Characteristics of the New Spectrometer (Electron).

The apparatus in which these improvements have been incorporated (« elotron ») is shown in Fig. 1. « A » designates the bent target; above line BB the magnetic field is homogeneous; below this line it decreases according to a law deduced by PAVINSKIJ [4]. The ^{60}Co γ-spectrum was measured with this instrument in 1953. A cellophane target of 5 μ thickness, slits of (2×11) and (2×15) mm² were used; helium pressure in the apparatus was 120 mm_{Hg}.

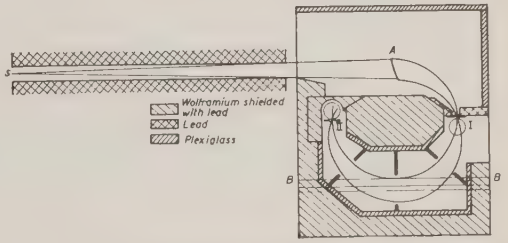

Fig. 1. – Schematic cross-section of the apparatus (« elotron ») in a horizontal plane.

Under these conditions a relative half-width of the order of 1.8-2.0% was attained. However the relative aperture of the apparatus was very small. After testing the apparatus we proceeded to select the most favourable conditions for the investigation of the RaC γ-spectrum.

In order to measure the weak RaC γ-lines the target thickness was increased to 35 μ. The relative half width of the lines in the neighborhood of 1 MeV rose to 2.7%. The counters used in the experiment were filled with a mixture of He (165 mm_{Hg}) + CH_4 (5 mm_{Hg}). The remaining conditions were as those previously described. The Ra source consisted of 4 grams of $RaBr_2$.

3. – Experimental Curve Obtained for the RaC γ-Spectrum and Corrections Brought to it.

The experimental curve thus obtained is shown in Fig. 2 (black circles). E_γ is plotted along the axis of abscissae. This quantity is computed from the formula

$$E_\gamma = \frac{1}{2} m_0 c^2 (E_\beta + \sqrt{E_\beta^2 + 2E_\beta}) ; \qquad E_\beta = \sqrt{1 + \left(\frac{e}{m_0 c^2}\right)^2 \cdot (H\varrho)^2} - 1 ,$$

where H is the measured field strength and ϱ the radius of curvature of the

circular trajectory in the apparatus ($\varrho = 65$ mm); the coincidence counting rate in relative units is plotted along the ordinates axis. Partially blackened circles refer to the background, i.e. to the coincidence counting rate with the target removed from the beam.

The experimental curve in Fig. 2 was subjected to further treatment, namely: 1) the background was subtracted; 2) a correction was included to account for the dependence of the counter efficiencies on the electron energy [5] (under our conditions the variation of the electron energy between 600 keV and 2200 keV caused an efficiency variation of about 7 %); 3) the results were reduced to equal $H\varrho$ intervals; 4) the curve was separated into components of standard form and the area of each of these components was then determined; 5) the area of each component was multiplied by a coefficient (depending on the absorption of the given γ-line in the target and counter wall) and divided by the spectral sensitivity of the apparatus, a quantity that was taken from paper [6]. The quantities thus obtained were accepted as yielding the relative intensities of the lines. A calibration curve was used to change the abscissae

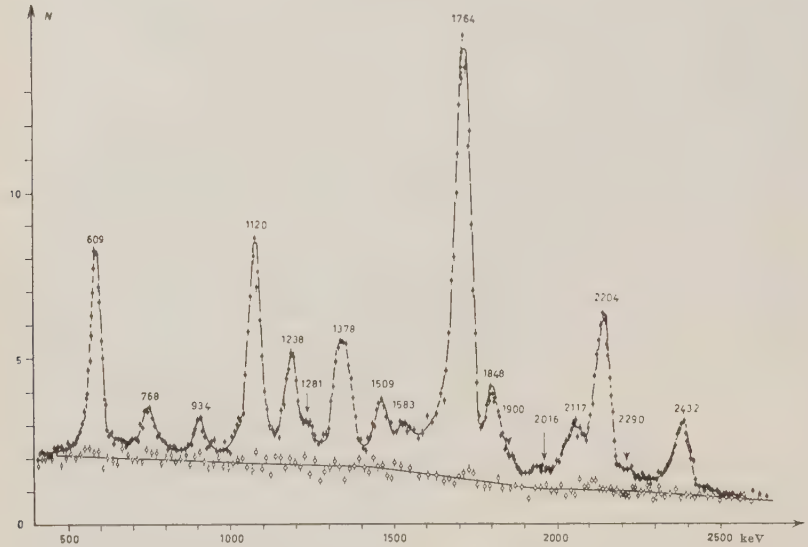

Fig. 2. – Experimental RaC γ-ray spectrum.

values E_γ into E_{tr}. γ-lines from ^{137}Cs, ^{60}Co, ^{65}Zn and line 2204.25 keV from RaC were used in the calibration. The difference between E_γ and E_{tr} did not exceed 3.8 %. No correction to account for dE_γ/dE_{tr} was included in the relative intensity as the magnitude of dE_γ/dE_{tr} is very small.

The following remarks concerning points 4 and 5 should be made. A knowledge of the form of the spectral line at various energies is necessary if one wishes to separate the spectrum into its components. Single γ-lines from ^{137}Cs ($h\nu$=661.6 keV) and ^{65}Zn ($h\nu$=1120 keV) were measured under the conditions described above. The results are shown in Fig. 3 and 4. Relative half-widths of the following γ-lines were also determined: 606 keV-^{124}Sb, 1367.9 keV-^{24}Na, 1700 keV-^{124}Sb, 2432 keV-RaC, 2614.3 keV-ThC″ and 2753.5 keV-^{24}Na.

4. – Conclusions and Discussion About a Possible $0 \rightarrow 0$ Transition Existing at 1415.9 keV.

An examination of the data enables one to draw the following conclusions: *a*) the relative half-width of the spectral lines is a smooth function of energy (Fig. 5); *b*) if the lines 661.6 keV, 1120 keV, 1700 keV and 2432 keV are reduced to the same half width, their form will be found to be very similar and only the rise at low energies differs. Using points *a*) and *b*) and linearly extrapolating the low energy ascent, the shape of spectral lines of any energy can be determined.

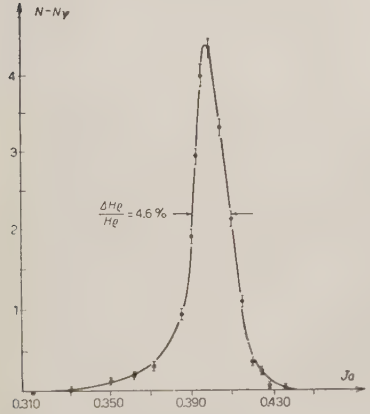

Fig. 3. – ^{137}Cs line; $h\nu$=661.6 keV.

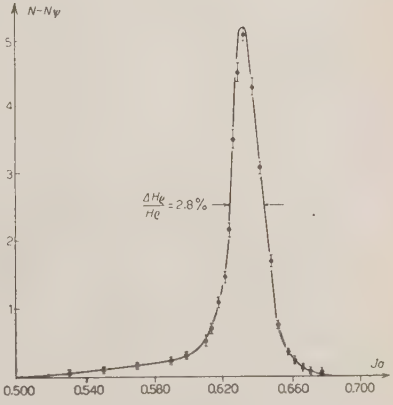

Fig. 4. – ^{65}Zn line; $h\nu$=1120 keV.

The spectral sensitivity of the apparatus was determined by DŽELEPOV, ŽUKOVSKIJ and NEDOVESOV. These authors compared the γ-spectrum of ^{152,154}Eu in elotron and ritron and found that the spectral sensitivities of both instruments are the same.

Relative intensities of RaC γ-lines after inclusion of corrections are shown in Fig. 6 and presented in Table I.

It is possible that, after further investigation of the shape of single lines and of the spectral sensitivity of the apparatus, some refinements in the data of the relative intensities of RaC-lines will be introduced.

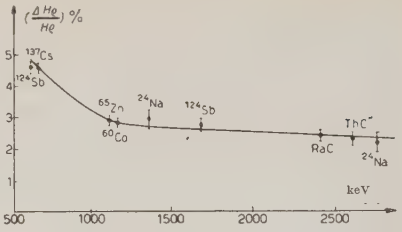

Fig. 5. – Dependence of the half-width of the lines on γ-ray energy.

The interval between $h\nu = 1350$ keV and 1450 keV deserves special attention as a $0 \rightarrow 0$ transition exists at 1 415.9 keV. The observed relative half-width of line 1378 keV is almost twice the value one would expect from the plot in Fig. 5. As MLADJENOVIČ and HEDGRAN [7] have previously remarked, the line is undoubtedly complex. In MLADJENOVIČ and SLÄTIS's [9] table for Ra(B+C) conversion electrons, among the unidentified lines are lines N 112, 113, 114, 115, 116 and 118; if one assumes that conversion K electrons from RaC are involved, then the energy of the lines would be 1385.3, 1391.9, 1396.5, 1401.7, 1408.0 and 1438.0 keV. It is possible that just these lines and also the line $h\nu = 1378.2$ keV are responsible for the broad maximum in the region of 1350÷1450 keV.

Our measurements indicate that the yield of γ-quanta with energy

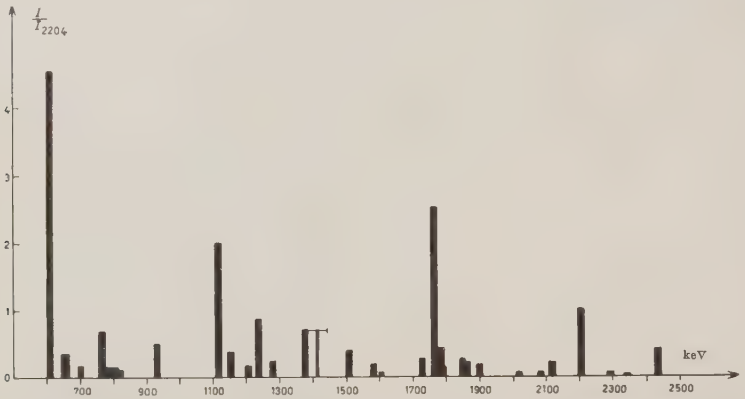

Fig. 6. – Relative γ-ray intensities in RaC spectrum. The intensity conventionally designated 1400 keV refers to the energy interval 1385÷1438 keV. A horizontal short line is used to indicate this.

1415.9 keV does not exceed 0.03 quantum per disintegration. According to KONSTANTINOV and LATYŠEV [10], the number of conversion electrons per

TABLE I. – *Energy and relative intensities of the* RaC γ-*lines.*

No.	E_γ, in keV	Relative intensity		
		Our data	MLADJENOVIČ and HEDGRAN [7]	LATYŠEV [8]
1	2	3	4	5
1	609.3	4.64	5.13	
2	652.4	0.38		
3	660.9			
4	703.2	0.19		
5	768.7	0.70	1.11	
6	787.1	0.17		
7	806.3	0.17		
8	821.3	0.13		
9	934.8	0.52	0.54	
10	1 120.4	2.06	3.9	1.76
11	1 155.3	0.40		
12	1 207.1	0.19		
13	1 238.3	0.88	1.42	0.41
14	1 281.3	0.26		
15	1 378.2	0.72	1.66	1.32
16	1 385.3	0.73		
17	1 391.1			
18	1 396.5			
19	1 401.7			
20	1 408.0			
21	1 438.0			
22	1 509.3	0.43	0.56	0.56
23	1 582.9	0.21		
24	1 605.2	0.07		
25	1 728.3	0.29		
26	1 764.4	2.52	3.14	2.51
27	1 783.8	0.44		
28	1 790.7	0.14		
29	1 848.5	0.28	0.33	0.32
30	1 862.3	0.22		
31	1 900	0.19		
32	2 016.7	0.06		
33	2 085	0.09		
34	2 117.0	0.23		
35	2 204.2	1	1	1
36	2 290	0.07		
37	2 340	0.04		
38	2 432	0.41	0.36	0.34

Note. – The energy values corresponding to numbers 1, 5, 9, 10, 11, 13, 14, 15, 22, 25, 26, 29, 32, 34, 35 in the table are taken from a paper by MLADJENOVIČ and SLÄTIS [9] who measured conversion electrons of the respective γ-lines. Several lines not identified by these authors have been indentified by us. They were listed under numbers 81, 82, 88, 90, 91, 92, 93, 102, 112-116, 118, 123, 124, 126, 127, 128, 132, 133 and 137 and in our table correspond to numbers 2, 3, 4, 6, 7, 8, 12, 16-21, 23, 24, 27, 28, 30. The energies of γ-lines N. 31, 33, 36 and 37 have been determined by us.

disintegration due to this line is $p\alpha = 3.5 \cdot 10^{-3}$. With our γ-ray intensity $p < 0.03$ per disintegration, this leads to a K-shell conversion coefficient which exceeds 0.12. A conversion coefficient of such magnitude can originate only if a multipole of high order is involved, e.g. E 8 or M 6. However in this case RaC with an excitation energy of 1 415.9 keV would be very long-lived.

Moreover, for such multipoles the ratio $\alpha k/\alpha(L_1+L_2)$ would be much smaller than 4.2, while experimentally a ratio of 5.3 is observed; finally it has been established in [11] that the lower limit of the ratio L_1/L_2 excludes all electric multipoles above E 4 and the lower limit of L_1/L_3 all magnetic multipoles above M 4.

This confirms the assumption, suggested firstly by FOWLER, that the $E = 1\,415.9$ keV transition is a $0 \rightarrow 0$ transition.

REFERENCES

[1] B. S. DŽELEPOV, N. N. ŽUKOVSKIJ, A. S. KARAMJAN and S. A. ŠESTOPALOVA: *Izv. Akad. Nauk SSSR, Ser. Fiz.*, **17**, 518 (1953).
[2] B. S. DŽELEPOV: *Dokl. Akad. Nauk SSSR*, **77**, 389 (1951).
[3] B. S. DŽELEPOV and A. A. BAŠILOV: *Izv. Akad. Nauk SSSR, Ser. Fiz.*, **14**, 263 (1950).
[4] P. P. PAVINSKIJ: *Izv. Akad. Nauk SSSR, Ser. Fiz.*, **18**, 175 (1954).
[5] G. CLURE: *Phys. Rev.*, **90**, 796 (1953).
[6] B. S. DŽELEPOV, N. N. ŽUKOVSKIJ and JU. V. HOL'NOV: *Izv. Akad. Nauk SSSR, Ser. Fiz.*, **18**, 599 (1954).
[7] M. MLADJENOVIČ and A. HEDGRAN: *Ark. f. Fys.*, **8**, 49 (1954).
[8] G. D. LATYŠEV: *Žu. Éksper. Teor. Fiz.*, **14**, 65 (1944).
[9] M. MLADJENOVIČ and A. SLÄTIS: *Ark. f. Fys.*, **8**, 65 (1954).
[10] G. LATYŠEV: *Rev. Mod. Phys.*, **19**, 132 (1947).
[11] D. ALBURGER and A. HEDGRAN: *Ark. f. Fys.*, **7**, 423 (1954).

SUPPLEMENTO AL VOLUME III, SERIE X
DEL NUOVO CIMENTO

N. 1, 1956
I° Semestre

Experimental Investigation of Neutron-Nucleon and Neutron-Deuteron Interaction in the Energy Region 380-590 MeV (*).

V. P. Dželepov, Ju. M. Kazarinov, B. M. Golovin,
V. B. Fljagin and V. I. Satarov

Institute of Nuclear Problems of the Academy of Sciences of the USSR - Moscow

Contents. — **1.** The neutron beam. – **2.** A general description of equipment and measurements methods. – **3.** Elastic neutron-proton scattering at 380 MeV. – **4.** Determination of the total cross sections for neutron-proton and neutron-deuteron interaction at 380, 500 and 590 MeV. – **5.** Discussion of results of the neutron-proton scattering experiments. – **6.** Exchange scattering of 380 MeV neutrons on deuterons. – **7.** Elastic neutron-neutron scattering at 300 MeV. – **8.** conclusion.

Introduction.

Experimental data on the scattering of identical nucleons permits one to obtain data on the nuclear interaction of particles in antisymmetric states. The interaction properties of high-energy nucleons in symmetric states may be studied only by observing neutron-proton scattering.

The present paper is devoted to a description of the main part of the investigations conducted by the authors in 1950-1952, on the synchrocyclotron of the Institute of Nuclear Problems of the Academy of Sciences of the USSR, with neutrons having a mean energy of 380 MeV.

The investigations cover the study of elastic neutron-proton and neutron-deuteron scattering, as well as the experimental study of exchange neutron-deuteron scattering conducted with the purpose of ascertaining the dependence of exchange forces on the spin [1-5].

(*) Reported at a session of the Academy of Sciences of the USSR, December 17, 1954.

A part of the data obtained by the authors in 1954 in experiments with neutrons having a mean energy of 500 and 590 MeV [6-8] is also discussed in the paper.

1. – The Neutron Beam.

High-energy neutrons were obtained as a result of exchange interaction between protons, accelerated in the synchrocyclotron, and neutrons of the beryllium target nuclei. For this purpose, a beryllium target of 2.5 or 5 cm thickness was introduced into the vacuum chamber of the accelerator and bombarded by protons with an energy $E_p = 480$ MeV or 680 MeV. A neutron beam of 2 or 5 cm diameter was selected from the high-energy neutron beam by a brass collimator placed in the concrete shield wall (see Fig. 1, where the general scheme of the experiments is given). Angular divergence of the neutrons in the beam did not exceed 0.3°.

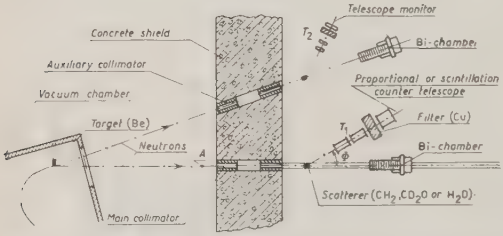

Fig. 1. – The general scheme of the experiments.

All experiments described here were carried out with non-polarized neutron beams. The intensity of the neutron beam for energies above 300 MeV was approximately $2 \cdot 10^4$ neutrons/cm² s at the site of the experimental arrangement.

The energy distribution of the neutrons in the beam was determined from

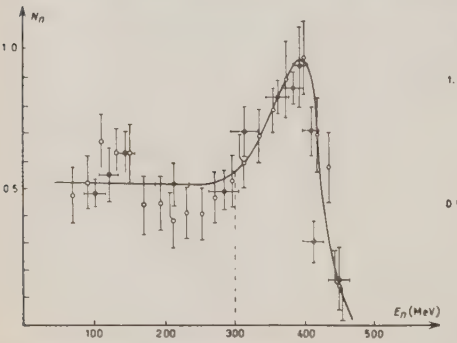

Fig. 2*a*. – Energy distribution of neutrons: $E = 480$ MeV. ○ first method.

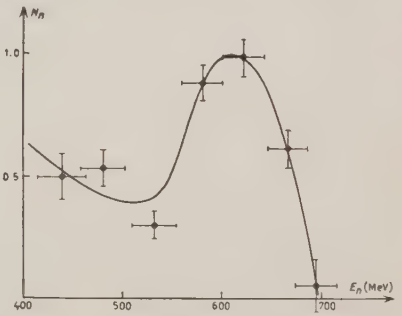

Fig. 2*b*. – Energy distribution of neutrons: $E_p = 680$ MeV. ● second method.

the energy spectrum of recoil protons from n-p collisions measured by two independent methods [3] at a recoil angle 20°. In one series of experiments the unknown neutron spectrum was determined from the curve of ionization losses of recoil protons in copper; in another series, the number of recoil protons was successively measured over the spectrum in energy intervals from E_p to $E_p+\Delta E_p$. Both types of experiments produced results that satisfactorily agree with each other. The energy distributions of neutrons in the beam, found for two energies of the primary protons 480 MeV and 680 MeV, are given in Fig. 2*a* and 2*b*. The circles indicate the results of spectrum measurements with the aid of the absorption curve. Data obtained by the differential method are denoted by points.

2. – A General Description of Equipment and Measurement Methods.

The basic measurement method used in the experiments described below was the method of counting recoil protons from n-p collisions in hydrogeneous scatterers placed in the collimated neutron beams.

The chief difference between the various experiments was the use of different recoil proton detectors. In those experiments, in which the elastic n-p scattering cross-sections and the neutron spectrum (represented in Fig. 2*a*) were measured, the recoil protons were counted by telescopes, each of which consisted of three proportional counters connected in coincidence. The counters were filled with 90% argon and 10% carbon dioxide at a total pressure of 760 mm_{Hg}. The operating voltage was $2000 \div 2500$ V. The resolving time of the proportional counter coincidence circuit was $4 \cdot 10^{-7}$ s. Under conditions of pulse operation of the accelerator this resolution was quite sufficient.

The use of proportional counters in such experiments was convenient also because the telescope could very easily be converted into a differential detector, necessary for neutron spectrum measurements. This was achieved by reducing the potential on the last counter. The gas amplification in the counter was reduced and only counter pulses produced by protons with an energy of 20-30 MeV could trigger the electronic circuit. Preliminary reduction of the energy of the recoil protons to the required value was done with the aid of filters placed beween the counters.

For experimental determination of the differential cross-section for exchange n-d scattering and of the cross-sections for neutron-neutron scattering, recoil proton detectors of higher resolving power were required. Scintillation counter telescopes connected in coincidence were therefore also used in the experiments. Photomultipliers of the FEU-19 type, and naphthalene crystals with a 2% admixture of anthracene (1952 experiments) or tolane crystals (1954) were employed in the telescopes. The resolving time of the coincidence

circuit for telescopes of this type was $5 \cdot 10^{-8}$ s. The plateau of the telescopes under typical conditions was 200 V wide and was carefully controlled before each series of experiments. Scintillation counter telescopes were also used by the authors to determine the neutron spectrum (shown in Fig. 2*b*) and to measure the total n-p and n-d interaction cross-sections.

In order to investigate only high-energy neutron scattering and to exclude the possibility that the telescope could record recoil protons produced by neutrons of lower energy, the energy sensitivity threshold of the measuring telescope T_1 (see Fig. 1) was artificially raised. This was achieved by placing copper or tungsten filters between the 2nd and 3rd counters; the thickness of the filter was varied with the proton scattering angle in such a way that only recoil protons produced by neutrons with an energy above a given value, passed through the filters. The diameter of the last telescope counter was always considerably larger than that of the first two (in the case of the proportional counters, for example, the first two counters had a diameter of 2 cm, and the last a diameter of 4 cm). This was done to reduce to a minimum the losses in proton counting due to multiple Coulomb or diffraction scattering in the filters. Under the conditions of the experiments, these losses did not exceed 5-10 %.

The neutron beam intensity was monitored during the experiments by a similar telescope T_2 and by a multilayer fission ionization chamber with electrodes coated with bismuth. These instruments were usually placed in a neutron beam, selected by an auxiliary collimator.

3. Elastic Neutron-Proton Scattering at 380 MeV [1, 2].

In order to determine the relative angular differential cross-sections of neutrons of a given energy scattered by protons, measurements were made on the angular distribution of recoil protons ejected from the hydrogeneous scatterer by neutrons, i.e. the function $N_p(\Phi) = k\sigma_{np}(\Phi)$ was measured; here Φ is the angle of emission of the recoil proton from the scatterer in the laboratory system (see Fig. 1), $\sigma_{np}(\Phi)$ is the unknown n-p scattering cross-section and k is a constant.

Chemically pure paraffin ($CH_{2.08}$) and graphite (C) disks with equal proton stopping powers were used as neutron scatterers. The effect of neutron scattering by free protons was determined by taking the difference of the effects observed in these two scatterers, account being made for the difference in the number of the carbon atoms contained in each of them. In the measurements carried out in the angle range $0^\circ \leqslant \Phi \leqslant 50^\circ$ the thickness of the paraffin scatterers was 3 g/cm²; for $50^\circ \leqslant \Phi \leqslant 70^\circ$ it was 1.5 g/cm². The mean energy losses of the protons in the scatterers for these two angle ranges respectively varied from $4 \div 8$ MeV to $5 \div 10$ MeV. The curve $N_p(\Phi)$ was determined in the recoil angle range from 0° to 70° with an angular resolution of $2.5^\circ \div 3^\circ$.

SOCIETÀ ITALIANA DI FISICA

SCUOLA INTERNAZIONALE DI FISICA

Sotto gli auspici del Ministero della Pubblica Istruzione
e del Consiglio Nazionale delle Ricerche

4° Corso estivo a Varenna, sul Lago di Como

15 Luglio - 4 Agosto 1956

1. Quest'anno 1956, col contributo del Ministero della Pubblica Istruzione, del Consiglio Nazionale delle Ricerche, del Comitato Nazionale per le Ricerche Nucleari, dell'Università di Milano, delle Autorità, di Enti, Società e privati della Provincia di Como, la Scuola terrà a Varenna, nella Villa Monastero, messa gentilmente a disposizione dall'Ente Villa Monastero, il *4° Corso estivo*.
   Il Corso sarà dedicato alle *proprietà magnetiche della materia*. In particolare verranno organicamente trattati i seguenti argomenti:
   — *Paramagnetismo nei cristalli*;
   — *Rilassamento paramagnetico*;
   — *Ferromagnetismo, ferrimagnetismo, antiferromagnetismo*;
   — *Risonanza paramagnetica, ferromagnetica, antiferromagnetica e diamagnetica*;
   — *Risonanza magnetica nucleare nei liquidi e nei cristalli*;
   — *Larghezza della riga nella risonanza magnetica*;
   — *Il concetto di temperatura nei fenomeni magnetici*;
   — *Magnetismo a basse temperature, polarizzazione nucleare*;
   — *Proprietà magnetiche dei superconduttori.*
   Le lezioni verranno affidate ai seguenti professori:
   C. J. Gorter, Kamerlingh Onnes Laboratorium der Rijksuniversiteit, Leiden.
   C. Kittel, University of California, Berkeley, California (U.S.A.).
   N. Kurti, Clarendon Laboratory, Oxford.
   L. Néel, Laboratoire d'Électrostatique et de Physique du Métal, Grenoble.
   M. H. L. Pryce, H. H. Wills Physical Laboratory, Bristol.
   E. M. Purcell, Harvard University, Cambridge, Massachusetts (U.S.A.).
   J. H. Van Vleck, Harvard University, Cambridge, Massachusetts (U.S.A.).
   Altri specialisti terranno seminari e conferenze su argomenti connessi con quelli che sono l'oggetto del Corso.
   Le lezioni, i seminari, le conferenze e le discussioni saranno generalmente tenute in inglese o in francese.
2. L'organizzazione e la Direzione del Corso sono affidate al prof. Luigi Giulotto, professore di Fisica Superiore all'Università di Pavia.
3. La durata del Corso sarà di 21 giorni. L'inaugurazione avrà luogo Domenica 15 Luglio alle ore 18 e la chiusura nel pomeriggio di Sabato 4 Agosto.
4. Il numero totale degli allievi sarà di 35.
   Chi desidera partecipare al Corso dovrà inviare entro il 31 Maggio 1956 la domanda al

Prof. LUIGI GIULOTTO
Istituto di Fisica dell'Università
PAVIA (Italia)

fornendo, ben chiaramente, le seguenti indicazioni:

a) Nome e Cognome.
b) Data e luogo di nascita.
c) Indirizzo attuale.
d) Titoli di studio universitari ottenuti e presso quale Università.
e) Professione attuale.
f) Elenco delle pubblicazioni di Fisica.
g) Quale conoscenza orale e scritta ha dell'inglese e del francese.
h) Se verrà a Varenna da solo o accompagnato da familiari e, nel caso che venga da solo, se è disposto a prendere alloggio in camera in comune con altro allievo.

Inoltre, il richiedente deve allegare alla domanda una lettera di presentazione, rilasciata da un professore universitario di Fisica, il quale assicuri che il richiedente ha interesse per i suoi studi a frequentare il Corso e che possiede già adeguata preparazione.

L'accettazione delle domande è decisa dalla Presidenza della Società unitamente alla Direzione del Corso, tenendo conto dei documenti presentati dai singoli richiedenti e di una equa ripartizione dei posti tra le varie nazioni cui questi appartengono.

Le comunicazioni delle deliberazioni saranno inviate agli interessati entro il 10 Giugno 1956.

5. Gli allievi saranno alloggiati o nella foresteria della Villa Monastero o in alberghi di Varenna, vicino alla Villa, in camere da 1 o 2 letti. Nella stessa Villa o in un albergo di Varenna sarà organizzata la mensa della Scuola.

6. Grazie alle sovvenzioni di cui la Scuola dispone, la spesa totale che ogni allievo deve sostenere per la frequenza al Corso, alloggio e vitto alla mensa della Scuola, è limitata a L. 30000, se egli prende alloggio in camera da solo, e a L. 25000, se prende alloggio in camera con altro allievo o con familiari. Dette somme sono da versarsi, non più tardi del 23 Luglio, all'Amministrazione della Scuola, a Varenna, in valuta italiana.

Borse di studio, in numero molto limitato, potranno essere accordate a quegli allievi che ne giustifichino il bisogno.

7. La Scuola cercherà, nei limiti delle possibilità locali (che sono però assai limitate causa la stagione balneare), di trovare una sistemazione adeguata in alberghi di Varenna per i familiari che intendessero accompagnare gli allievi.

I familiari possono essere accolti, insieme con l'allievo, alla mensa della Scuola.

Tutte le spese per alloggio, vitto, ecc., relative ai familiari sono da computarsi a parte e totalmente a carico dell'allievo: esse, per trattamento uguale a quello fatto all'allievo, si aggirano intorno a L. 3000 per giorno e per persona adulta, e dovranno essere regolate direttamente dall'allievo con l'albergatore.

8. Per ogni informazione relativa al Corso rivolgersi direttamente al Direttore di questo.

Milano, 25 Febbraio 1956

Il Segretario della S.I.F.
G. C. Dalla Noce

Il Direttore del Corso
L. Giulotto

Il Presidente della S.I.F.
G. Polvani

ITALIAN PHYSICAL SOCIETY

INTERNATIONAL SCHOOL OF PHYSICS

Under the auspices of the Ministero della Pubblica Istruzione
and the Consiglio Nazionale delle Ricerche

4th Summer Course to be held in Varenna, Lake Como

15th July - 4th August 1956

1. This year, 1956, thanks to contributions from the Ministero della Pubblica Istruzione, the Consiglio Nazionale delle Ricerche, the Comitato Nazionale per le Ricerche Nucleari, the University of Milan, and Authorities, Companies and private individuals of the Province of Como, the *4-th Summer Course* will be held at Varenna in the Villa Monastero, the use of which has been kindly granted by the Ente Villa Monastero.
   The Course will be devoted to the *magnetic properties of matter*. In particular the following subjects will be organically treated:
   — *Paramagnetism in crystals*;
   — *Paramagnetic relaxation*;
   — *Ferromagnetism, ferrimagnetism and antiferromagnetism*;
   — *Paramagnetic, ferromagnetic, antiferromagnetic and cyclotron resonance*;
   — *Nuclear magnetic resonance in liquids and in crystals*;
   — *Line-widths in magnetic resonance*;
   — *The concept of temperature in magnetic phenomena*;
   — *Magnetism at low temperatures, nuclear polarisation*;
   — *Magnetic properties of superconductors.*
   The lectures will be given by following Professors:
   C. J. Gorter, Kamerlingh Onnes Laboratorium der Rijksuniversiteit, Leiden.
   C. Kittel, University of California, Berkeley, California (U.S.A.).
   N. Kurti, Clarendon Laboratory, Oxford.
   L. Néel, Laboratoire d'Électrostatique et de Physique du Métal, Grenoble.
   M. H. Pryce, H. H. Wills Physical Laboratory, Bristol.
   E. M. Purcell, Harvard University, Cambridge, Massachusetts (U.S.A.).
   J. H. Van Vleck, Harvard University, Cambridge, Massachusetts (U.S.A.).
   Other specialists will hold seminars and lectures on questions related to the basic subjects of the course.
   The lectures, seminars, conferences and discussions will be held generally in English or French.
2. The person intrusted with the organisation and Direction of the Course is Mr. Luigi Giulotto, Professor at the University of Pavia.
3. The Course will last 21 days. It will open at 6.00 p.m. on Sunday the 15-th July and will close on the afternoon of Saturday the 4-th August.
4. The total number of students will be 35.
   Those wishing to attend the course shoulds end not later than 31-st of May 1956 an application to:

Prof. LUIGI GIULOTTO
Istituto di Fisica dell'Università
PAVIA (Italy)

and should furnish the following information, which should be set out clearly and legibly:

a) Christian name and surname.
b) Date and place of birth.
c) Present address.
d) Degrees and other qualifications obtained, with name of university in each case.
e) Present professional activity.
f) List of publication in physics.
g) Standard of knowledge of English and French – written and spoken.
h) Whether intending to stay at Varenna unaccompanied or with members of family and in the former case, whether willing to share a room with other students.

The applicant should send, together with his application, a note of reference from an university professor of Physics, to testify for the applicant's interest and preparation in the activities of the School.

Each application will be considered by the President of the Italian Physical Society and by the Direction of the School on the basis of the information submitted, with regard also to a fair distribution of the places available, among students of various Nations. The decisions on the admittance to the School will be made known to the applicants by 10th June 1956.

5. Accomodation for the students will be provided in rooms with 1 or 2 beds either in the guest quarters of the Villa Monastero or in hotels at Varenna, near the Villa. Meals will be taken at the villa itself or at a hotel in Varenna.

6. Thanks to the grants made available to the School the total fee (for attendance' hotel accomodation and full board) will be 30000 Lire for each student having single hotel accomodation, and 25000 Lire for each student sharing hotel accodation with other students or with members of his family. Fees should be paid to the management of the School, at Varenna, in Italian currency, not later than the 23rd of July.

A very limited number of scholarships may be granted to those students whose economic conditions might otherwise prevent them from attending the School.

7. The School will do everything possible to find suitable accomodation in local hotels for members of families accompanying the students. It should be noted, however, that, in view of the holiday season, local possibilities are limited.

Members of student's families may avail themselves of the catering arrangements being organised for the School.

All expenditure involved in the hotel accommodation, board etc., for student's relatives will be payable separately. These expenses, covering full service similar to that enjoyed by the student, will be of about 3000 Lire per adult person per day and are to be settled directly with the hotel management.

8. For all further information regarding the School, application should be made directly to Professor Luigi Giulotto.

Milan, the 25-th February 1956

The Secretary of the Society
G. C. Dalla Noce

The Director of the Summer Course
L. Giulotto

The President of the Society
G. Polvani

ONORANZE AD AMEDEO AVOGADRO

CONGRESSO INTERNAZIONALE SULLE COSTANTI FONDAMENTALI

E

XLII CONGRESSO DELLA SOCIETÀ ITALIANA DI FISICA

TORINO, 6-11 SETTEMBRE 1956

In occasione del centenario della morte di AMEDEO AVOGADRO, Torino, sua città natale, organizza quest'anno un ciclo di manifestazioni per onorare degnamente il grande scienziato.

Nel quadro di queste manifestazioni, la Società Italiana di Fisica organizzerà, sotto gli auspici dell'Unione Internazionale di Fisica Pura ed Applicata e del Consiglio Nazionale delle Ricerche, un Congresso Internazionale di Fisica sulle « costanti fondamentali », che avrà luogo a Torino dal 6 all'11 Settembre 1956. Intendiamo comprendere, sotto questa denominazione generale, non soltanto quelle grandezze fisiche che sono comunemente chiamate « costanti universali », ma anche le grandezze della fisica atomica e nucleare, quali i pesi atomici dei nuclidi, le costanti delle forze nucleari, ecc.

Pertanto il Congresso non tratterà soltanto il problema particolare dei valori più probabili da attribuire alle costanti fondamentali, ma — più generalmente — le questioni connesse con quei rami della Fisica sperimentale e teorica ai quali si può in qualche modo assegnare, come caratteristica, questa o quella costante. È precisamente:

- per la costante di Avogrado: **questioni relative alle molecole e ai cristalli**;
- per la velocità della luce: **questioni relative a particelle molto veloci**;
- per la carica elettrica elementare, la costante di Planck e le costanti delle forze nucleari: **questioni relative ai fenomeni elettrodinamici, alle interazioni mesone-nucleone e alla Fisica dei neutrini**;
- e finalmente, per le costanti caratteristiche dei nuclidi: **questioni relativi ai pesi atomici, ai processi nucleari, ecc.**

Il Congresso sarà evidentemente diviso in diverse Sezioni, che verranno precisate più tardi.

Inoltre, contemporaneamente al Congresso Internazionale, avrà luogo a Torino nella sua forma consueta il XLII Congresso della Società Italiana di Fisica.

Segretario Generale di tutta l'organizzazione è il prof. R. DEAGLIO, Istituto di Fisica dell'Università di Torino (via P. Giuria 1, Torino), al quale coloro che desiderano partecipare al Congresso possono rivolgersi per informazioni, non più tardi del 30 Aprile 1956.

CELEBRATION OF AMEDEO AVOGADRO

INTERNATIONAL CONGRESS ON FUNDAMENTAL CONSTANTS

AND

XLII CONGRESS OF THE ITALIAN PHYSICAL SOCIETY

TURIN, 6th-11th SEPTEMBER, 1956

On occasion of the centenary, 1956, of the death of AMEDEO AVOGADRO, the city of Turin, his birth-place, is going to organize celebrations in honour of the great scientist.

The Italian Physical Society takes part in these celebrations organizing, under the auspices of the International Union of Pure and Applied Physics and of the National Research Council, an International Congress on Fundamental Constants of Physics, to be held in Turin from September 6th to 11th 1955. We wish to include, under this general denomination, not only the physical quantities which are generally called « universal constants », but also the quantities of atomic and nuclear physics such as the atomic weights of nuclides, the constants of nuclear forces, etc.

The Congress will therefore treat not only the particular problem of the most probable values which are to be attributed to the fundamental constants, but more generally, the questions concerning those branches of experimental and theoretical physics to which one can attach, as a characteristic, this or that constant. And exactly:

— for the constant of Avogadro: **questions concerning molecules and crystals**;

— for the velocity of light: **questions concerning very fast particles**;

— for the elementary electric charge, the constant of Planck and the constants of nuclear forces: **questions concerning electrodynamic phenomena, meson-nucleon interactions and the physics of neutrinos**;

— and lastly, for the characteristic constants of nuclides: **questions concerning atomic weights, nuclear processes, etc.**

Of course, the Congress will be divided into several Sections, which will be specified later.

At the same time the XLII Congress of the Italian Physical Society will take place in Turin in its customary form.

Secretary General of the whole organization is prof. R. DEAGLIO, Institute of Physics of the University of Turin (via P. Giuria 1, Turin), to whom those wishing to attend the Congress may send their application or apply for information not later than April 30th 1956.

Corrections were introduced to account for the losses of recoil protons due to nuclear absorption and multiple scattering in the filters. These corrections were experimentally determined by the authors with an high accuracy in special experiments conducted with a proton beam removed from the synchrocyclotron. The maximum value of the correction ($\Phi = 0°$) was 40% of the uncorrected value of $N_p(\Phi)$.

As an analysis showed, under the conditions of the experiments described, charged π-mesons produced in n-p collisions were absorbed in copper filters and were not recorded by the proton detector. As a result of this, it was not necessary to introduce into the curve $N_p(\Phi)$ corrections for meson counting.

The absolute differential elastic n-p scattering cross-sections were determined, as usual, by normalizing the curve $\sigma_{np}(\Phi)$ to the total n-p scattering cross-section σ_t^{elast}(n-p) in accord with the equation

$$\sigma_t^{elast}(\text{n-p}) = 2\pi \int_0^{\pi/2} \sigma_{np}(\Phi) \sin \Phi \, d\Phi \,. \tag{1}$$

The total n-p interaction cross-section was determined for neutrons of the same mean energy in special experiments by the method of ejecting neutrons from the beam under conditions of « good » geometry (see section 4). According to these measurements, at $E_n = 380$ MeV, $\sigma_t(\text{n-p}) = (34 \pm 2) \cdot 10^{-27}$ cm² (*).

Since at the same energy the total cross-section for production of neutral and charged mesons in n-p collisions is, according to data in the literature (see for example [9]), about $1 \cdot 10^{-27}$ cm², the total cross-section of elastic n-p scattering is: $\sigma_t^{elast}(\text{n-p}) = (33 \pm 2) 10^{-27}$ cm².

Fig. 3 gives the final results of the measurements of the differential cross-sections for elastic n-p scattering, obtained after normalizing (1) to $33 \cdot 10^{-27}$ cm² and recalculating to the centre of mass system of the colliding nucleons (+). The errors given in the graph are the statisti-

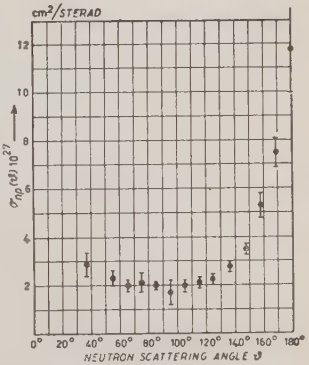

Fig. 3. – Differential n-p scattering cross section at average neutron energy 380 MeV.

(*) Here and henceforward we give data (improved in comparison with [1], concerning σ_t(n-p) and σ_t(n-d), obtained by the authors in the 1954 experiments.

(+) The results given in Fig. 3 were obtained taking account of the weak change in the cross-sections of $\sigma_{np}(\vartheta)$ in the angle region less than 40° (center of mass system) found in [10] for neutrons with an energy (400 ± 25) MeV.

cal errors. The total error in the values of differential cross-sections, with account for a small ambiguity in the extrapolation of the curve $N_p(\Phi)$ from $\Phi = 70°$ to 90°, is, according to our estimates, on the average about 15%.

4. – Determination of the Total Cross Sections for Neutron-Proton and Neutron-Deuteron Interaction at 380, 500 and 590 MeV.

In the experiments dealing with the determination of the total cross-sections for n-p interaction, the experimental samples were placed in a neutron beam directly in front of the main collimator (at point A in Fig. 1). Neutrons that had passed through the absorber and collimator were detected by a standard telescope which recorded recoil protons emerging at an angle of 20° from a polythene scatterer permanently placed in the beam. The energy threshold of the detector in the neutron experiments (the spectrum of the neutrons is shown in Fig. 2*a*) was 300 MeV. Calculations show that cross-sections measured at such threshold value refer to a mean effective energy of 380 MeV. The cross-sections for neutrons with effective energies of 500 and 590 MeV (spectrum Fig. 2*b*) were determined under the condition that the detector did not respond to neutrons with energies of less than 320 or 471 MeV respectively. The geometrical conditions of the experiment were such that neutrons scattered in the sample at an angle of more than 15′ were not recorded by the telescope.

Total cross sections were found from the formula: $\sigma_t = (1/nx)\ \ln\ (N_0/N_n,)$ where N_n and N_0 are the relative intensities of neutrons (corrected for background) of corresponding effective energy; these intensities were measured with and without the sample in the beam; n is the number of nuclei per cm³ of the sample, and x the thickness of the sample in cm.

The cross-section for neutrons interacting with hydrogen was determined from the difference of the total cross-sections for paraffin ($CH_{2.08}$) and graphite (C), or polyethylene $(CH_2)_n$ and graphite. The total cross-section for deuterium was found from experiments with heavy (99.8% concentration) and ordinary water. Quantitative chemical analysis showed that the samples of the investigated materials were of high grade of purity (the content of heavy impurities in them did not exceed 0.1 per cent).

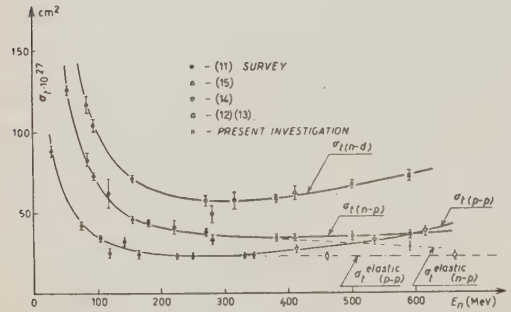

Fig. 4. – Dependence on energy of total cross-sections of n-p, n-d, and p-p interactions.

The results of the measurements of the total cross-sections for n-p and n-d interaction (in 10^{-27} cm^2) for three mean energies of neutrons are given in Table I.

TABLE I.

Cross-section (in 10^{-27} cm^2)	$E_n = 380$ MeV	$E_n = 500$ MeV	$E_n = 590$ MeV
σ_t(n-p)	34 ± 2	35 ± 2	36 ± 2
σ_t(n-d)	57 ± 2	65 ± 2.5	72 ± 2.5

A comparison of these cross-sections with the cross-sections at lower neutron energies found in the literature ([11-15], see Fig. 4) shows, that in a wide energy region from 250 to 500 MeV the total n-p interaction cross-section practically does not change. The smallest cross-sections were observed for $E_n = 350 \div 450$ MeV. The total n-d interaction cross-section has minimum values in the energy region $250 \div 350$ MeV and appreciably grows in passing to higher neutron energies; thus, the variation of σ_t(n-d) on energy, when E_n rises from 200 to 600 MeV, is to a considerable extent similar to the variation, in the same energy range, of the total p-p interaction cross-sections (*).

5. – Discussion of Results of the Neutron-Proton Scattering Experiments.

The first conclusion which may be drawn on the basis of our experimental data (see Fig. 3) is that at neutron energies of 380 MeV the contribution of forces of an exchange character to n-p interaction is approximately equal to the contribution due to forces of the usual type (+).

Differential cross-sections for elastic n-p scattering in a wide range of angles ($55^\circ \div 125^\circ$) vary but slightly with the angle and have a relatively large value close to $2 \cdot 10^{-27}$ cm^2/sterad, just as it was found for neutrons with energies

(*) The values, given in Fig. 4, of the total p-p scattering cross-sections up to energies of 345 MeV were not obtained directly from the experimental data but by integrating the curves of the differential cross-sections [11]. The cross sections σ_t^{elast}(p-p) for $E_p = 460$ and 660 MeV were determined in [12] and [13] in a similar way.

(+) Data obtained in 1954 in [10] on the (n-p) differential scattering cross-sections for energies $E_n = (400 \pm 25)$ MeV and for angles $13 < \vartheta_n \leqslant 180^\circ$ indicate a certain asymmetry in the $\sigma_{np}(\vartheta_n)$ curve with respect to the angle 90°; the cross-sections for angles $13^\circ < \vartheta_n < 30^\circ$ were noticeably less than those for angles $150^\circ < \vartheta_n < 170^\circ$. As the contribution of small angle scattering to the integral cross-section, for n-p interaction, is small, the conclusion that the contributions of ordinary and exchange forces to the nuclear interaction at an energy of about 400 MeV are approximately equal remains true, even if the asymmetry is taken into account.

of 180 [16] and 260 MeV [17]. In agreement with this fact, the total cross-section for n-p scattering also exhibits a relatively weak decrease with energy in the neutron energy interval of 200÷400 MeV.

The results of our experiments are in sharp contradiction with the predictions of perturbation theory and, as the analysis [2] showed, cannot be interpreted on the basis of phenomenological theory involving static potentials.

Under these conditions, and also in view of the absence of an exact theory, the hypothesis of charge independence of nuclear forces seems to be a promising approach to the phenomenological study of the problem of nucleon-nucleon interactions. A confirmation of this hypothesis can be found in the region of small nucleon energies (equality of n-p and p-p interactions in the $^1S_0$ state, similarity of the levels of mirror nuclei, etc.).

If we turn to experimental facts available at present on the scattering of high-energy nucleons by nucleons (including the results of the experiments described here), it may be stated that the data of these experiments also do not contradict the hypothesis of charge independence of nuclear forces. A consequence of this hypothesis is the following relation between the differential cross-sections for n-p and p-p scattering

$$2[\sigma_{np}(\vartheta) + \sigma_{np}(\pi - \vartheta)] - \sigma_{np}(\vartheta) > 0 \,. \tag{2}$$

This relation is fulfilled in a broad range of energies up to 400 MeV. This hypothesis facilitates to a certain extent the analysis of the experimental results on nucleon-nucleon scattering. First of all, it should be pointed out that this hypothesis and the experimental results on n-p scattering and also the well-known results on p-p scattering permits one (as SMORODINSKIJ has demonstrated [18]) to separate the interactions of two nucleons in states of different isotopic spin $T=0$ and $T=1$. It then appears that the angular dependence of the nucleon scattering cross-sections strongly differs for states of different T. If $\sigma_{T=1}(\vartheta)$ (which, according to the condition of charge independence, is equal to $\sigma_{pp}(\vartheta)$), in the neutron energy region of 150÷400 MeV, does not depend on the angle and is conditioned fundamentally by interaction in states $^1S_0$ and $^3P_0$, the phases of which are close to $\pi/2$, then the neutron-proton scattering cross-section in states with $T=0$, $\sigma_{T=0}(\vartheta)$ (which is equal to the left hand side of the inequality (2)) is described by a curve resembling that obtained from perturbation theory. The strong dependence on scattering angle of cross-sections for states with $T=0$ can be seen from the figures given in Table II (fifth and sixth column), where the averaged values of the cross-sections for several neutron energies are given; these values were obtained by treating all available experimental data on n-p and p-p scattering.

The strong scattering anisotropy observed for nucleon states with $T=0$ indicates that a considerable number of symmetric states, such as $^3S_1$, $^1P_1$, ^3D, etc.,

the phases of which are considerably less than $\pi/2$, participate in n-p interactions at high energies. A result of participation of a considerable number of states with such phases in n-p interactions (in states with $T=0$) may be

TABLE II.

E_n (MeV)	$\sigma^t_{T=0} = 2\cdot\sigma^{\text{elast}}_t(\text{n-p}) - \sigma^{\text{elast}}_t(\text{p-p})$	$\sigma^t_{T=1} = \sigma^{\text{elast}}_t(\text{p-p})$	$\sigma^{\text{elast}}_t(\text{n p})$	$\sigma^{90^0}_{T=0}$	$\sigma^{0^0}_{T=0}$	$\sigma^{90^0}_{T=1}$
	in 10^{-27} cm^2			in 10^{-27} cm^2/sterad		
100	110	32	71	10.8	54	5
150	69	27	48	5.0	40	4.3
200	59	23	41	4.2	36	3.7
300	47	23	35	3.6	32	3.7
400	43	23	33	3.0	31	3.7

the experimental fact that neutrons scattered by protons are polarised to a smaller degree than are high energy protons scattered by protons.

The difference in the energy dependence of total nucleon scattering cross-sections in states with different T, points to a difference in the character of nucleon interaction in such states. Indeed, as it may be seen from data in Table II, in the nucleon energy range from 150 to 400 MeV, $\sigma^t_{T=0}$ changes by one and one half times, whereas $\sigma^t_{T=1}$ remains practically constant.

In this connection, it may be of interest to mention another fact which is observed at still greater neutron energies. From our data on σ_t(n-p) (see Table I) and on the cross-sections for the production of π-mesons by 590 MeV neutrons on hydrogen (*) the total elastic n-p scattering cross-section for neutrons of 590 MeV is only $28\cdot10^{-27}$ cm^2, instead of $33\cdot10^{-27}$ cm^2 observed at $E_n = 380$ MeV. Since, on the other hand, it is known that the total elastic p-p scattering cross-section, which characterizes the nucleon interaction in the state with an isotopic spin of $T=1$, remains constant throughout the whole energy region from 150 to 600 MeV (see Fig. 4), the decrease of the elastic n-p scattering cross-section observed when the energy increases from 400 to 600 MeV should be due to further weakening of the interaction between nucleons in the state with an isotopic spin $T=0$.

Apparently, a result of the different dependence on energy of nucleon interaction cross-sections in states with different isotopic spins is that the total elastic n-p scattering cross-sections in the energy range from 100 to 590 MeV

(*) According to [7] the total cross-section of π^0-meson production in n-p collisions at $E_n = 590$ MeV is $5 \div 6\cdot10^{-27}$ cm^2, and according to the data in [8], $\sigma(\text{n}+\text{p}\rightarrow\pi^{\pm}+\ldots)\approx$ $\approx 3\cdot10^{-27}$ cm^2.

is in rough accordance with an empirical formula of the form:

$$\sigma_t^{\text{elast}}(\text{n-p}) = a + \frac{b}{E_n}. \tag{3}$$

Within the limits of the hypothesis of charge invariance of nuclear forces, the asymmetry of the n-p scattering curve with respect to a 90° angle (observed in experiments at energies of ~ 400 MeV) may be explained by assuming interference between states with different isotopic spins.

6. – Exchange Scattering of 380 MeV Neutrons on Deuterons.

The results of investigations of neutron-proton scattering carried out with high-energy neutrons, clearly testify to the large contribution of exchange-type forces to neutron-proton interaction. However, on the basis of these investigations it is not possible to draw any definite conclusion concerning the spin dependence of exchange forces.

Experiments with polarised beams of nucleons and polarised targets are necessary to elucidate this important aspect of the nuclear interaction of nucleons.

In 1951, I. POMERANČUK [19] pointed out a new way of obtaining data concerning the dependence of the exchange forces on spin. This method consists in investigating the angular distribution of fast protons arising in exchange collisions of high energy neutrons with deuterons, in accord with the reaction

$$\text{n} + \text{d} \rightarrow \text{p} + (\text{n} + \text{n}) \quad (*) \tag{4}$$

and in comparing the results of such experiments with the data of scattering of neutrons by free protons.

The basic point, on which he centered attention, was that as a result of the parallelism of the spins of the particles, including the deuteron, the probability of n-d exchange scattering accompanied simultaneously by an exchange of spins between the nucleons, sharply decreases, if the momentum of the proton after the collision is close to the momentum of the incident neutron. This means that the appearance, in reaction (4), of protons with energies close to the energy of the incident neutrons, is possible only at the expense of exchange collisions taking place without an exchange of spins (×). If we conduct

---

(*) The notation (n+n) signifies that the two neutrons remaining after the collision have a small relative velocity.

(×) Similar conclusions are to be found in paper [20].

comparative experiments in n-d and n-p exchange scattering, then, as the theory developed by I. POMERANČUK shows, it is possible to find the relation between the amplitudes of spin-exchange ($\bar{b}$) and spin-non-exchange ($\bar{a}$) scattering.

The difference $N_1^p(\Phi)$ in the number of recoil protons emerging at a given angle Φ (laboratory system) to the neutron beam from scatterers of ordinary and heavy water containing equal numbers of atoms of hydrogen and deuterium was measured with a scintillation counter telescope [2, 4]. The neutron beam had a diameter of 2 cm and the geometry of the detector made it possible to carry out measurements of the differential cross-sections with an angular resolution of $\pm 0.75°$. The energy threshold of the proton detector was about 300 $\cos^2 \Phi$ in MeV (*).

The value of $N_1^p(\Phi)$ is proportional to the difference of the cross-sections of n-p and n-d exchange collisions, and, for a given angle is determined, in relative units, by the equality

$$N_1^p(\Phi) = K[\sigma_{np}(\Phi) - \sigma_{nd}^{exch}(\Phi)] . \tag{5}$$

The absolute values of σ_{nd}^{exch} may be obtained if the values of $N_1^p(\Phi)$ found in the above manner are referred to the number of recoil protons $N_2^p(\Phi) = K\sigma_{np}(\Phi)$ from free n-p collisions recorded by the detector under similar conditions (in respect to neutron beam intensity geometry of the detector, and to the number of protons in the scatterer). The values of $N_2^p(\Phi)$ were measured as usual by the difference of the effects observed in paraffin and graphite. The ratios

$$\frac{N_1^p(\Phi)}{N_2^p(\Phi)} = 1 - \frac{\sigma_{nd}^{exch}(\Phi)}{\sigma_{np}(\Phi)} \tag{6}$$

thus determined made it possible to find, with satisfactory accuracy, the values of $\sigma_{nd}^{exch}(\Phi)/\sigma_{np}(\Phi)$ for angles Φ from 0° to 40°, and then (with the aid of the n-p scattering cross-section measured before) to find the absolute cross-sections $\sigma_{nd}^{exch}(\Phi)$ for the same mean neutron energy of 380 MeV.

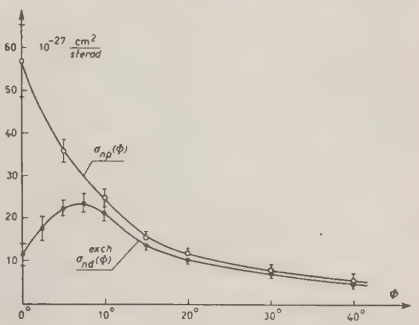

Fig. 5. – Differential cross-section of n-p and n-d exchange scattering at neutron energy 380 MeV.

The results of the measurements of the cross-sections $\sigma_{dn}^{exch}(\Phi)$ and of the ratios $\sigma_{nd}^{exch}(\Phi)/\sigma_{np}(\Phi)$ are given in Fig. 5 and 6. An especially sharp reduction

(*) At such a threshold, the elastically scattered deuterons were not registered by the detector and did not introduce distortions into the experimental results.

in the proton yield of exchange n-d collisions in comparison with n-p collisions is observed in the recoil angle region close to 0°. A 10-15% lower proton yield in n-d collisions is also found in the recoil angle range from 15° to 40°. This qualitatively agrees with results obtained in experiments with neutrons of 90 MeV [21] and 270 MeV [22], according to which the yields of fast protons in the angle region $\Phi > 10°$ was about 70-80% of $\sigma_{np}(\Phi)$. The reduction of the ratio $\sigma_{nd}^{exch}(\Phi)/\sigma_{np}(\Phi)$ in the region of large recoil angles with decreasing neutron energy may also be partially due to operation of Pauli's principle, and possibly to the fact that at lower energies of the incident neutrons (resulting from the internal motion of nucleons in the deuteron) the energy of a relatively large portion of recoil protons falls below the threshold of the detector.

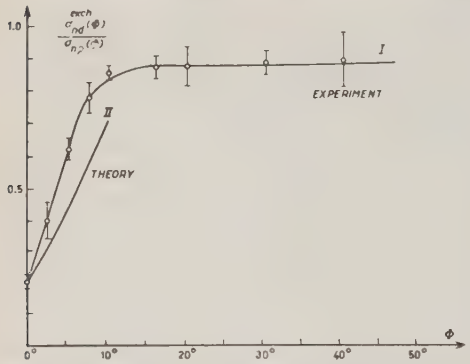

Fig. 6. – Ratio of cross-sections of n-p and n-d exchange scattering at neutron energy 380 MeV.

Fig. 6 gives a theoretical curve, calculated for angles $\Phi \leqslant 5°$ with the aid of formulae (35) and (39) of paper [19]. It may be seen that this curve exhibits qualitative agreement with the experimental data. However, the quantitative difference between them is considerable. The fundamental reason for the observed discrepancy, apparently, is that in [19] the non central interaction between nucleons was not taken into account.

Using the value of the ratio of the cross-sections $\sigma_{nd}^{exch}(\Phi)/\sigma_{np}(\Phi) = 0.2 \pm 0.035$ experimentally found for the angle $\Phi = 0°$, and the result obtained in [19], one can roughly estimate the limits of variation of the ratio of the spin-non-exchange and spin-exchange scattering amplitudes. It appears that the value of this ratio lies within the limits:

$$(7) \qquad 0.5 \leqslant \left|\frac{\bar{a}}{\bar{b}}\right| \leqslant 1.2 .$$

Inequality (7) makes it possible to draw an essentially new conclusion concerning the character of n-p interaction at high energies; it shows that in n-p exchange collisions, spin exchange also takes place simultaneously with a relatively greater probability. This means that the contributions made by spin-exchange and spin-non-exchange forces to n-p exchange interaction are of the same order of magnitude.

In the light of our knowledge on exchange, central, and tensor forces, it seems that the last conclusion permits one to generalize, stating that approximate equality in the magnitude of various forces involved in nuclear interactions of nucleons is a characteristic feature of this type of interaction.

7. – Elastic Neutron-Neutron Scattering at 300 MeV.

In the experiments [2, 5] described below the elastic cross-sections for scattering of neutrons with a mean effective energy of 300 MeV by neutrons were determined by comparing the angular distribution of neutrons scattered by deuterons and free protons, measured in the same conditions. The possibility of utilising the data on n-d scattering for obtaining data on elastic n-n scattering is based on the fact that, according to present-day conceptions, if the energy of the incident nucleons is sufficiently high, in the majority of cases, they interact intensively with only one of the nucleons making up the deuteron.

Calculations of the total n-d scattering cross-section for a given angle, made by one of the authors [23] in the impulse approximation, showed that at scattering angles (in the center of mass system) $\theta \leqslant 100^\circ \div 120^\circ$, the n-d scattering cross-section may be written as follows:

$$\sigma_{nd}(\theta) = \{\sigma_{nn}(\theta) + \sigma_{np}(\theta)\}\alpha + \sigma_{int}(\theta)\,, \tag{8}$$

where $\sigma_{nn}(\theta)$ and $\sigma_{np}(\theta)$ are the cross-sections for the scattering of neutrons respectively by free neutrons and protons through an angle θ, α is a coefficient, and $\sigma_{int}(\theta)$ is the «interference cross-section», due to superposition of neutron waves scattered by deuteron, neutron and proton.

The dependences of the values of α and $\sigma_{int}(\theta)$ on the scattering angle, found in paper [23], testify to the fact that at $E_n = 300 \div 400$ MeV and $\theta \leqslant 100^\circ \div 120^\circ$ the coefficient α is practically equal to unity, and $\sigma_{int}(\theta)$ in the angle range $50 \leqslant \theta \leqslant 100^\circ \div 120^\circ$ does not exceed, in a maximum evaluation, 15% of the n-p scattering cross-section measured at the same angle. In passing to larger θ (in the stated angle range) and with an energy increase of the incident neutrons, $\sigma_{int}(\theta)$ rapidly declines (see column 5 of Table III). This fact makes it possible to consider that, in the stated conditions, the cross-sections for scattering of neutrons by free neutrons may be determined with satisfactory accuracy by the difference

$$\sigma_{nn}(\theta) \cong \sigma_{nd}(\theta) - \sigma_{np}(\theta)\,. \tag{9}$$

From formula (9) it follows that in order to find the elastic n-n scattering

cross sections it is sufficient to determine the flux of neutrons scattered by hydrogen and deuterium at the same angle. Since in such experiments the neutron beam intensity produced by the accelerator is low, and also because of the low efficiency of present-day methods of counting fast neutrons, a method was used in the first experiments which enables one to measure the relative differential cross-sections of n-n scattering by using thick scatterers and large-angle neutron detectors.

In these experiments the neutron beam had a diameter of 3 cm, the scatterers were cylindrical thin walled containers 6 cm in diameter and 80 cm in length, filled with heavy water (99.8% concentration) and ordinary water. The neutron detector was a fission chamber with circular electrodes (outer diameter 52 cm, inner diameter 12 cm) covered with bismuth. The initial experimental data for determining the relative values of differential n-n scattering cross-sections were the relative counting rates of the detector, $\nu_1(x)$ and $\nu_2(x)$, obtained when scatterers of D_2O and H_2O containing an equal number of nuclei were alternately placed in the neutron beam at equal distances x from the detector (see Fig. 7) (*). As this distance is gradually varied, the region of angles of incidence of the scattered neutrons entering detector also varies, and thus a wide range of scattering angles can be investigated.

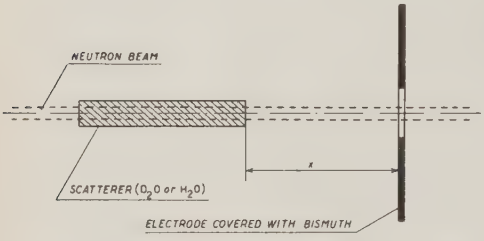

Fig. 7. – Experimental scheme with circular division chamber.

The method used by the authors was treated mathematically by E. F. TAMBOVCEV [24]. He obtained equations, relating the quantities $\nu_1(x)$ and $\nu_2(x)$ (found from experiments with a circular chamber) with the relative values of the function

$$S(\theta) = K[\sigma_{nn}(\theta) + \sigma_{int}(\theta)] , \tag{10}$$

where K is a constant.

In the calculations, account was taken of the absorption of neutrons in the scatterer, of the energy distribution of neutrons in the beam, and of the efficiency of the fission chamber for neutrons of various energies; the efficiency was determined from our experimental data on the fission cross-section of

(*) An analysis showed that under the conditions of the experiments described here there was no necessity to introduce into $\nu_1(x)$ corrections to account for triggering of the detector by elastically scattered deuterons.

bismuth at $E_n = 120$ MeV and 300 MeV [3], and also on the fission of bismuth by high energy protons.

The numerical values of the functions $S(\theta)$ found in [24], in relative units, are given in column 2 of Table III (*).

TABLE III.

θ^0 c.m.s.	$S(\theta)$ rel.	$S'(\theta)$	$S''(\theta)$	$\sigma_{int}^{max}(\theta)$	$\overline{S(\theta)}$	
		in 10^{-27} cm^2/sterad				
12	2.1 $\pm$ 0.4	7.7 $\pm$ 1.5	8.4 $\pm$ 2.3	—	7.9 $\pm$ 1.5	
16	1.6 $\pm$ 0.3	5.8 $\pm$ 1.2	6.4 $\pm$ 1.7	—	6.0 $\pm$ 1.0	
20	1.3 $\pm$ 0.2	4.7 $\pm$ 0.8	5.2 $\pm$ 1.6	—	4.8 $\pm$ 0.7	
30	0.85 $\pm$ 0.2	3.1 $\pm$ 0.8	3.4 $\pm$ 1.2	—	3.2 $\pm$ 0.6	
40	0.85 $\pm$ 0.2	3.1 $\pm$ 0.8	3.4 $\pm$ 1.2	0.6	3.2 $\pm$ 0.6	
50	0.94 $\pm$ 0.2	3.4 $\pm$ 0.8	3.8 $\pm$ 1.3	0.36	3.5 $\pm$ 0.8	$\sigma_{nn}(\theta)$
60	1.03 $\pm$ 0.2	3.7 $\pm$ 0.8	4.1 $\pm$ 1.3	0.20	3.8 $\pm$ 0.6	
70	1.00 $\pm$ 0.2	3.6 $\pm$ 0.8	4.0 $\pm$ 1.1	0.10	3.75 $\pm$ 0.6	
80	1.00 $\pm$ 0.2	3.6 $\pm$ 0.8	4.8 $\pm$ 1.1	0.09	3.75 $\pm$ 0.6	
90	0.97 $\pm$ 0.25	3.5 $\pm$ 1.0	3.9 $\pm$ 1.4	0.04	3.6 $\pm$ 0.8	

According to calculations, these values of $S(\theta)$ refer to an effective energy of 300 MeV.

In the present work, two independent methods were used for determining the values of $S(\theta)$ in absolute units. In the first case, the integral $S(\theta)$ over all scattering angles was equated to the difference between the total n-d and n-p scattering cross-sections:

$$\int S(\theta)\mathrm{d}\Omega = \sigma_t(\text{n-d}) - \sigma_t(\text{n-p})\,. \tag{11}$$

In view of a slight dependence of the cross-sections on energy, we used for the normalization a value of the difference which was corrected for meson production; this value was obtained from measurements with neutrons having a mean effective energy of 380 MeV and was found to be $(22 \pm 5)\cdot 10^{-27}$ cm^2. The values of the functions $S(\theta)$ thus normalized are given in column 3 of Table III.

The second method of normalizing $S(\theta)$ is based on a method worked out by the authors, for determining the absolute n-n scattering cross-sections by comparison of these cross-sections with those for n-p scattering. In the new instrument which has been called a « neutron telescope », high energy neutrons

(*) The calculations were carried out by E. P. TAMBOVCEV in the laboratory of the Academician N. N. BOGOLJUBOV, for which the authors of this paper take the opportunity to express their gratitude.

from n-p and n-n collisions were recorded by counting the charge exchange protons formed in a converter made of a light substance placed in the path of the neutrons being counted (see Fig. 8) (*).

The protons were counted by a telescope, placed at an angle of 40° to the neutron beam, consisting of three scintillation counters connected in coincidence (the C I system). In order to exclude that the telescope could count the charged particles emitted from the scatterer, a double coincidence circuit was used, the counters being placed directly in front of and behind the converter (C II system): these counters were in anticoincidence with the C I system. The energy threshold for neutron counting was determined as usual by the thickness of a copper filter placed in the path of the charge exchange protons between counters two and three of the C I system.

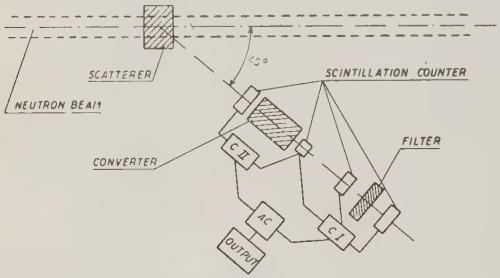

Fig. 8. – Neutron Telescope.

As a result of experiments carried out with the neutron telescope and small-size scatterers made of D_2O and H_2O and CH_2 and C, it was found (with the aid of data on $\sigma_{np}(\theta)$) that for neutrons with a mean energy of 380 MeV and for an angle $\theta = 85°$ (center of mass system), $S(\theta)$ is

$$S\,(85°) = (4.0 \pm 1.1)\cdot 10^{-27}\ \text{cm}^2/\text{sterad}\,. \tag{12}$$

The function $S(\theta)$, normalized with the aid of (12) to absolute values, is given in column 4 of Table III. Column 6 of the table contains the values of $\overline{S(\theta)}$, obtained averaging over both methods of normalization. Since $\sigma_{int}(\theta)$ for $\theta \geqslant 50°$ is only a small correction, the cross-sections given in column six are, for $\theta \geqslant 50°$, differential cross-sections for scattering of neutrons by free neutrons. On the average they are equal to

$$\sigma_{nn}(\theta) = (3.7 \pm 0.6)\cdot 10^{-27}\ \text{cm}^2/\text{sterad}\,.$$

It may be seen that in the investigated range of angles ($50° \leqslant \theta \leqslant 90°$) the cross-sections $\sigma_{nn}(\theta)$, within experimental accuracy, coincide in magnitude with the cross-sections $\sigma_{pp}(\theta)$, measured at the same energy, and apparently depend but slightly on the scattering angle. These facts permit us to conclude that

(*) A similar instrument was independently used later in [25] for measuring the total cross-sections of n-p and n-n interactions at $E_n = (1.4 \pm 0.2)$ GeV.

at 300 MeV the n-n scattering cross-sections are determined mainly by neutron interaction in the same $^1S_0$ and $^3P_0$ states, which play the main role likewise as in p-p scattering.

The equality of n-n and n-p interaction at high energies and thus the charge symmetry of nuclear forces also follow from the experimentally established fact that (within the experimental errors) the total cross-sections for n-d and p-d interactions at the same energy of the incident nucleons are equal; thus, according to our measurements (see Table II), $\sigma_t(\text{n-d}) = (57 \pm 2) \cdot 10^{-27}$ cm^2 at $E_n = 380$ MeV, and according to the data of [26], at $E_p = (408 \pm 10)$ MeV, $\sigma_t(\text{p-d}) = (55.6 \pm 2.2) \cdot 10^{-27}$ cm^2.

A convincing argument in favour of the equality of n-n and p-p forces at high energies is that the difference $\sigma_t(\text{n-d}) - \sigma_t(\text{n-p})$ in a broad region of neutron energies (from 160 to 600 MeV) coincides, with satisfactory accuracy, with the total cross-section of p-p interaction measured at the same energies (Fig. 4). The relatively rapid growth of this difference above 300 MeV is apparently due to a sharp increase of the probability of meson production in n-n collisions, similar to that observed in the case of p-p collisions.

A comparison of the measured differential n-n scattering cross-sections, with those for n-p scattering shows that the inequality

$$\sigma_{np}(90^\circ) \geqslant \tfrac{1}{4}\sigma_{nn}(90^\circ)$$

is fulfilled and that, consequently, also the results of the experiments on n-n scattering do not contradict the hypothesis of charge independence of nuclear forces.

8. – Conclusion.

A discussion of the experimental material obtained in this work leads to the following conclusions:

1) For neutron energy of 380 MeV, the contributions made to neutron-proton interaction by exchange and ordinary forces are approximately equal in magnitude; spin-exchange and spin-non-exchange forces also participate in the exchange interaction of nucleons in about the same degree.

2) The differential and total elastic n-p scattering cross-sections weakly vary as the neutron energy varies between 260 MeV and 380 MeV.

3) The interaction of neutrons of 380 MeV energy with protons is chiefly of an elastic character. The cross section for meson production at this energy is about 3% of the total n-p interaction cross-section. As the energy increases,

the contribution of inelastic processes (meson production) grows rapidly and at $E_n = 590$ MeV it includes about 25% of σ_t(n-p).

4) The data obtained in the study of the interaction of neutrons with energies from 300 to 600 MeV with neutrons and deuterons, testify to the charge symmetry of nuclear forces in this energy region.

5) The results of the experiments on the scattering of 380-300 MeV neutrons by nucleons do not contradict the charge invariance of nuclear forces. A qualitative consideration of the experimental data indicates that the interactions of nucleons in states with various values of isotopic spin appreciably differ and that the intensity of the interaction in states with $T = 0$ considerably decreases with increase of energy up to 590 MeV.

6) The next stage of these investigation, as far as utilization of the hypothesis of charge invariance of nuclear forces is concerned, is, in addition to obtaining more precise data on scattering of unpolarized beams of nucleons, the separate determination (in experiments with polarized beams) of the interaction between nucleons in various spin states at a given value of T.

* * *

In concluding, the authors take the opportunity to express their deep gratitude to M. G. MEŠČERJAKOV, I. JA. POMERANČUK, JA. A. SMORODINSKIJ, and L. I. LAPIDUS for the interest taken in their work and discussions. We are grateful to the synchrocyclotron staff of the Institute of Nuclear Problems of the Academy of Sciences of the USSR, headed by A. V. ČESTNOJ, for the good work of the accelerator, which contributed to the success of the experiments described.

REFERENCES

[1] V. P. DŽELEPOV, JU. M. KAZARINOV: *Report of the Institute of Nuclear Problems. Acad. of Sciences, USSR* (June, 1951): *Dokl. Akad. Nauk SSSR*, **99**, 939 (1954).

[2] V. P. DŽELEPOV: *Doctor's Dissertation, Institute of Nuclear Problems, Acad. of Sciences, USSR* (March 1954).

[3] V. P. DŽELEPOV, JU. M. KAZARINOV, B. M. GOLOVIN and V. B. FLJAGIN: *Report of the Institute of Nuclear Problems, Acad. of Sciences, USSR* (1953); V. B. FLJAGIN: *ibid.* (1954).

[4] V. P. DŽELEPOV, JU. M. KAZARINOV and V. B. FLJAGIN: *Report of the Instiutte of Nuclear Problems, Acad. of Sciences, USSR* (1952); *Dokl. Akad. Nauk SSSR*, **100**, 655 (1955).

[5] V. P. Dželepov, B. M. Golovin and V. I. Satarov: *Report of the Institute of Nuclear Problems, Acad. of Sciences, USSR* (1953); *Dokl. Akad. Nauk SSSR*, **99**, 943 (1954).
[6] V. P. Dželepov, V. I. Satarov and B. M. Golovin: *Report of the Institute of Nuclear Problems, Acad. of Sciences, USSR* (1954).
[7] V. P. Dželepov, V. B. Fljagin and K. O. Oganesjan: *Report of the Institut of Nuclear Problems, Acad. of Sciences, USSR* (1954).
[8] Ju. M. Kazarinov and Ju. N. Simonov: *Report of the Institute of Nuclear Problems, Acad. of Sciences, USSR* (1954).
[9] H. Rosenfeld: *Phys. Rev.*, **96**, 139 (1954).
[10] A. Hartzler, R. Siegel and W. Opitz: *Phys. Rev.*, **95**, 591 (1954).
[11] V. I. Gol'danskij, A. L. Ljubimov and B. V. Medvedev: *Usp. Fiz. Nauk*, **48**, N. 4, 531 (1952); **49**, N. 1, 3 (1953).
[12] M. G. Meščerjakov, N. P. Bogačev, B. S. Neganov and E. V. Piskarev: *Dokl Akad. Nauk SSSR*, **99**, 955 (1954).
[13] N. P. Bogačev and I. K. Vzorov: *Dokl. Akad. Nauk SSSR*, **99**, 931 (1954).
[14] A. Shapiro, C. Leavitt and F. Chew: *Bull. Am. Phys. Soc.*, **29**, N. 4, 75 (1954).
[15] V. Nadzel: *Phys. Rev.*, **94**, 174 (1954).
[16] G. Guernsey, R. Mott and B. Nelson: *Phys. Rev.*, **88**, 15 (1952).
[17] E. Kelly, C. Leith, E. Segre and C. Wiegand: *Phys. Rev.*, **79**, 96 (1950).
[18] Ja. A. Smorodinskij: *Report of the Academy of Sciences, USSR* (1953); *Problems of the Present-Day Physics*, Moscow, **7**, 7 (1954).
[19] I. Ja. Pomerančuk: *Dokl. Akad. Nauk SSSR*, **78**, 249 (1951); *Žu. Èksper. Teor. Fiz.*, **21**, 1113 (1951).
[20] F. Chew: *Phys. Rev.*, **84**, 710 (1951).
[21] W. Powell: the results of his work are given in paper [20].
[22] J. Cladis, J. Hadley and W. Gess: *Phys. Rev.*, **86**, 110 (1952).
[23] B. M. Golovin: *Report of the Institute of Nuclear Problems, Acad. of Sciences, USSR* (1954).
[24] E. P. Tambovcev: *Report of the Academy of Sciences, USSR* (1952) and (1954).
[25] D. Hill, T. Coor, N. Hornyak, L. Smith and G. Snow: *Bull. Am. Phys. Soc.*, **29**, N. 1, 54 (1954).
[26] J. Marshall, L. Marshall and V. Nadzel: *Phys. Rev.*, **91**, 717 (1953).

SUPPLEMENTO AL VOLUME III, SERIE X
DEL NUOVO CIMENTO

N. 1, 1956
1° Semestre

On the Quantum Theory of Fields.

L. D. LANDAU, A. ABRIKOSOV and L. HALATNIKOV

Academy of Sciences of the USSR – Moscow

CONTENTS. — **1.** The fundamental equations. – **2.** The asymptotical expression for the photon Green function. – **4.** The mass of the electron in quantum electrodynamics. – **5.** The infrared catastrophe. – **6.** The gauge transformations of the Green functions of charged particles. – **7.** The Green functions in the meson theory with weak pseudoscalar coupling.

1. – The Fundamental Equations. [1]

As is well known, the main difficulties of the quantum field theory arise from the infinities. The existing methods of removing these infinities (regularisation) sometimes give quite correct results, but in general are of a very artificial nature and in many cases become inapplicable. Therefore it seems necessary to construct a theory without considering actually infinite quantities.

In accordance with the usual methods of theoretical physics, it is natural to regard the point interaction as a limit of a smeared out interaction with a finite decreasing radius. The order of magnitude of the radius we will denote by a. Then $\Lambda \sim 1/a$ is the upper limit of integration in momentum space. All the calculations will be made under the assumption, that the unrenormalized bare charge e_1, which appears in the interaction term in the Lagrangian, satisfies the condition $e_1^2 \ll 1$.

The Green functions of the electron $G(p)$ and photon $D_{\mu\nu}(k)$ are connected

FONDAZIONE FRANCESCO SOMAINI
PRESSO IL TEMPIO VOLTIANO, A COMO

BANDI DI CONCORSI
AL PREMIO E ALLA BORSA PER IL 1958

Con lo scopo di premiare e incoraggiare nel nome di ALESSANDRO VOLTA gli studi di Fisica in Italia, la « Fondazione Francesco Somaini », presso il Tempio Voltiano a Como, indice i seguenti concorsi.

A) **Concorso al " Premio Triennale per la Fisica Francesco Somaini " per il 1958.** di L. 1 500 000 (un milione e cinquecentomila) nette, da assegnarsi al concorrente che, fra quelli che la Commissione Giudicatrice giudicherà in senso assoluto meritevoli del premio per i risultati conseguiti nello studio della Fisica durante il Triennio 1° Luglio 1955-30 Giugno 1958, sia, a parere della Commissione stessa, il più meritevole.

B) **Concorso alla " Borsa Francesco Somaini per lo studio della Fisica " per il 1958.** di L. 750 000 (settecentocinquantamila) nette, da assegnarsi al concorrente che, tra quelli che la Commissione Giudicatrice giudicherà in senso assoluto meritevoli della Borsa, verrà dalla Commissione stessa giudicato il più meritevole, sia per titoli, preparazione scientifica, lavori già svolti e risultati già conseguiti nella Fisica, sia anche per il vantaggio che gli studi, per i quali è richiesta la Borsa, possono portare allo sviluppo della Fisica, in Italia.

1. – Ad entrambi i Concorsi possono prendere parte singolarmente i cittadini, d'ambo i sessi, italiani e svizzeri del Canton Ticino purchè di stirpe italiana. Sono esclusi dal Concorso i membri della Commissione Amministratrice e della Commissione Scientifica della « Fondazione Francesco Somaini ».

2. – Le norme particolareggiate dei singoli Concorsi verranno pubblicate in apposito volantino che potrà essere richiesto dagli interessati alla Segreteria della Fondazione presso il Tempio Voltiano a Como.

3. – La domanda, i documenti, i lavori, ecc., presentati dai singoli concorrenti dovranno pervenire, tra il 1° Gennaio e le ore 12 del 1° Luglio 1958, alla Commissione Amministratrice della « Fondazione Francesco Somaini » a Como presso il Tempio Voltiano.

4. – Il Premio Triennale per la Fisica potrà essere anche conferito a uno studioso che non abbia preso parte al Concorso, ma sia stato segnalato da un Membro della Commissione Giudicatrice, con proposta motivata, come meritevole di particolare considerazione oppure ritenuto degno di premio dalla Commissione Giudicatrice, indipendentemente da ogni segnalazione.

* * *

La procedura dei suddetti Concorsi è regolata secondo lo Statuto della Fondazione, il quale è ostensibile a Como presso il Tempio Voltiano ed è depositato negli atti del Notaio Dr. Raoul Luzzani di Como.

Como, dal Tempio Voltiano, il giorno 6 Agosto 1955.

Il Segretario Conservatore del Tempio — CESARE MORLACCHI

Il Presidente Sindaco di Como — PAOLO PIADENI

[Il bando in esteso di detti Concorsi è stato pubblicato nel fascicolo di Gennaio del *Nuovo Cimento* 1956].

SOCIETÀ ITALIANA DI FISICA

CONCORSO SPECIALE A UN PREMIO PER STUDI SUI MATERIALI SEMICONDUTTORI

Prendendo occasione dalla prossima inaugurazione a Forlì del Centro di Ospitalità per scrittori, artisti e scienziati, fondato, in memoria di Livio e Maria Garzanti, dal figlio, l'Editore Aldo Garzanti, questi ha istituito un premio scientifico, del quale ha fissato la natura e lo scopo con la sequente dichiarazione:

« Considerando la grande importanza che in questi ultimi anni hanno acquistato, sia nel campo strettamente scientifico sia nelle applicazioni, i materiali semiconduttori, viene istituito un premio di un milione di lire a favore di uno studioso italiano che, entro il 31 Maggio 1956, abbia presentato una memoria, nella quale, premesso un breve riassunto sulla Fisica di questi materiali, siano indicate, nei termini più concreti, le possibilità di fabbricazione e di impiego di essi in Italia, con riferimento alle materie prime qui esistenti, ai costi e alle condizioni della nostra industria. Sarà tenuto conto dei contributi scientifici e tecnici personali che il candidato abbia eventualmente portato alla conoscenza delle proprietà e delle applicazioni di questi materiali. Il premio sarà assegnato alla migliore tra le memorie giudicate degne dalla apposita Commissione. La proprietà letteraria e il diritto di eventuale pubblicazione della memoria vincitrice spettano all'Editore Garzanti ».

La Società Italiana di Fisica, richiesta dall'Editore Garzanti, ha ben volentieri acconsentito, applaudendo alla iniziativa di lui, a patrocinare il Concorso e curare tutte le operazioni che esso comporta: e quindi d'intesa con l'Editore stesso ha formulato il seguente Bando.

1. – È aperto un concorso a un premio di L. 1000000 (un milione) intitolato « Premio Livio e Maria Garzanti », per studi sui materiali semiconduttori.

2. – Possono partecipare al Concorso le persone di nazionalità italiana che non facciano parte della Commissione esaminatrice.

3. – Le domande di ammissione al Concorso, redatte su carta libera e recanti le generalità e il recapito del concorrente, dovranno pervenire alla Presidenza della Società Italiana di Fisica (Milano, Via Saldini, 50) entro il 31 Maggio 1956.

Alla domanda il concorrente dovrà unire: *a*) la dichiarazione firmata che egli è di nazionalità italiana; *b*) cinque copie (dattilografate) di una memoria originale, da lui compilata, nella quale, premesso un breve riassunto sulla Fisica dei materiali semiconduttori, siano indicate, nei termini più concreti, le possibilità di fabbricazione e d'impiego di essi in Italia, con riferimento alle materie prime qui esistenti, ai costi e alle condizioni della nostra industria; *c*) quei titoli, documenti e pubblicazioni (queste in cinque copie) che possano attestare il contributo portato dal concorrente alla conoscenza delle proprietà fisiche e alle applicazioni tecniche e pratiche dei materiali semiconduttori; *d*) sei copie (dattiloscritte) dell'elenco completo di tutte le carte presentate.

4. – La Commissione giudicatrice del concorso è costituita da cinque membri, di cui quattro nominati dal Consiglio di Presidenza della Società Italiana di Fisica e uno dall'Editore Aldo Garzanti in sua rappresentanza.

5. – Il Premio sarà assegnato alla migliore tra le memorie giudicate degne dalla Commissione. La proprietà letteraria e il diritto dell'eventuale pubblicazione della memoria vincitrice spettano all'Editore Aldo Garzanti.

6. – Il giudizio della Commissione è inappellabile.

7. – La proclamazione del vincitore avrà luogo, per quanto in tempo, alla inaugurazione del Centro di Ospitalità di Forlì, altrimenti, insieme con il conferimento del Premio stesso al Congresso Internazionale di Fisica che si terrà nel prossimo Settembre a Torino per celebrare il grande fisico e chimico italiano Amedeo Avogadro nel centenario della sua morte.

Il Segretario: G. C. Dalla Noce *Il Presidente*: G. Polvani

with the vertex part $\Gamma_\mu(p, p-k; k)$ by the Dyson equations

$$(1.1) \qquad G(p)\left\{\hat{p} - m_1 - \frac{e_1^2}{\pi i}\int \Gamma_\mu(p, p-k; k) G(p-k)\gamma_\nu D_{\mu\nu}(k)\,\mathrm{d}^4k\right\} = 1\,,$$

$$(1.2) \quad D_{\mu\nu}(k) = D^0_{\mu\nu}(k) - \frac{e_1^2}{\pi i} D_{\mu\sigma}(k)\,\mathrm{Sp}\left[\int G(p)\Gamma_\sigma(p, p-k; k)G(p-k)\gamma_\tau \mathrm{d}^4p\right]\cdot D^0_{\tau\nu}(k).$$

Here and further the Feynman notations will be used. $D^0_{\mu\nu}$ is the photon Green function in zeroth approximation. Usually it is taken to be equal to $\delta_{\mu\nu}/k^2$. This choice is however inconvenient. Actually the longitudinal (proportional to $k_\mu k_\nu$) part of the tensor $D_{\mu\nu}$, in consequence of gauge invariance, can be taken arbitrarily and is not altered by perturbations (owing to the transversality of the Dirac current, the integral term in (1.2)).

We will take $D^0_{\mu\nu}$ in the form of $(1/k^2)(\delta_{\mu\nu} - (k_\mu k_\nu/k^2))$. Then the equation for the transversal part of the tensor $D_{\mu\nu}$ is

$$(1.3) \quad D^t_{\mu\sigma}\left(k^2\delta_{\sigma\nu} + \frac{e_1^2}{\pi i}\,\mathrm{Sp}\left[\int G(p)\Gamma_\sigma(p, p-k; k)G(p-k)\gamma_\nu \mathrm{d}^4p\right]\right) = \delta_{\mu\nu} - \frac{k_\mu k_\nu}{k^2}\,.$$

The unpleasant feature of the integrals in (1.1) and (1.3) is the integration over the pseudoeuclidean space. Let the k-vector in (1.3) have the time-like component equal zero. Then the whole integrated expression is a function of p_0. After some simple operations we are left with a function of p_0^2. As is well known, this function is regular in the upper halfplane. Owing to the smearing out it vanishes in the infinity. Therefore we have

$$\int_{-\infty}^{\infty} f(p_0^2)\,\mathrm{d}p_0 = \int_0^\infty f(x)\frac{\mathrm{d}x}{\sqrt{x}} = i\int_0^\infty f(-x)\frac{\mathrm{d}x}{\sqrt{x}} = i\int_0^\infty f(-p_0^2)\,\mathrm{d}p_0\,.$$

This corresponds to the fact that p_0 in the integral is changed to ip_0. Then the integration will be extended over an euclidean space. By this transformation G and D, for space vectors, will be expressed through the space-like Γ_μ. G and D, for time-like vectors, may be found by means of analytical continuation. The exception is G for p^2 nearing m^2, but this case will be discussed later. As to the $\Gamma_\mu(p, q; k)$ which we obtain here, the analytical continuation will give only the cases when the p^2, q^2 and k^2 are of the same order or, if one of these squares is small, the two others should be near to each other.

As is well known, the power of the logarithmic divergence never exceeds the implied order of the perturbation theory (+). This means, that the main terms in the perturbation series are the terms proportional to $(e_1^2 \ln A^2/p^2)^n$ (*), which are the only terms we will account for in calculations of the principal approximation.

First we will show that for the space-like Γ_μ a closed integral equation can be written. For this purpose we will use the fact that the addition of a virtual photon line surrounding two vertices will give only a convergent integral. Therefore in the diagrams representing successive approximations for the vertex part we may neglect the lines belonging to the interference of vertices, which contain powers of logarithms lower then the order of perturbation theory. Particularly we may neglect diagrams with crossing photon lines. In the same manner more complicated diagrams are also excluded. The diagrams which are left form ladders where every vertex has an additional ladder of the same kind, and the photon and electron lines are summed over all approximations, i.e. are represented by the true G and D. The summation of the described scheme with the assumptions implied may be easily performed. Then we arrive to the following equations

$$\Gamma_\sigma(p, p-l; l) = \gamma_\sigma + \frac{e_1^2}{\pi i}\int \Gamma_\mu(p, p-k; k) G(p-k) \Gamma_\sigma(p-k; p-k-l; l) \cdot G(p-k-l)\Gamma_\nu(p-k-l, p-l; k) D_{\mu\nu}(k)\, \mathrm{d}^4k \,. \tag{1.5}$$

2. – The Asymptotical Expression for the Electron Green Function. [3]

In the preceding section we have derived the equations for the fundamental functions in quantum electrodynamics. Since our purpose is the exact solution of these equations we cannot use the usual expressions for the quantities G, $D_{\mu\nu}$ and Γ_μ even with renormalized coefficients.

It was mentioned above that in view of the analytical properties of the functions G and $D_{\mu\nu}$, they may be determined only for negative values of p^2 and k^2 (space vectors). The main interest in solving the equations is the

---

(+) The quadratically divergent photon mass should be put equal zero. The presence of a finite photon mass would violate the charge conservation law.

(*) We should mention, that in general this is not true for not space like Γ_μ. So when k^2 is large compared to p^2 and q^2 the formulae include $\ln k^2/p^2$, $\ln k^2/q^2$, and their common power may be twice the power of e_1^2. This question is discussed in more detail by V. V. Sudakov [2].

behaviour of all functions at large values of momenta $p \gg m$, $k \gg m$. We will suppose the functions G and $D_{\mu\nu}$ to have the form

$$G(p) = \frac{\beta(p^2)}{\hat{p}}, \tag{2.1}$$

$$D_{\mu\nu}(k) = \frac{1}{k^2}\left[d_t(k^2)\left(\delta_{\mu\nu} - \frac{k_\mu k_\nu}{k^2}\right) + d_l(k^2)\,\frac{k_\mu k_\nu}{k^2}\right], \tag{2.2}$$

where the functions $\beta(p^2)$, $d_t(k^2)$, $d_l(k^2)$ are slowly varying functions of p^2 and k^2. As to the Γ_μ, we shall show that the equation (1.5) is satisfied by the following form:

$$\Gamma_\mu(p, q; l) = \gamma_\mu \alpha(f^2), \tag{2.3}$$

where $\alpha(f^2)$ is a slowly varying function and f^2 is any of p^2, q^2 and l^2, if they are of the same order of magnitude. If one of the squares is small compared to the other two, f^2 should be the largest square.

Let us substitute the expressions (2.1), (2.2) and (2.3) in the equation (1.5). It is easy to see that the integral on the right hand side of the equation, excepting from the slowly varying functions, diverges logarithmically at $|k^2| \gg |p^2|$ and $|k^2| \gg |q^2|$. Hence this region plays the main role in the integration. Here we can neglect p, q and l as compared to k and the whole integrated expression becomes a function of k only. After averaging over the directions of k, the integral becomes equal to a scalar function multiplied by γ_μ. This confirms the supposed form (2.3). To transform the integration over the k space to a simple integration over k^2 we use the substitution $k_0 \to ik_0$. Then d^4k transforms to $i(2\pi)^{-2}\mathrm{d}\Omega$. $\mathrm{d}\Omega$ is a volume element in the four dimensional euclidean space and has the form $2\pi^2R^3\,\mathrm{d}R$, where R is the radius equal to $\sqrt{-k^2}$. So we have

$$\mathrm{d}^4k \to \frac{i}{4}\,(-k^2)\,\mathrm{d}(-k^2)\,. \tag{2.4}$$

Introducing a new variable $\xi = \ln(-p^2/m^2)$ we obtain the final equation

$$\alpha(\xi) = 1 + \frac{e_1^2}{4\pi}\int_\xi^\infty \alpha^3(z)\beta^2(z)\,d_l(z)\,\mathrm{d}z\,. \tag{2.5}$$

It should be mentioned that d_t does not enter this equation.

Now we turn to the equation (1.1) for G. It can be seen that the integral in this equation diverges at $k \gg p$. Although this divergence at first sight is linear in k, the averaging over the directions gives again, owing to the vector

character of k, a logarithmic divergence. That means that by expansion of the integrated expressions in reciprocal powers of k we should account everywhere for the terms of the next order. The corresponding terms in G are found directly from the formula (2.1) where we can, of course, in spite of the week dependence of β on p^2, restrict ourselves to the expansion of the denominator, i.e.

$$G(p-k) \approx -\frac{\beta(k^2)}{\hat{k}} - \beta(k^2)\frac{1}{\hat{k}}\hat{p}\frac{1}{\hat{k}}. \tag{2.6}$$

However the corrections of the order of p/k arising from $\Gamma_\mu(p, p-k; k)$ should be also taken into account. To find these corrections we will turn again to the equation for Γ_μ. Since we want to calculate small corrections occurring by passing from $p=0$ to finite p's, we may consider the change of the integral on the right hand side of (1.5) as a sum of changes arising separately from each term of the integrated expression. The evaluation of the resulting expression shows that at $k \gg l$ the integrated function is of the order of $1/k^5$, i.e. the integral converges at large k. However when k is in the interval $l \gg k \gg p$ the integral becomes logarithmic. So this interval is the main region of integration. At larger and smaller values of k the integral gives relatively small corrections which we may disregard within the accepted approximation.

In the mentioned region of integration it is enough to consider only corrections of the order of p/k, since they are considerably larger than p/l. It may be shown that the corrections in the expression for $\Gamma_\sigma(p, p-l; l)$ will have the form

$$[\Delta_1(p^2, l^2)\hat{l}\gamma_\sigma + \Delta_2(p^2, l^2)\gamma_\sigma\hat{l}]\frac{\hat{p}}{l^2}. \tag{2.7}$$

Indeed it is easy to verify that corrections of other types do not appear for G taken in the form (2.6), and if substituted in the integral give again expressions of the form (2.7), and therefore turn out to be zero by comparison of the right and left sides of the equation.

Substituting (2.6) and (2.7) in the equation for Γ_σ and using the transformation (2.4) we come to the following equations for Δ_1, and Δ_2:

$$\begin{cases} \Delta_1(\xi,\eta) = \dfrac{e_1^2}{8\pi}\alpha^2(\eta)\beta(\eta)\displaystyle\int_\xi^\eta \beta(z)\{\Delta_1(\xi,z)[d_l(z)-d_t(z)] + \\ \qquad + [\Delta_2(\xi,z)+\alpha(z)][d_l(z)+d_t(z)]\}\,\mathrm{d}z \\ \Delta_2(\xi,\eta) = \dfrac{e_1^2}{8\pi}\alpha^2(\eta)\beta(\eta)\displaystyle\int_\xi^\eta \beta(z)\{\Delta_1(\xi,z)[d_t(z)+d_t(z)] + \\ \qquad + [\Delta_2(\xi,z)+\alpha(z)][d_l(z)-d_t(z)]\}\,\mathrm{d}z \end{cases} \tag{2.8}$$

where $\xi = \ln(-p^2/m^2)$, $\eta = \ln(-l^2/m^2)$; substituting (2.6) and (2.7) in the integral of the equation for G, where the main region of integration is $p \ll k < \infty$, we obtain, after similar transformations,

$$\frac{1}{\beta(\xi)} = 1 + \frac{e_1^2}{4\pi}\int_{\xi}^{\infty}[\alpha(z)\Delta_1(\xi, z) + \Delta_2(\xi, z)]\beta(z)d_l(z)\,\mathrm{d}z\,. \tag{2.9}$$

Adding the two equations (2.8) we have

$$\Delta_1(\xi, \eta) + \Delta_2(\xi, \eta) = \frac{e_1^2}{4\pi}\alpha^2(\eta)\beta(\eta)\int_{\xi}^{\eta}\beta(z)d_l(z)\,[\Delta_1(\xi, z) + \Delta_2(\xi, z) + \alpha(z)]\,\mathrm{d}z\,.$$

It should be noted that the quantity d_l does not enter in the formulae (2.9) and (2.10). Therefore the equations for Γ_μ and G can be solved independently of calculating the photon Green function $D_{\mu\nu}$. The longitudinal part d_l, as mentioned previously, is an arbitrary quantity which we retain in the equations in order to prove their gauge invariance. Of course the dependence of G and Γ_μ upon d_l does not contradict the gauge invariance. The general gauge transforms of G and Γ_μ shall be found afterwards. Here we restrict ourselves to slowly varying $d_l(k^2)$.

Let us introduce the notation

$$q(\xi, \eta) = \frac{\Delta_1(\xi, \eta) + \Delta_2(\xi, \eta)}{\alpha^2(\eta)\beta(\eta)}\,. \tag{2.11}$$

The function $q(\xi, \eta)$ satisfies the equation

$$q(\xi, \eta) = \frac{e_1^2}{4\pi}\int_{\xi}^{\eta}\alpha^2(z)\beta^2(z)d_l(z)\,q(\xi, z)\,\mathrm{d}z + \frac{e_1^2}{4\pi}\int_{\xi}^{\eta}\alpha(z)\,\beta(z)d_l(z)\,\mathrm{d}z\,. \tag{2.12}$$

The equation (2.9) can now be written in the form

$$\frac{1}{\beta(\xi)} = 1 + q(\xi, \infty)\,. \tag{2.13}$$

The equations (2.5), (2.12), (2.13) can be solved for α and β. After differentiating equations (2.5) and (2.12) (the second with respect to η) we obtain

$$\frac{\mathrm{d}\alpha}{\mathrm{d}\xi} = -\frac{e_1^2}{4\pi}\alpha^3(\xi)\beta^2(\xi)d_l(\xi)\,, \tag{2.14}$$

$$\frac{\partial q(\xi, \eta)}{\partial \eta} = \frac{e_1^2}{4\pi}\alpha^2(\eta)\beta^2(\eta)d_l(\eta)\,q(\xi, \eta) + \frac{e_1^2}{4\pi}\alpha(\eta)\beta(\eta)d_l(\eta)\,. \tag{2.15}$$

There should be added the boundary conditions:

$$\alpha \to 1 \qquad \text{when} \qquad \xi \to 1\,,$$

$$q = 0 \qquad \text{at} \qquad \xi = \eta\,.$$

Introducing a new function $r(\xi, \eta) = \alpha(\eta) q(\xi, \eta)$ we have

$$\frac{\partial r(\xi, \eta)}{\partial \eta} = \frac{e_1^2}{4\pi} \alpha^2(\eta) \beta(\eta) d_l(\eta)\,.$$

Hence

$$r(\xi, \eta) = \frac{e_1^2}{4\pi} \int_{\xi}^{\eta} \alpha^2(z) \beta(\eta) d_l(z)\, \mathrm{d}z\,,$$

$$\frac{\partial r(\xi, \eta)}{\delta \xi} = -\frac{e_1^2}{4\pi} \alpha^2(\xi) \beta(\xi) d_l(\xi)\,.$$

From (2.13) we have that, when $\eta \to \infty$, $r(\xi, \infty) = (1/\beta(\xi)) - 1$. Hence:

$$\mathrm{d}\beta/\mathrm{d}\xi = (e_1^2/4\pi)\alpha^2(\xi)\beta^3(\xi) d_l(\xi).$$

From this equation and (2.14) it follows that $\alpha\beta = \text{const}$, and taking into account the boundary conditions we have:

$$\alpha(\xi)\beta(\xi) = 1\,. \tag{2.16}$$

It is easy to see that this formula follows immediately from the Ward's theorem [4]

$$\Gamma_\mu(p, p; 0) = \frac{\partial G^{-1}(p)}{\partial p_\mu}\,,$$

if we mention that the slowly varying function β gives terms of higher order by differentiation.

After the substitution of (2.16) into the equation (2.14) we obtain finally, making use also of the boundary condition

$$\alpha(\xi) = \exp\left[\frac{e_1^2}{4\pi} \int_{\xi}^{\infty} d_l(z)\, \mathrm{d}z\right], \quad \beta(\xi) = \exp\left[-\frac{e_1^2}{4\pi} \int_{\xi}^{\infty} d_l(z)\, \mathrm{d}z\right]. \tag{2.17}$$

The formulae express in fact the gauge transformation of G and Γ_μ (for slowly varying d_l). The most convenient choice is evidently $d_l = 0$ (contrary to the usual assumption $d_l = 1$). Then to the considered order Γ_μ and G have no divergences at all and these quantities (Γ_μ with the mentioned

limitations) are equal to their zeroth approximation values. It should be mentioned that this calibration actually corresponds to the Lorenz condition $\partial A_i/\partial x_i = 0$.

3. – The Asymptotic Expression for the Photon Green Function. [5]

Now we proceed to the calculation of the photon Green function $D_{\mu\nu}$. The integral standing in the equation for $D_{\mu\nu}$ (1.3) diverges at large k, this time quadratically. However, as the value of the integral at $k = 0$ should vanish in consequence of charge conservation (the transverse character of the Dirac current), we may consider only the difference between this integral and its value at $k = 0$. Taking in view that terms having p^3 in the denominator give zero being averaged over the angles, we arrive again to a logarithmic integral. According to the fact that the region $p \ll k$, as it is easily seen, gives nothing noticeable in the integral, it is enough to consider only the region $p \gg k$.

Calculating the logarithmic integral we have to take into account the corrections in $\Gamma_\mu(p, p-k; k)$ of the second order in (k/p), as it was done in the preceding section. To find these corrections we will use the equation for Γ_σ (1.5) with the following transformation of the variable in the integral: $k' \to p - k$. Then the integral takes the form

$$\int D_{\mu\nu}(p-k')\,\Gamma_\mu(p, k'; p-k')\cdot$$
$$\cdot\, G(k')\,\Gamma_\sigma(k', k'-l; l)\,G(k'-l)\,\Gamma_\nu(k'-l, p-l; k'-p)\,\mathrm{d}^4k'.$$

Here it is assumed $p \gg l$. It is evident that in the expansion of $G(k'-l)$ in powers of l, terms of the second order in l arise which give a logarithmic integral in the region $p \gg k' \gg l$. The terms of the first order in l cannot appear because they have k'^3 in the denominator and vanish after integration over the angles. The terms of considered order may come from $G(k'-1)$ and from $\Gamma_\sigma(k', k'-l; l)$. The l dependence of the last Γ_ν gives terms not of the order l^2/k^2, but of the order of l^2/p^2, which may be neglected.

We start with the calculation of corrections coming from $G(k'-l)$. After some calculations we find

$$(3.1)\qquad \frac{e_1^2}{24\pi}\left\{2d_t(\xi)\,\frac{\hat{l}\hat{\gamma}_\sigma\hat{l} - l^2\gamma_\sigma}{p^2} + [d_l(\xi) - d_t(\xi)]\,\frac{l^2\hat{p}\hat{\gamma}_\sigma\hat{p} - \hat{p}\hat{l}\hat{\gamma}_\sigma\hat{l}\hat{p}}{p^4}\right\}\alpha^2(\xi)\int_\eta^\xi \alpha(z)\,\beta^2(z)\,\mathrm{d}z\,,$$

where $\xi = \ln(-p^2/m^2)$, $\eta = \ln(-l^2/m^2)$.

It turns out that the corrections to $\Gamma_\sigma(p, p-l; l)$ should be supposed

to have the form

$$(3.2)\qquad s(\xi,\eta)\alpha^2(\xi)\left\{2d_l(\xi)\frac{\hat{l}\gamma_\sigma\hat{l}-l^2\gamma_\sigma}{p^2}+[d_l(\xi)-d_l(\xi)]\frac{l^2\hat{p}\gamma_\sigma\hat{p}-\hat{p}\hat{l}\gamma_\sigma\hat{l}\hat{p}}{p^4}\right\}.$$

Substituting this expression in the integral and comparing terms on the left and right sides of the equation (1.5) for Γ_σ, we obtain the following equation for $s(\xi,\eta)$:

$$(3.3)\qquad s(\xi,\eta)=\frac{e_1^2}{4\pi}\int_\eta^\xi \alpha^2(z)\beta^2(z)d_l(z)s(z,\eta)\,\mathrm{d}z+\frac{e_1^2}{24\pi}\int_\eta^\xi \alpha(z)\beta^2(z)\,\mathrm{d}z\,.$$

Substituting the expression (3.2) giving the correction to Γ_σ, into the equation for $D_{\mu\nu}$ (1.3) we obtain

$$(3.4)\qquad \mathrm{d}_l(\eta)=1-8d_l(\eta)\left[\frac{e_1^2}{4\pi}\int_\eta^L \alpha^2(z)\beta^2(z)d_l(z)s(z,\eta)\,\mathrm{d}z+\frac{e_1^2}{24\pi}\int_\eta^L \alpha(z)\beta^2(z)\,\mathrm{d}z\right].$$

In this formula L denotes the upper limit of the considered values of the quantity η, which is determined by the radius of smearing out of the interactions. As already said, according to our scheme of smeared out interaction, the magnitude of interaction should drop rapidly when the momentum exceeds the critical value $\Lambda\sim 1/a$, where a is the radius of interaction. The condition $p\ll\Lambda$ turns to $\xi\ll L$ on logarithmic scale, because considerable changes of p correspond to relatively small changes of $\ln(-p^2/m^2)$. Therefore the fact of smearing out produces an upper limit L in all integrals. It should be emphasized that, according to the general scheme, the constant e_1 is actually a function of the range of interaction i.e. of the quantity Λ. In calculating G and Γ_μ it was unnecessary to use the smearing out because of the divergence of $d_l(\xi)$, which is arbitrary and independent of the character of interaction. But if we introduce the smearing out we have to put the upper limit L, instead of the infinity, in the integrals standing in the exponents of α and β.

It should be mentioned that then we have $\beta(L)=1$. This corresponds to the evident fact that at $p\gg\Lambda$ the electron must behave as free, not interacting with the photon field. Comparing the formula (3.4) with the formula (3.5) we obtain:

$$(3.5)\qquad \frac{1}{d_l(\eta)}=1+8s(L,\eta)\,.$$

Differentiating the equation (3.3) with respect to ξ and taking into account

the relations $\alpha = 1/\beta$ and $\mathrm{d}\beta/\mathrm{d}\xi = (e_1^2/4\pi)d_t(\xi)\beta(\xi)$ we have

$$\frac{\partial s(\xi, \eta)}{\partial \xi} = s(\xi, \eta)\frac{1}{\beta(\xi)}\frac{\mathrm{d}\beta(\xi)}{\mathrm{d}\xi} + \frac{e_1^2}{24\pi}\beta(\xi)\,. \tag{3.6}$$

Hence

$$\frac{\partial}{\partial \xi}\left(\frac{s(\xi, \eta)}{\beta(\xi)}\right) = \frac{e_1^2}{24\pi}\,.$$

Noting that $s = 0$ for $\xi = \eta$ in accordance with (3.3) we have

$$s(\xi, \eta) = \frac{e_1^2}{24\pi}(\xi - \eta)\beta(\xi)\,. \tag{3.7}$$

Substituting here $\xi = L$ and remembering $\beta(L) = 1$ we come to the final expression

$$d_t(k^2) = \frac{1}{1 + (e_1^2/3\pi)\ln\left(\Lambda^2/(-k^2)\right)}\,. \tag{3.8}$$

It should be mentioned that, contrary to G and Γ_μ, this expression does not include the arbitrary function d_t, quite as it should be according to gauge invariance. At $k^2 \ll m^2$, $\ln(\Lambda^2/m^2)$ stands in place of $\ln(\Lambda^2/(-k^2))$. If particles other than electrons participate in vacuum polarisation, then the formula takes the form

$$d_t(k^2) = \frac{1}{1 + (\nu e_1^2/3\pi)\ln\left(\Lambda^2/(-k^2)\right)}\,, \tag{3.9}$$

where the contribution of particles with spin 1/2 and charge Ze equals Z^2, and that of particles with spin 0 equals $Z^2/4$. Particles with higher spins give quadratically divergent expressions which we disregard here, the more so, as there is no indication on the existence of such particles in nature.

The analysis of physical effects shows that the physical charge e is expressed in terms of e_1 by means of the relation

$$e^2 = e_1^2 \lim_{k^2 \to 0} d_t(k^2). \tag{3.10}$$

From formula (3.9) it follows therefore

$$e^2 = \frac{e_1^2}{1 + (\nu e_1^2/3\pi)\ln\left(\Lambda^2/m^2\right)}\,, \tag{3.11}$$

or

$$e_1^2 = \frac{e^2}{1-(ve_1^2/3\pi)\ln(\Lambda^2/m^2)}. \tag{3.12}$$

Expressing d_t through e^2 we have

$$d_t(k^2) = \frac{e^2}{e_1^2}\frac{1}{1-(ve^2/3\pi)\ln(-k^2/m^2)}. \tag{3.13}$$

The formula (3.13) is evidently renormalizable, i.e. we can change in all the formulae the « bare » charge e_1 into the physical charge e multiplying simultaneously $D_{\mu\nu}$ by the renormalizing factor $Z_3 = e_1^2/e^2$. Thereafter all the quantities will not depend upon the cut-off limit and the charge e_1, which is connected with it.

From the formula (3.12) it follows that, for sufficiently large Λ, e_1^2 may become of the order of unity and the considered approximation fails. Hence the electrodynamics with weak coupling is a logically unclosed theory. It could be supposed that this theory should be supplemented by a strong-coupling theory at great energies. However I. Ja. Pomerančuk and L. D. Landau suggested that there is a reason to understand the situation in a different way. According to their considerations, the formula (3.11) will be correct not only for small e_1^2 but also for $e_1^2 \gtrsim 1$. Then regarding the physical charge e as a function of e_1 and Λ, it may be seen that under a given Λ, however large e_1^2 may be, it cannot make e^2 exceed some limit, tending to zero with increasing Λ. This brings us to the conclusion that point interaction is impossible in pure electrodynamics.

It should be mentioned however that the whole question for electrodynamics has only a methodological sense, since at great energies other types of interactions may play a considerable role, in particular the gravitation.

Here we assumed everywhere that the radii of smearing out in the Dirac current and in the interaction of this current with electromagnetic potentials are equal. This assumption may be put aside. We will show how the results are changed if the radii are different. Let us introduce two different cut-off limits, Λ_ψ corresponding to the smearing out of the Dirac current, and Λ_A corresponding to the smearing out of the electromagnetic interaction of the current. It should be noticed that the Λ's must satisfy the condition $\Lambda_A \lesssim \Lambda_\psi$. Then the formula (2.17) for $\alpha(\xi)$ and $\beta(\xi)$ will change to

$$\alpha(\xi) = \beta^{-1}(\xi) = \exp\left[\frac{e_1^2}{4\pi}\int_{\xi}^{L_A} d_l(z)\,dz\right] \qquad L_A = \ln(\Lambda_A^2/m^2). \tag{3.14}$$

As to the d_t a simple calculation gives the following result

$$d_t = \frac{1}{1 + (ve_1^2/3\pi) \ln (\Lambda_\varphi^2/ - k^2)} \qquad \text{for } |k^2| < \Lambda_\Delta^2 \tag{3.15}$$

$$d_t = 1 \qquad \text{for } |k^2| > \Lambda_\Delta^2. \tag{3.16}$$

It may be seen that in the case $\Lambda_\varphi \gg \Lambda_\Delta$, the d_t function undergoes a rapid change in the vicinity of $k^2 = \Lambda_\Delta^2$.

4. – The Mass of the Electron in Quantum Electrodynamics. [6]

Now we will consider the mass of the electron, particularly the roles of electromagnetic and « bare » masses. The most important point in this respect is the behaviour of the electron Green function $G(p)$ when p^2 becomes of the order of m^2. In Section 2 we have obtained an asymptotic form of the electron Green function, justified for $p \gg m$. For the mass calculation it is insufficient to consider this expression of $G(p)$ at $p \sim m$, but we have to find corrections to this expression. Let us suppose that $G(p)$ has the form

$$G(p) = \frac{\beta(p^2)}{\hat{p} - m(p^2)}, \tag{4.1}$$

where $\beta(p^2)$ is the function introduced in Section 2 and $m(p^2)$ a new slowly varying function of p^2. At large values of p, the ratio of the second term in the denominator to the first one becomes negligible, in any case considerably smaller than the inaccuracy in the calculated function $\beta(p^2)$. Nevertheless the consideration of this term is justified because, contrary to the first term, it is an even function of the vector p. Therefore the inaccuracy in β cannot have any influence upon the value of $m(p^2)$. For large values of p, $G(p)$ may be written in the form

$$G(p) = \frac{\beta(p^2)}{\hat{p}} + \frac{\beta(p^2) m(p^2)}{p^2}, \tag{4.2}$$

where the first term is an odd and the second an even function of p.

Let us write the equation for the G function

$$G^{-1}(p) = \hat{p} - m_1 + \frac{e_1^2}{\pi i} \int \Gamma_\mu(p, p-k; k)\, G(p-k) \gamma_\nu D_{\mu\nu}(k)\, \mathrm{d}^4 k \tag{4.3}$$

and separate from both sides the even function of p which must be equal

to each other. Determining the even part of the integral on the right side we will change the sign of the variable k also. Then the even part of the integrated expression will consist of the product of the even part of Γ_μ (with respect to the change of sign of all variables) and the even part of G, and of the product of the odd part of Γ_μ and the odd part of G. In the first case we can use $\alpha(k^2)\gamma_\mu$ for Γ_μ, and the second term of (4.2) for G. In the latter case G is taken with the old form $\beta(p^2)/\hat{p}$, and the odd part of Γ_μ should be defined from the equation for Γ_σ (1.5).

Equating the odd parts of the expressions on either side of the equation, we will change the sign of the variable k together with the signs of p and e. Thereafter the odd part of the integral expression will contain either the even part of one of the G's or the odd part of one of the Γ's. Other possibilities give terms of higher order. At first we will consider the influence of the even addition to G. Suppose $p \ll 1$. Then it is easy to see that the principal term of the expression comes from the even addition only to one of the G's, namely to $G(p-k)$. The corresponding integral is logarithmic in the region $p \ll k \ll l$ and converges rapidly in the other regions. Direct calculation gives the following expression

$$-\frac{e_1^2}{4\pi}\frac{l_\sigma}{l^2}\alpha^2(\eta)\beta(\eta)\int_\xi^\eta \beta(z)\alpha(z)\,m(z)[3d_t(z)+d_l(z)]\mathrm{d}z\,,$$

where, as before,

$$\xi=\ln\left(\frac{-p^2}{m^2}\right),\qquad \eta=\ln\left(\frac{-l^2}{m^2}\right).$$

Now we will find the odd part of Γ_σ, which we suppose to have the form $(l_\sigma/l^2)\alpha^2(\eta)\beta(\eta)t(\xi,\eta)$.

One can easily verify that only the addition to the first $\Gamma_\mu(p, p-k; k)$ in (1.5) will give important terms. After substitution in (1.5), we obtain an integral equation for $t(\xi,\eta)$

$$t(\xi,\eta)=\frac{e_1^2}{4\pi}\int_\xi^\eta \alpha^2(z)\beta^2(z)d_l(z)\,t(\xi,z)\mathrm{d}z-\frac{e_1^2}{4\pi}\int_\xi^\eta \alpha(z)\beta(z)\,m(z)[3d_t(z)+d_l(z)]\,\mathrm{d}z\,. \tag{4.4}$$

Substituting into equation (4.3) the expressions of the addition made to G and Γ_μ, we obtain from the even part of this equation

$$-\frac{m(\xi)}{\beta(z)}=-m_1+\frac{e_1^2}{4\pi}\int_\xi^L \alpha^2(z)\beta^2(z)d_l(z)\,t(\xi,z)\,\mathrm{d}z- \tag{4.5}$$

$$-\frac{e_1^2}{4\pi}\int_\xi^\eta \alpha(z)\beta(z)\,m(z)[3d_t(z)+d_l(z)]\,\mathrm{d}z\,.$$

Then it follows

$$m(\xi) = \beta(\xi)[m_1 - t(\xi, L)] . \tag{4.6}$$

Differentiating the equation (4.4) with respect to η, and using the formulae $\alpha\beta = 1$ and $\mathrm{d}\beta/\mathrm{d}\xi = (e_1^2/4\pi)\beta d_t$, we obtain

$$\frac{\partial t(\xi, \eta)}{\partial \eta} = \frac{1}{\beta(\eta)} \frac{\mathrm{d}\beta(\eta)}{\mathrm{d}\eta} t(\xi, \eta) - \frac{e_1^2}{4\pi} m(\eta)[3d_t(\eta) + d_l(\eta)]$$

or

$$\frac{\partial}{\partial \eta}\left(\frac{t(\xi, \eta)}{\beta(\eta)}\right) = -\frac{e_1^2}{4\pi} \frac{m(\eta)}{\beta(\eta)} [3d_t(\eta) + d_l(\eta)] .$$

Taking into account that, according to (4.4), $t(\xi, \eta) = 0$ at $\xi = \eta$, we have

$$\frac{t(\xi, \eta)}{\beta(\eta)} = -\frac{e_1^2}{4\pi} \int_{\xi}^{\eta} \frac{m(z)}{\beta(z)} [3d_t(z) + d_l(z)] \, \mathrm{d}z .$$

Differentiating with respect to ξ we obtain

$$\frac{1}{\beta(\eta)} \frac{\partial t(\xi, \eta)}{\partial \xi} = \frac{e_1^2}{4\pi} \frac{m(\xi)}{\beta(\xi)} [3d_t(\xi) + d_l(\xi)] .$$

Substituting $\eta = L$, and noting that $\beta(L) = 1$, we have

$$\frac{\mathrm{d}}{\mathrm{d}\xi} \frac{m(\xi)}{\beta(\xi)} = -\frac{e_1^2}{4\pi} \frac{m(\xi)}{\beta(\xi)} [3d_t(\xi) + d_l(\xi)] ,$$

or, using the relation $\mathrm{d}\beta/\mathrm{d}\xi = (e_1^2/4\pi)\beta d_t$

$$\frac{\mathrm{d}m}{\mathrm{d}\xi} = -\frac{3e_1^2}{4\pi} d_t(\xi) \, m(\xi) .$$

Substituting d_t in formula (3.11) we arrive to the final expression

$$m(\xi) = m(0)\left(1 - \frac{e^2}{3\pi} \nu\xi\right)^{9/4\nu} , \tag{4.8}$$

where the constant $m(0)$ is the value of $m(\xi)$ at $\xi = 0$, i.e. the observable mass of the electron.

In the usual notation, (4.8) is

$$m(p^2) = m\left[1 - \frac{e^2}{3\pi} \nu \ln\left(\frac{-p^2}{m^2}\right)\right]^{9/4\nu} . \tag{4.9}$$

The formula (4.8) defines $m(p^2)$ for $p^2 \gg m^2$. The case $|p^2| \ll m^2$ does not differ essentially from the case $p^2 \sim m^2$, i.e. in this case $m\,(p^2) = m$. At $p^2 = m^2$ the denominator of the formula (4.1) becomes zero, therefore the case of p^2 approaching m^2 to such an extent that $e^2 \ln\,(m^2/(p^2 - m^2)) \sim 1$ should be treated separately.

The formula (4.9) is gauge invariant and does not depend on the smearing out radius. It follows from (4.9) that the mass of the particle decreases by increasing k^2. The quantity m_1, according to (4.6), is equal to $m(L)$, i.e. corresponds to the value k^2 related to the smearing out radius

$$m_1 = m\left(\frac{e^2}{e_1^2}\right)^{9/4\nu}. \tag{4.10}$$

At the limit of applicability of the theory, $e_1 \sim 1$ and $m_1 \sim m_e^{9/2\nu}$, that is a very small quantity. According to (4.10), m_1 decreases with increasing L. Therefore it may be supposed that if the theory were closed, m_1 would turn to zero. It means that the mass of the electron is of electromagnetic nature. So the concept stated above brings us back to the idea of pure electromagnetic electron mass, which was abandoned long ago.

5. – The Infrared Catastrophe. [7]

Up to now we did not consider the behaviour of the electron Green function when the momentum p approaches m to such an extent that $e_1^2 \ln\,(m^2/(p^2 - m^2)) \gtrsim 1$. We were also not interested in the vertex parts Γ_μ whose argument did not satisfy the inequalities of a triangle.

We begin with the calculation of $G(p)$ for p approaching m. According to the general method, we will sum up the terms containing, for a given power of e, the greatest power of $\ln\,(m^2/(p^2 - m^2))$. Here we will use the physical charge together with the renormalized D-function. In this case the considered terms are of the type $[e^2 \ln\,(m^2/(p^2 - m^2))]^n$. Analysing the diagrams for Γ_μ, we see that such terms appear only from diagrams with parallel virtual lines. So the equation (1.5) is completely applicable. Since p is essentially a time-like vector in the interesting region we cannot, in the integral of the equation (1.1), pass to the euclidean space in the same way as before, however we may do it by means of a rotation of space axes: $k_m \to -ik_m$ $(m = 1, 2, 3)$. Then it turns out that again Γ_μ's are needed whose arguments satisfy the triangle rule. These Γ_μ's, together with G, form a closed system.

The G function at $p^2 \approx m^2$ is supposed to have the form

$$G(p) = \frac{p^2 + m}{p^2 - m^2}\,\beta(m^2)\,\sigma(m^2 - p^2)\,, \tag{5.1}$$

where σ is a new slowly varying function. Analysing the integral in the equation (1.5) we come to the conclusion that the region where $p^2 - m^2 \ll (p-k)^2 - m^2 \ll m^2$ plays the main role in the integral. In this region we will suppose $\Gamma_\mu(p, p-l; l)$ to have the form

$$(5.2)\quad (\hat{p}+m)\Gamma_\mu(p, q; l)(\hat{q}+m) = (\hat{p}+m)\gamma_\mu(\hat{q}+m)\tau(m^2-p^2)\alpha(m^2) \qquad \hat{q} = \hat{p} - \hat{l},$$

where τ is a new slowly varying function.

It can be seen that in all applications we use not Γ_μ itself, but its product with $\hat{p}+m$ on the left and $\hat{q}+m$ on the right. This is the quantity we have to find. In the integral of the equation for Γ_μ the main region is $q^2 - m^2 \ll (p-k)^2 - m^2 \ll m^2$. Transforming the equation for Γ_μ in this region we obtain the equation for τ

$$(5.3)\qquad \tau(\eta) = 1 - \frac{3e^2}{2\pi}\int_0^\eta \tau^3(z)\,\sigma^2(z)\,\mathrm{d}z\,,$$

where

$$\eta = \ln\frac{m^2}{m^2-q^2}\,, \qquad z = \ln\frac{m^2}{m^2-(p-k)^2}\,.$$

Analysing the integral in the equation (1.1) we see that, as before, we have to find corrections to the expression (5.2) of Γ_μ proportional to $(p^2-m^2)/(q^2-m^2)$.

These corrections are found from the equation (1.5) where the main region of integration is $p^2 - m^2 \ll (p-k)^2 - m^2 \ll q^2 - m^2$. Omitting the detailed calculations we will write the final results.

$$(5.4)\qquad \tau(\xi)\,\sigma(\xi) = 1\,,$$

$$(5.5)\qquad \sigma(p) = \left(\frac{m^2}{m^2-p^2}\right)^{(e^2/2\pi)(3-d_i^0)}, \quad \text{where} \qquad d_i^0 = d_i(k^2=0)\,.$$

So G appears to have, at $p^2 = m^2$, not a pole but in general a critical point.

The calculated τ belongs to a $\Gamma_\mu(p, q; l)$ with $p^2 \approx m^2$, $q^2 \approx m^2$ and $l^2 \ll m^2$. Γ_μ was determined also in a more general case: $(pq) \gg p^2 - m^2$, $q^2 - m^2$. As before, only terms with highest powers of logarithms were accounted for, those corresponding to $[e^2 \ln((m^2/(p^2-m^2))]^n$ and $(e^2 \ln^2(pq/m^2))^n$. To calculate the Γ_μ one has to sum up diagrams with all virtual lines surrounding the original vertex. We will omit the calculations. The result is

$$(5.6)\quad (\hat{p}+m)\Gamma_\mu(p, q; l)(\hat{q}+m) = \alpha(m^2)\,(\hat{p}+m)\gamma_\mu(\hat{q}+m)\exp\left[-\frac{e^2}{2\pi}f\right],$$

where f is equal to

$$f = \frac{a}{\sqrt{a^2-1}} S + \frac{1}{2\sqrt{2}}(1-d_1^0)(L_1+L_2)\,. \tag{5.7}$$

Here $a = (pq)/m^2$, S is the area on the plane λ and μ, restricted by the conditions

$$\begin{cases} 0 < \lambda < \ln \dfrac{(pq)}{p^2 - m^2}\,, \\ 0 < \mu < \ln \dfrac{(pq)}{q^2 - m^2}\,, \end{cases} \tag{5.8}$$

$$\mu + \ln(a + \sqrt{a^2-1}) > \lambda > \mu - \ln(a - \sqrt{a^2-1}) \tag{5.9}$$

and L_1, L_2 are the lengths of the pieces of the lines $\lambda = \mu \pm \ln(a + \sqrt{a^2-1})$ which are cut out by the conditions (5.8).

A method analogous to that applied to calculation of Γ_μ was then used to investigate the question about the radiation of additional quanta in physical effects, the so called infrared catastrophe. The probability of such radiation appears to be represented by the Poisson formula

$$W(n) = \frac{e^{-\bar{n}}}{n!}(\bar{n})^n\,. \tag{5.10}$$

The factor $e^{-\bar{n}}$ in this formula comes from the integrals over virtual quanta and is essentially defined by the formula (4.6). So it becomes clear that the found deviation of Γ_μ from the zeroth approximation of perturbation theory comes from the infrared catastrophe.

The results represented here are essentially the same for the additional radiation in other physical effects.

So it occurs that at great energies the major department from the zeroth approximation of perturbation theory (effects of order $e^2 \ln^2 (E/m)$) comes from the infrared catastrophe.

6. - The Gauge Transformations of the Green Functions of Charged Particles.

The theory describing the field of charged particles coupled to the electromagnetic field has the property of gauge invariance. By the gauge transformation of potentials of the electromagnetic field

$$A_\mu \to A_\mu + \frac{\partial \varphi}{\partial x_\mu} \tag{6.1}$$

(φ is an arbitrary scalar operator) the ψ operators of the particles transform in the following way

$$\psi \to \psi \exp[ie\varphi] . \tag{6.2}$$

Here we will consider how the Green functions of the particles are changed under the gauge transformation. The particle Green function, as it is well known, is

$$G(x, x') = -i\langle(\psi(x)\psi(x'))_+\rangle . \tag{6.3}$$

Here the bracket means the vacuum expectation value.

By the gauge transformation (6.1) the Green function will change. According to (6.2), this may be written in the form

$$G(x, x') = G_0(x, x')\langle(\exp[ie\varphi(x)]\exp[-ie\varphi(x')])_+\rangle . \tag{6.4}$$

Here $G_0(x, x')$ is the Green function calculated for the particular case when the longitudinal (in four dimensional sense) part of the photon Green function is equal to zero.

In accordance with the transverse character of the Dirac current, the longitudinal part of the potential does not participate in the interaction of fields and therefore the task consists in averaging the expression $\exp[ie\varphi(x)]\cdot\exp[-ie\varphi(x')]$ over the vacuum state where the operators φ belong to a free field. Then we have

$$G(x, x') = G_0(x, x')\exp\left[ie^2(\Delta_F(0) - \Delta_F(x, x'))\right] , \tag{6.5}$$

where Δ_F is a Green function of the φ field

$$\Delta_F(x, x') = i\langle(\varphi(x)\varphi(x'))_+\rangle . \tag{6.6}$$

The photon Green function in general contains a longitudinal part as well as a transverse part (formula (2.2)). It is easy to see that $d_l(k^2)$ is connected with the Fourier component $\Delta_F(k)$ of the function $\Delta_F(x, x')$ in the following manner

$$\Delta_F(k) = 4\pi\frac{d_l(k^2)}{k^4} . \tag{6.7}$$

The gauge transforms of Fourier components of the Green functions can be found only for infinitesimal gauge transformations of potentials.

Variating the relation (6.5) we have:

$$\delta G(x, x') = ie^2 G(x, x')(\delta\Delta_F(0) - \delta\Delta_F(x, x')) . \tag{6.8}$$

Taking Fourier transforms of both sides and taking into account (6.7), we find:

$$\delta G(p) = -\frac{e^2}{\pi i}\int \frac{\delta d_l(k^2)}{k^4}\{G(p) - G(p-k)\}\,\mathrm{d}^4k\,. \tag{6.9}$$

For a particle having spin 1/2 in the case when $d_l(k^2)$ is a slowly varying function this formula reduces to (2.17).

The gauge transform of Γ_μ may be obtained in an analogous manner. Omitting the detailed calculation we will write only the result

$$\begin{aligned} G(p)\,\delta\Gamma_\mu(p,\, p-k;\, k)\,G(p-k) = \frac{e^2}{\pi i}\int\{&G(p)\,\Gamma_\mu(p,\, p-k;\, k)\cdot \\ &\cdot[G(p-k) - G(p-k-r)] + G(p-r)[\Gamma_\mu(p-r,\, p-r-k;\, k)\cdot \\ &\cdot G(p-r-k) - \Gamma_\mu(p,\, p-k;\, k)G(p-k)]\}\,\frac{\delta d_l(r)}{r^4}\,\mathrm{d}^4r\,. \end{aligned} \tag{6.10}$$

For a particle with spin 1/2 and slowly varying $d_l(k^2)$ this gives (2.17). However the formulae (6.9) and (6.10) are applicable indeed for charged particles of any spin.

7. – The Green Functions in the Meson Theory with Weak Pseudoscalar Coupling. [8]

Now we will try to apply the methods used in the preceding sections for quantum electrodynamics to the meson theory with weak pseudoscalar coupling. As in electrodynamics, we will find the expressions of the fundamental functions: $G(p)$ the Green function of a nucleon, $D(k)$ the Green function of a meson and the related vertex part $\Gamma(p)$ of space vectors p, q and l. The fundamental equations are analogous to those derived in section 1, and have the form

$$G(p)\left\{\hat{p} - M_1 - \frac{g_1^2}{\pi i}\int \Gamma_\mu(p,\, p-k;\, k)\,G(p-k)\tau_\nu\gamma_5 D_{\mu\nu}(k)\,\mathrm{d}^4k\right\} = 1 \tag{7.1}$$

$$D_{\mu\tau}(k)\left\{(k^2-\mu_1^2)\,\delta_{\tau\nu} + \frac{g_1^2}{\pi i}\,\mathrm{Sp}\left[\int G(p)\,\Gamma_\tau(p,\, p-k;\, k)\,G(p-k)\tau_\nu\gamma_5\,\mathrm{d}^4p\right]\right\} = \delta_{\mu\nu}\,, \tag{7.2}$$

$$\begin{aligned} \Gamma_\sigma(p,\, p-l;\, l) = \gamma_5\tau_\sigma + \frac{g_1^2}{\pi i}\int &\Gamma_\mu(p,\, p-k;\, k)\,G(p-k)\,\Gamma_\sigma(p-k,\, p-k-l;\, l)\cdot \\ &\cdot G(p-k-l)\,\Gamma_\nu(p-k-l,\, p-l;\, k)\,D_{\mu\nu}(k)\,\mathrm{d}^4k\,. \end{aligned} \tag{7.3}$$

Here the following notations were used: $\gamma_5 = i\gamma_1\gamma_2\gamma_3\gamma_0$ ($\gamma_{1,2,3} = \beta\alpha_{1,2,3}$, $\gamma_0 = \beta$);

M_1, μ_1 are the bare masses of the nucleon and meson, g_1 the bare coupling constant depending on the cut-off limit, the Greek indices here denote the components in isotopic space, τ_μ are the operators of isotopic spin. It should be mentioned also that the Sp in (7.2) is extended over the isotopic as well as over the Dirac matrices.

From (7.2) it is easy to see that $D_{\mu\nu}(k) = \delta_{\mu\nu} D(k)$. This gives us a possibility to eliminate the τ_μ operators from the equations, introducing $\Gamma_\mu = \tau_\mu \Gamma$. After this, the equations take the form:

$$\Gamma(p, p-l; l) = \gamma_5 - \frac{g_1^2}{\pi i}\int \Gamma(p, p-k; k) G(p-k) \Gamma(p-k, p-k-l; l) \cdot \cdot G(p-k-l)\Gamma(p-k-l, p-l; k) D(k) \, \mathrm{d}^4(k) , \tag{7.4}$$

$$G(p)\left\{\hat{p} - M_1 - \frac{3g_1^2}{\pi i}\int \Gamma(p, p-k; k) G(p-k)\gamma_5 D(k) \, \mathrm{d}^4 k\right\} = 1 , \tag{7.5}$$

$$D(k)\left\{k^2 - \mu_1^2 + \frac{2g_1^2}{\pi i} \operatorname{Sp}\left(\int G(p)\Gamma(p, p-k; k) G(p-k)\gamma_5 \, \mathrm{d}^4 p\right)\right\} = 1 , \tag{7.6}$$

where the Sp sign belongs to the Dirac matrices.

We will find from these equations the asymptotic form of the functions G, D and Γ. We suppose the functions $G(p)$ and $D(k)$, for large values of momenta $p \gg M$, $k \gg M$, to have the form

$$G(p) = \frac{\beta(p^2)}{\hat{p} - M(p^2)} , \quad D(k) = \frac{d(k^2)}{k^2} . \tag{7.7}$$

As before, although $M(p^2) \ll p$, the function $M(p^2)$ can be derived because it is the even part of $G^{-1}(p)$. As to the function $\mu(k^2)$, the definition of this function is impossible in our consideration, because it cannot be separated from the much bigger k^2. Therefore we will restrict ourselves to the form (7.7) of $D(k)$.

The Γ function in the case when p, q and l are of the same order, or two of them are much greater than the third, is given by the formula $\Gamma = \gamma_5 \varkappa(f^2)$, where f^2 is the greatest of the squares. Noticing that the integral in (7.4) is logarithmic in the region $f^2 \ll k^2 \ll \infty$, the equation for $\varkappa$ may be written in the form

$$\alpha(\xi) = 1 + \frac{g_1^2}{4\pi}\int_{\xi}^{L} d(z)\, \alpha^3(z)\, \beta^2(z) \, \mathrm{d}z, \tag{7.8}$$

where $\xi = \ln(-p^2/M^2)$, $L = \ln(-\Lambda^2/M^2)$, Λ being the momentum corresponding to the smearing out radius.

In accordance to the fact that the expression in the integral of equation (7.5) has a k^3 in the denominator we have to account for terms of the first order with respect to p/k in G and Γ. These terms arise in G directly from the formula (7.7), and in Γ from the equation (7.4).

Finding the alterations occurring in the integral of the equation (7.4) from $G(p-k)$, it may be seen that the addition to Γ must have the form

$$\alpha^2(l^2)\beta(l^2)\left(\frac{\hat{p}\,\hat{l}}{l^2}\Delta_1(p^2, l^2) + \frac{\hat{l}\,M}{l^2}\Delta_2(p^2, l^2)\right)\gamma_5 . \tag{7.9}$$

Here the first term in the brackets belongs to the even part, and the second term to the odd part of Γ. Equating the even and odd parts of equation (7.4) we find the equations for Δ_1 and Δ_2

$$\Delta_1(\xi, \eta) = \frac{g_1^2}{4\pi}\int_{\xi}^{\eta}\alpha^2(z)\beta^2(z)d(z)\Delta_1(\xi, z)\,\mathrm{d}z - \frac{g_1^2}{8\pi}\int_{\xi}^{\eta}\alpha(z)\beta(z)d(z)\,\mathrm{d}z , \tag{7.10}$$

$$\Delta_2(\xi, \eta_l) = \frac{g_1^2}{4\pi}\int_{\xi}^{\eta}\alpha^2(z)\beta^2(z)d(z)\Delta_2(\xi, z)\,\mathrm{d}z - \frac{g_1^2}{4\pi}\int_{\xi}^{\eta}\alpha(z)\beta(z)d(z)\,\mathrm{d}z , \tag{7.11}$$

where $\xi = \ln(-p^2/M^2)$, $\eta = \ln(-l^2/M^2)$.

Substituting the formula (7.9) in the equation (7.5), we note that there appear the same integrals as in the formulae (7.10) and (7.11), but with the limit L, i.e., correspondingly, $\Delta_1(\xi, L)$ and $\Delta_2(\xi, L)$. Separating the even and odd parts of the derived equation, we obtain two equations

$$\frac{1}{\beta(\xi)} = 1 - 3\Delta_1(\xi, L) , \tag{7.12}$$

$$\frac{M(\xi)}{\beta(\xi)} = M_1 + 3\Delta_2(\xi, L) . \tag{7.13}$$

The equations obtained: (7.8), (7.10)-(7.13) do not form a complete system because they contain the quantity $d(\xi)$, the equation of which has not yet been written. But all the same we can use the equations obtained to find out the connection between the functions $\alpha(\xi)$, $\beta(\xi)$ and $M(\xi)$.

Differentiating (7.9) we obtain:

$$\frac{\mathrm{d}\alpha(\xi)}{\mathrm{d}\xi} = -\frac{g_1^2}{4\pi}\alpha^3(\xi)\beta^2(\xi)d(\xi) . \tag{7.14}$$

Introducing the new variables $\tau_1(\xi, \eta) = \alpha(\eta)\Delta_1(\xi, \eta)$; $\tau_2(\xi, \eta) = \alpha(\eta)\Delta_2(\xi, \eta)$,

differentiating the equations (7.10) and (7.11), and using the equation (7.14), we have:

$$\frac{\partial r_1(\xi, \eta)}{\partial \eta} = -\frac{g_1^2}{8\pi}\alpha^2(\eta)\beta(\eta)d(\eta)\,, \tag{7.15}$$

$$\frac{\partial r_2(\xi, \eta)}{\partial \eta} = \frac{g_1^2}{8\pi}\alpha^2(\eta)\beta(\eta)d(\eta)\,M(\eta)\,. \tag{7.16}$$

According to (7.10) and (7.11), $\tau_1(\xi, \eta)$ and $\tau_2(\xi, \eta)$ should turn to zero at $\xi = \eta$, i.e. they have the form of integrals from ξ to η. Therefore $\partial\tau_1(\xi, \eta)/\partial\xi$ and $\partial\tau_2(\xi, \eta)/\partial\xi$ are represented by the right hand sides of equations (7.15) and (7.16), taken with the opposite sign and with the variable ξ instead of η.

Differentiating the equations (7.12) and (7.13) with respect to ξ and substituting the expressions of the derivatives of Δ (in consequence of $\alpha(L) = 1$, $\Delta_{1,2}(\xi, L) = \tau_{1,2}(\xi, L)$) we obtain:

$$\frac{\mathrm{d}\beta(\xi)}{\mathrm{d}\xi} = \frac{3g_1^2}{8\pi}\alpha^2(\xi)\,\beta^3(\xi)d(\xi)\,, \tag{7.17}$$

$$\frac{\mathrm{d}}{\mathrm{d}\xi}\left(\frac{M(\xi)}{\beta(\xi)}\right) = -\frac{3g_1^2}{4\pi}\alpha^2(\xi)\beta(\xi)d(\xi)\,M(\xi)\,. \tag{7.18}$$

Comparing the equations (7.17) and (7.14) and remembering that, according to (7.12), we have: $\beta(L) = 1$, we obtain

$$\alpha(\xi) = [\beta(\xi)]^{-\frac{1}{2}}\,, \tag{7.19}$$

$$\frac{\mathrm{d}\beta}{\mathrm{d}\xi} = \frac{3g_1^2}{8\pi}[\beta(\xi)]^{\frac{3}{2}}d(\xi)\,. \tag{7.20}$$

Comparing the equations (7.17) and (7.18) and taking into account that, according to (7.13), $M(L) = M_1$, we obtain

$$M(\xi) = \frac{M_1}{\beta(\xi)}\,. \tag{7.21}$$

Now we find the equation for $d(\xi)$. For this purpose let us consider the equation (7.6). It is easy to see that the integrated expression contains p^2 in the denominator. Therefore it is necessary to account for terms appearing in the expansion of the integrated expression up to the order of k^2/p^2. Then the terms of zeroth order give a quadratically divergent integral, which is independent of k and may be enclosed in the proper mass of the meson.

The terms of order k^2/p^2 in $G(p-k)$ are obtained by means of a direct expansion of (7.7). As to the addition coming from Γ it is obtained from equation (7.4), where the change of variable $k'=p-k$ should be done. Finding the change of the integral coming from the addition to G, we conclude that the addition to Γ should have the form:

$$\frac{l^2}{p^2}\alpha^2(p^2)d(p^2)\Delta(p^2, l^2)\,. \tag{7.22}$$

Performing the further derivation with the same procedure described above we come to the relation

$$d(\eta) = [\beta(\eta)]^{8/3}\,. \tag{7.23}$$

Substituting (7.23) in the equation (7.20) and taking into account that $\beta(L)=1$, we obtain

$$\beta(p^2) = \left[1+\frac{5g_1^2}{4\pi}\ln\left(\frac{\Lambda^2}{-p^2}\right)\right]^{-3/10}. \tag{7.24}$$

The functions $\alpha(p^2)$ and $d(p^2)$ are obtained from (7.19) and (7.23)

$$\alpha(p^2) = \left[1+\frac{5g_1^2}{4\pi}\ln\left(\frac{\Lambda^2}{-p^2}\right)\right]^{1/5}, \tag{7.25}$$

$$d(p^2) = \left[1+\frac{5g_1^2}{4\pi}\ln\left(\frac{\Lambda^2}{-p^2}\right)\right]^{-4/5}. \tag{7.26}$$

Considering now a particular process (for example the Compton-effect) we conclude that $g_1^2\alpha^2(0)\beta^2(0)d(0)$ plays the role of the physical coupling constant g^2, i.e.

$$g^2 = \frac{g_1^2}{1+(5g_1^2/4\pi)\ln(\Lambda^2/M^2)}\,,\quad g_1^2 = \frac{g^2}{1-(5g^2/4\pi)\ln(\Lambda^2/M^2)}\,. \tag{7.27}$$

Substituting (7.24) in (7.21) and defining the physical mass as $M(\xi=0)$, we obtain

$$M_1 = M\left(\frac{g^2}{g_1^2}\right)^{3/10}.$$

The results are close to those obtained in electrodynamics. As in electrodynamics, the effective coupling constant g_1^2 increases with increasing Λ. So

we could have made the conclusion that even weak coupling becomes strong at great energies. However there are certain considerations due to I. JA. POMERANČUK showing that the situation in this case is essentially the same as in electrodynamics, but here we will not discuss the matter in more detail.

It is worth to point out the following peculiar feature of the theory with weak pseudoscalar coupling of the meson and nucleon fields. V. B. BERESTECKIJ considered charged nucleons interacting with electromagnetic and pseudoscalar meson fields, under the assumption that the coupling constant of the nucleons with mesons, although much greater than the electric charge, is at the same time smaller than unity ($e^2 \ll g^2 \ll 1$). Then he could use our method of calculation. It appeared that the asymptotic expression of the photon Green function $D_{\mu\nu}$ did not depend on the coupling constant g^2. So the weak pseudoscalar interaction of the nucleons with mesons does not have any influence on the photon Green function.

Now we describe briefly how the expressions obtained will change under the assumption of a difference between the orders of magnitude of the cut-off's as it was done already in electrodynamics. Let Λ_ψ be the cut-off limit in the Dirac current, and Λ_φ that in the interaction of the current with the meson field (it must be of course $\Lambda_\psi \gtrsim \Lambda_\varphi$).

Then the expressions of α, β and d change to the following:

((7.29) $$\beta(p^2) = Q(p^2)^{-3/10}$$

(7.30) $$\alpha(p^2) = Q(p^2)^{1/5}$$

(7.31) $$d(p^2) = \frac{Q(p^2)^{-4/5}}{1 + (g_1^2/\pi) \ln (\Lambda_\psi^2/\Lambda_\varphi^2)}$$

if $p^2 \ll \Lambda_\varphi^2$, where

(7.32) $$Q(p^2) = 1 + \frac{5g_1^2}{4\pi} \frac{\ln (\Lambda_\varphi^2/-p^2)}{1 + (g_1^2/\pi) \ln (\Lambda_\psi^2/\Lambda_\varphi^2)}$$

and

(7.33) $$\beta(p^2) = d(p^2) = 1$$

if $p^2 \gg \Lambda_\varphi^2$.

We see again that the d-function undergoes a rapid change in the vicinity of $p^2 \cong \Lambda_\varphi^2$.

REFERENCES

[1] L. D. LANDAU, A. A. ABRIKOSOV and I. M. HALATNIKOV: *Dokl. Akad. Nauk SSSR*, **95**, 497 (1954).
[2] V. V. SUDAKOV: *Dissertation*, Institute of Physical Problems of the Academy of Sciences of the USSR, (1954).
[3] L. D. LANDAU, A. A. ABRIKOSOV and I. M. HALATNIKOV: *Dokl. Akad. Nauk SSSR*, **95**, 773 (1951).
[4] J. WARD: *Phys. Rev.*, **78**, 182 (1950).
[5] L. D. LANDAU, A. A. ABRIKOSOV and I. M. HALATNIKOV: *Dokl. Akad. Nauk SSSR*, **95**, 1177 (1954).
[6] L. D. LANDAU, A. A. ABRIKOSOV and I. M. HALATNIKOV: *Dokl. Akad. Nauk SSSR*, **96**, 261 (1954).
[7] A. A. ABRIKOSOV: *Dissertation*, Institute of Physical Problems of the Academy of Sciences of the USSR, (1955).
[8] A. A. ABRIKOSOV, A. D. GALANIN and I. M. HALATNIKOV: *Dokl. Akad. Nauk SSSR*, **97**, 793 (1954).

SUPPLEMENTO AL VOLUME III, SERIE X
DEL NUOVO CIMENTO

N. 1, 1956
1° Semestre

Investigation of Photoprotons from Copper and Nickel.

E. Lejkin, R. Osokina and B. Ratner
Academy of Sciences of the USSR - Moscow

Contents. — Introduction. – **1.** Apparatus and procedure. – **2.** Errors. – **3.** Experimental results. – **4.** Discussion.

Introduction.

The study of photonuclear reactions at $10 \div 30$ MeV is of considerable interest from the point of view of establishing the mechanism of γ-ray interaction with nuclei as well as providing a check for the validity of proposed nuclear models.

The results of a great number of experiments indicate that the cross-section curves of photonuclear reactions exhibit a maximum in this energy interval.

The decrease of the cross-section for a given reaction beyond the maximum cannot be ascribed to a competing reaction. Further work, however, showed that the « resonance » character of these reactions is due to the occurence of a strong dipole absorption of γ-rays by nuclei, already predicted in [1] on the basis of the drop model. Collective models were used by several authors [2, 3] for the description of the interactions between γ-rays and nuclei.

It has been shown recently [4, 5] that the characteristic features of these reactions may be accounted for also on the basis of an independent particle model. The study of photonuclear reactions showed further [6] the experimental (γ,p) to (γ,n) cross-sections ratios for a number of isotopes to be $100 \div 1000$ times those predicted by the statistical model.

In order to explain this result a new mechanism was suggested, known as the direct photoeffect [7]. According to this concept the γ-ray interacts directly with one of the nucleons within the nucleus, after which the nucleon is ejected without formation of a compound nucleus.

It appears that the discrepancies from the statistical model are most evident when the proton evaporation is prevented either by a too large binding energy or by the high coulomb barrier of the heavy nuclei. A detailed study of photoprotons from silver and copper nuclei [8, 9] showed a cross-section ratio of (γ,p) to (γ,n) in good agreement with theoretical prediction on the evaporation model.

The energy spectrum, however, exhibits an excess of fast photoprotons. The angular distribution of these particles, in contrast with that of the remaining protons, appears to be anisotropic. According to [7] the angular distribution in this case closely approximates that obtained by the assumption of a direct photoeffect. Further research on heavy nuclei (for instance [10]) revealed considerable divergencies from the evaporation theory.

It must be noted that the study of reactions induced by heavy particles (neutrons, protons) [11] likewise shows divergencies from predictions based on the theory of the compound nucleus.

Up to the present, experimental work was limited to the establishment of deviations from statistical theory. It seems therefore of interest to obtain experimental information on processes related with the direct photoeffect and to consider the latter in detail.

In working with accelerators giving a continuous bremsstrahlung spectrum a considerable number of details of the process is lost. It appears therefore advisable to study the process at various maximum γ-rays energies. Up to the present, however, energy and angular distributions were studied only at one unchanged value of energy.

The experimental observations reported in this paper were undertaken in order to study in detail the energy and angular distribution of photoprotons from neighbouring copper and nickel nuclei at different maximum values of bremsstrahlung energy (*).

1. – Apparatus and Procedure.

A synchrotron with maximum bremsstrahlung energy $E_{\gamma m}$ up to 30.5 MeV was used as a source of γ-rays and the protons were detected in nuclear emulsions. This method gives reliable information on the energy and angular distributions of protons even in presence of an appreciable electron background.

The experimental arrangement is shown in Fig. 1. The γ-ray beam from the synchrotron passed through a 20 cm lead collimator, with angular aperture of 0.5°. The irradiated target and the photographic plates were placed in a vacuum chamber with entrance and exit holes covered by 100 μm alu-

(*) The results of these investigations were briefly described in [12, 13].

minium foil. The alignment of the collimator, beam and chamber was checked by means of X-ray film before and after exposure. Adjustments were made until the beam and apparatus were aligned to ~ 0.5 mm. Behind the chamber, along the axis of the beam, was placed an integrating ionization chamber (monitor), for the measurement of the amount of γ-rays incident on the target. A ^{60}Co source was used for controlling the sensitivity of the monitor. The monitor was calibrated against a thick-walled graphite carbon ionization chamber. The sensitivity of the chamber was computed according to [14]. Copper and nickel foils 18.4 mg/cm^2 and 40 mg/cm^2 respectively, prepared from a mixture of natural isotopes, were used as targets. The content of impurities did not exceed 1% for copper and 0.01% for nickel. The foils were placed at an angle of 45° to the axis of the beam. Six 30 × 30 mm^2 plates were placed with their surfaces tangent to the edge of the irradiated portion of the target. The distance from the centre of the target to the nearest edge of the plate was 40 mm. The effective angles $\bar{\theta}$ between the direction of the outgoing proton and the γ-ray beam were 28°, 58°, 88°, 92°, 122° and 152° respectively for the various plates, the angular interval being $\theta \pm 10°$. This geometry was used for the measurement of the energy and angular distribution of photoprotons. Two plates placed at a much greater solid angle to the target were used for the determination of the dependence of copper photoproton yield on $E_{\gamma m}$. The relative solid angles of the plates vere calibrated against a polonium α-source placed at the target. The shape of the source duplicated that of the irradiated portion of the target (an ellipse with semi-axes of 8 and 12 mm). The plates used were 160, 280 and 450 μm NIKFI Ja-2 and 400 μm Ilford C-2. The borders of the plates before exposure were coated with shellac to prevent curling of the emulsion edges in vacuum. The plates were processed by dry temperature development with a standard amidol developer and underdeveloped in order to reduce the effect of background due to electrons (*).

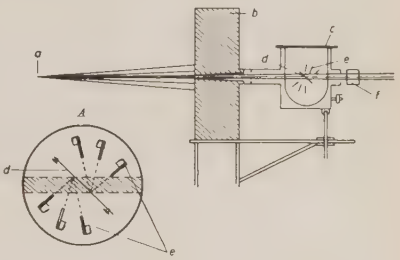

Fig. 1. – Scheme of the experimental set up: *a*) synchrotron target, *b*) Pb collimator, *c*) vacuum chamber, *d*) target, *e*) nuclear plates, *f*) monitor. *A*, inner geometry of the chamber.

(*) It must be noted that NIKFI Ja-2 plates are nearly similar to Ilford C-2 as to sensitivity to protons, but afford a better differenciation of proton tracks from background. Thus when the plates are dry, developed for 10 min instead of 20 min the background density is reduced three times and the density of proton tracks is diminished by 5%.

Binocular microscopes MBI-2×630 were used for scanning. Tracks beginning at the surface of the emulsion corresponding to protons of $\varepsilon_p \geqslant 3$ MeV and coming from the irradiated portion of the target were selected. The proton energy was determined from range-energy curves for Ilford C-2 emulsions [15]. This was made possible by the similarity of composition between these plates and the NIKFI Ja-2 emulsions. A correction was introduced for the energy loss of protons in the target, according to [16].

The energy distribution was further corrected for protons going through the emulsions, this correction being appreciable for 160 μm emulsions. In order to determine the proton background a special exposure was made with the target removed from the camera. The background amounted to $3 \div 4\%$ in all plates, excepting those placed at an angle $\theta = 28°$ and 152°, amounting to 20% for the latter case. The energy spectrum of background protons includes mostly protons with energies below 5 MeV. Since deuterons were not eliminated the energy distribution of photoprotons includes deuterons from the (γ,d) reaction. According to [9], the photodeuteron yield from copper at $E_{\gamma m} = 24.0$ MeV amounts to 30% of the total photoproton yield.

In the present work only protons of $\varepsilon_p \geqslant 3$ MeV were registered. Accordingly the deuteron contribution (allowing for their energy spectrum) amounts in our case to 10%, the distortion of the energy distribution being restricted to the $\varepsilon_p \leqslant 4.5$ MeV region. Since the dependence of the yield of the (γ,d) reaction from $E_{\gamma m}$ for copper is unknown, and for nickel these data are completely lacking, no correction for deuterons was made. The same applies to the correction for the proton contribution from the (n,p) reaction at the target at the expence of the neutrons in the γ-ray beam, since its contribution to [9] does not exceed 0.1%.

2. – Errors.

$E_{\gamma m}$ values, determined according to magnetic measurements, were checked with the results of the determination of the threshold of reaction $^{63}Cu(\gamma, n)^{62}Cu$. The value 10.7 MeV obtained is in good agreement with experimental results [17]. The uncertainty in the value $E_{\gamma m}$ due to the instability of the synchrotron power supply is of the order of 2%. The uncertainty in the determination of proton energies is due to a variety of causes, viz.: subjective error of the scanner, the uncertainty in the range-energy relation and multiple scattering of protons in the emulsion. Of less importance are errors due to uncertainties in the determination of the shrinking factor of the emulsion. The total error in the energy determination, due to the above factors, does not exceed 3%. The error in angular distribution, beside those due to statistical errors, may be ascribed to errors in the determination of relative solid angles

formed by the plates. The relative solid angles were measured with an accuracy of $6 \div 12\%$. The angular interval is 10°. The multiple proton scattering in the target is small. The mean square angle of multiple scattering for $\varepsilon_p = 3.5$ MeV is less than 2°. The results of all exposures are listed in Table I, including data on the substance of the target, its thickness in mg/cm², values of maximum energy in the bremsstrahlung spectrum in MeV, the dosage in readings of the monitor, type and thickness of the emulsion, number of plates, area scanned in mm², number of tracks measured, number of background tracks corresponding to the given exposure.

TABLE I. – *Results of various exposures for copper and nickel (for the study of energy and angular distribution).*

Substance of the target . .	copper	copper	copper	copper	nickel	nickel	nickel	nickel
Thickness of target in mg/cm²	18.9	18.9	18.9	18.9	40.1	40.1	40.1	—
Maximum energy $E_{\gamma m}$ (in MeV)	19.0	24.0	28.0	30.5	21.5	25.5	28.0	24.0
Dosage in readings of the monitor	3800	8000	4600	3670	2000	1350	1480	1600
Type of emulsion . . .	Ya-2	C-2	Ya-2	Ya-2	Ya-2	Ya-2	Ya-2	Ya-2
Thickness of emulsion in μm	280	400	160	280	450	280	160	160
Number of plates . . .	6	6	6	6	6	6	6	6
Scanned area in mm² . .	2672	2199	1989	1542	1997	1482	1644	1142
Number of tracks measured	1827	7952	3585	2684	5207	4415	4300	35
Number of background tracks	94	250	76	106	50	16	19	—
Number of tracks going through the emulsion	1	34	0 171	47	0	12	210	—

Note. – Each reading of the monitor corresponds to $6.3 \cdot 10^7$ quanta per 1 cm² in the 0.1 MeV interval at $E_{\gamma m} = 24.0$ MeV incident on a target normal to the direction of the γ-ray beam.

3. – Experimental Results.

3·1. *Copper.* – Copper was irradiated at $E_{\gamma m} = 19.0$ MeV, 24.0 MeV, 28 MeV and 30.5 MeV. At $E_{\gamma m} = 28$ MeV the results obtained lack the necessary

precision, owing to the large number of tracks not ending in the emulsion and to the considerable error in the calibration of solid angles. Accordingly the discussion is limited to $E_{\gamma m} = 19$ MeV, 24.0 MeV and 30.5 MeV. The total energy

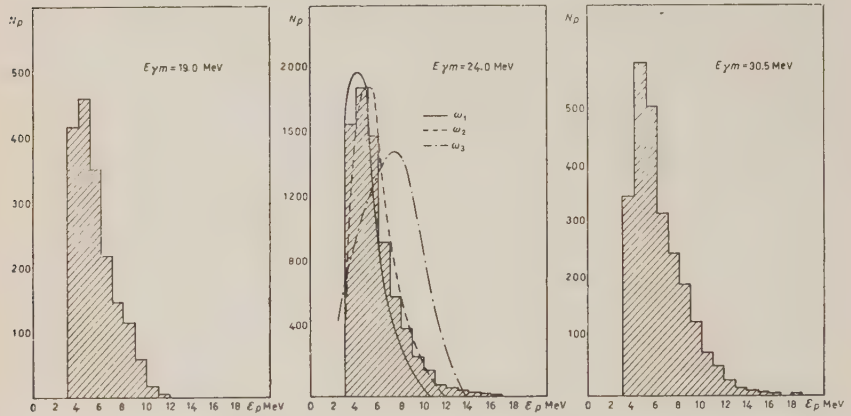

Fig. 2. – Total energy distribution of $\varepsilon_p \geqslant 3$ MeV photoprotons from copper. N_p = number of tracks in the given energy interval. Smooth curves are calculated on the statistical model of nuclear reactions and are normalized to the area of experimental distribution.

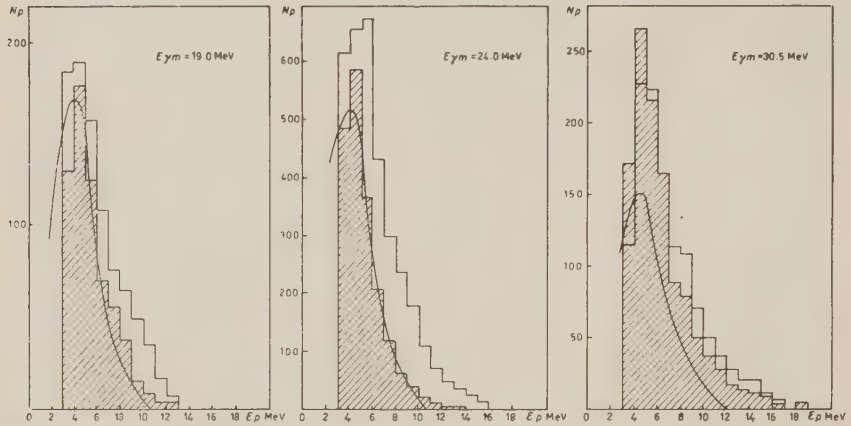

Fig. 3. – Energy distribution of $\varepsilon_p \geqslant 3$ MeV protons from copper, emitted at various angles to the γ-ray beam direction. Shaded regions represent cumulative data for angles $\theta = 28°$ and 152°, data for the angles 88° and 92° are contoured by a thick line. The spectra are normalized to the same solid angle. Smooth curves are calculated on the statistical theory in accordance with data on angular distribution (24.0 MeV) and yield (19.0 and 30.5 MeV).

distribution of photoprotons of $\varepsilon_p \geqslant 3$ MeV corrected for background and tracks not ending in the emulsion for $E_{\gamma m} = 19.0$ MeV, 24.0 MeV and 30.5 MeV is given in Fig. 2.

Fig. 3 shows the energy distribution of photoprotons emitted at various angles θ to the γ-ray beam for $E_{\gamma m} = 19.0$ MeV, 24.0 MeV and 30.5 MeV. Since the spectra of protons emitted at angles symmetric to $\theta = 90°$ (28° and 152°) are quite similar, data obtained for these angles, as well as those

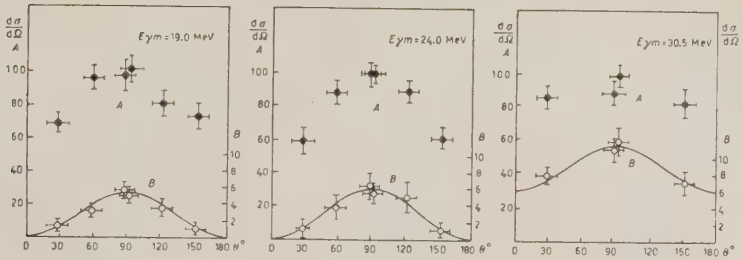

Fig. 4. – Angular distribution of photoprotons from copper. $d\sigma/d\Omega$, relative cross-section; A, for $\varepsilon_p \geqslant 3$ MeV protons; B, for $\varepsilon_p \geqslant 10$ MeV protons. The cross-section for the angle $\theta = 92°$ is taken equal to 100. Smooth curves correspond to a distribution $\sin^2\theta$ (19.0 and 24.0 MeV) and $a + b\sin^2\theta$ (30.5 MeV).

at angles corresponding to $\theta = 88°$ and 92°, are summed in order to increase statistical precision. The hystograms are reduced to the same solid angles.

The angular distribution of $\varepsilon_p \geqslant 3$ MeV photoprotons (A) and fast $\varepsilon_p \geqslant 10$ MeV photoprotons (B) for $E_{\gamma m} = 19.0$ MeV, 24.0 MeV and 30.5 MeV are shown in Fig. 4. Data on the dependence of photoproton yields from copper on $E_{\gamma m}$ are given in Fig. 5.

These data may be used for the evaluation of the cross-section of the (γ,p) reaction. This requires a knowledge of the shape of the $\sigma_{\gamma p}(E_\gamma)$ curve, which is unknown for copper. However, [18] showed the cross-section for neighbouring elements to differ only slightly from one another. Accordingly, using the $\sigma_{\gamma p}(E_\gamma)$ curve measured for nickel [18], we were able to calculate that the cross-section for copper, in the maximum of the $\sigma_{\gamma p}(E_\gamma)$ curve, must be of $4.0 \cdot 10^{-26}$ cm$^2 \pm 30$ %.

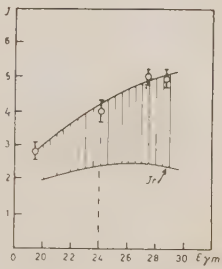

Fig. 5. – Dependence of $\varepsilon_p \geqslant 3$ MeV photoproton yield from copper on $E_{\gamma m}$. J_r, yield on the statistical model normalised to the experimental value according to angular distribution data at $E_{\gamma m} = 24.0$ MeV.

3·2. *Nickel.* – Nickel was irradiated at $E_{\gamma m} = 21.5$ MeV, 25.5 MeV and 28.0 MeV. For the reasons stated above the results obtained at $E_{\gamma m} = 28.0$ MeV

are not considered in detail. Energy distributions of photoprotons from nickel at $E_{\gamma m} = 21.5$ MeV, 25.5 MeV and 28.0 MeV are shown in Fig. 6, and the angular distribution of $\varepsilon_p \geqslant 3$ MeV (A) photoprotons and that of fast $\varepsilon_p \geqslant 10$ MeV (B) photoprotons in Fig. 7.

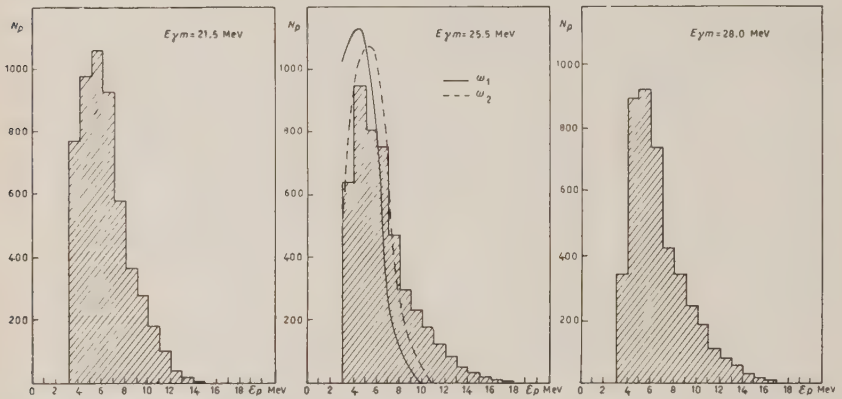

Fig. 6. - Total energy distribution of $\varepsilon_p \geqslant 3$ MeV photoprotons from nickel. N_p, the number of tracks in the given energy interval. Smooth cuvers are calculated for $E_{\gamma m} = 25.5$ MeV on the basis of the statistical model and normalized to the experimental spectrum area.

The cross-section in the maximum of the curve for nickel is $9.0 \cdot 10^{-26}$ cm$^2 \pm \pm 30$ % in agreement with the data of [18], within the limits of experimental error. The ratio of photoproton yields in nickel and copper, at $E_{\gamma m} = 25.5$ MeV, is 1.72 ± 10 %.

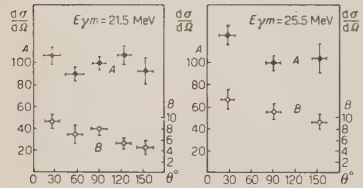

Fig. 7. – Angular distribution of photoprotons from nickel. $d\sigma/d\Omega$, relative cross-section: A, for $\varepsilon_p \geqslant 3$ MeV protons; B, for $\varepsilon_p \geqslant 10$ MeV protons. The cross-section for the angle $\theta = 92°$ is taken equal 100.

4. – Discussion.

The results obtained have been compared with predictions based on the statistical model. The energy distribution of protons emitted from the nucleus in the (γ, p) reaction induced by the γ-ray spectrum $N(E_\gamma, E_{\gamma m})$ (*) is given

(*) Taken from [27].

by the expression

$$I(\varepsilon_p) = \text{const}\ \varepsilon_p \sigma(\varepsilon_p) \int_0^{E_{\gamma m}} \frac{\sigma_{\gamma n}(E_\gamma) N(E_\gamma, E_{\gamma m}) \omega(E_\gamma - E_{p^0} - \varepsilon_p)}{\Gamma_n(E_\gamma)} \, dE_\gamma ,$$

where $\sigma(\varepsilon_p)$ is the penetration cross-section for protons, $\sigma_{\gamma n}(E_\gamma)$ is the cross-section of the (γ, n) reaction, $\Gamma_n = \text{Const} \int_0^{E_{n\,max}} \varepsilon_n \omega(E_\gamma - E_{p^0} - \varepsilon_n) d\,\varepsilon_n$ is the neutron width, $\omega(E_\gamma - E_{p^0} - \varepsilon_p)$ the level density of the residual nucleus, E_{n^0} and E_{p^0} the values of the binding energies of the neutron and proton respectively.

The theoretical spectrum was compared with the total energy spectrum of protons obtained experimentally at $E_{\gamma m} = 24.0$ MeV (in this exposure the highest accuracy was achieved). The value of the penetration cross-section $\sigma(\varepsilon_p)$ for $r_0 = 1.5 \cdot 10^{-13}$ cm^2 was taken from [19]; the dependence of the cross-section for the (γ, n) reaction on the energy of the γ-ray, $\sigma_{\gamma n}(E_\gamma)$, was taken from (17). In the last paper $\sigma_{\gamma n}(E_\gamma)$ has been measured up to $E_\gamma = 22$ MeV. Extrapolation to high energies was made in accordance with our preliminary measurements. The values of the neutron binding energies E_{n^0} were assumed equal to 10.9 MeV for ^{63}Cu [20], and to 10.0 MeV for ^{65}Cu (mean value from the data in [20]). The value of the proton binding energy E_{p^0} was obtained from E_{n^0} values and β-decay data according to the formula

$$E_{p^0} = E_{n^0} - 1.8 - E_{\beta^+} ,$$

where E_{β^+} is the maximum positron energy in the decay spectrum of the product nucleus of the (γ, n) reaction of the isotope under consideration. The values of E_{β^+} are taken from [21]. The values of E_{p^0} were found to be 6.5 MeV and 7.6 MeV for ^{63}Cu and ^{65}Cu respectively.

In calculations the following equations were used, describing the dependence of the level density of the residual nucleus with mass number A on its excitation energy $E_R = E_\gamma - E_{p^0} - \varepsilon_p$:

$$\omega_1 = \text{const} \exp\left[\sqrt{3.35(A-40)^{\frac{1}{2}} E_R}\right] \qquad \text{(taken from [19])},$$

$$\omega_2 = \text{const} \exp\left[\sqrt{1.6(A-40)^{\frac{1}{2}} E_R}\right] \quad \text{(used by several authors: see [8, 9])},$$

as well as

$$\omega_3 = \begin{cases} \text{const} & \text{for } 0 < E_R < 3\,\text{MeV}, \\ \omega_1 & \text{for } E_R \geqslant 3\ \text{MeV}, \end{cases}$$

The latter makes it possible to take into consideration the fact that the

nuclear level density at small excitation appears to grow more slowly than expected according to the exponential law [22].

The energy distribution has been calculated both for ^{65}Cu and for ^{63}Cu. Since, however, the contribution of the heavier isotope to the spectrum of the evaporation protons is but small (5% for the case of ω_1), all the curves calculated are referred to ^{63}Cu. In the theoretical spectrum only protons from the (γ,p) reaction are taken into account. The protons may be emitted also in the (γ, np) reaction, which is energetically possible at $E_\gamma > 22$ MeV. Experiments on photoneutron registration (23) showed, however, that at $E_\gamma = 22 \div 23$ MeV $\sigma(\gamma, np)$ is small.

As one can see from Fig. 2, the photoproton spectrum exhibits an excess of fast particles as compared with the distribution calculated for level densities ω_1 and ω_2, in agreement with [9]. The level density described by ω_3 gives a distribution sharply contrasting with the observed spectrum. Thus neither of the expressions used to describe the level density $\omega(E_R)$ is able to account satisfactorily for the observed energy distribution of photoprotons. On the other hand, the differential proton energy spectra at $E_{\gamma m} = 19.0$ and 24.0 MeV show (Fig. 3) that the proton energy distribution for the angles $\theta = 28°$ (152°) fairly agrees as to form with the evaporation spectrum, while that for the angles close to 90° exhibits a considerable departure from the calculated spectrum. A further examination of Fig. 3 shows, however, that while at $E_{\gamma m} = 19.0$ and 24.0 MeV the photoproton energy spectra considerably differ for various angles, this difference is practically non existing at $E_{\gamma m} = 30.5$. The spectra in Fig. 3 have been calculated on the basis of the statistical theory for the level density of residual nucleus ω_1. At $E_{\gamma m} = 24.0$ MeV the theoretical spectrum has been normalized to the same area as the experimental distribution obtained for the angles $\theta = 28°$ (152°). At other values of $E_{\gamma m}$ the normalization of the theoretical curves is made in accordance with available data on the dependence of the proton yields on $E_{\gamma m}$.

The shape of the total proton energy spectrum depends also on $E_{\gamma m}$. If we take as a characteristics of the shape of the spectrum the fraction of protons having $\varepsilon_p > 10$ MeV (Fig. 8), it becomes evident that the fast proton fraction, which remained fairly unchanged over the $19 \div 24$ MeV and $28 \div 30$ MeV intervals, shows a sharp rise by a factor of ~ 2.5 over the interval

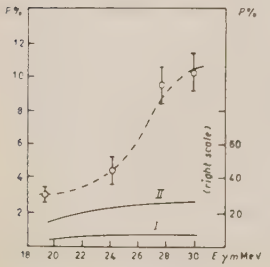

Fig. 8. – Dependence of the fast photoproton fraction p% from copper on energy $E_{\gamma m}$. The dashed curves represent experimental results. The solid curves are calculated on the statistical model in the various assumptions on the level density of the residual nucleus: I) $\omega = \omega_1$, II) $\omega = \text{const}$.

$24 \div 28$ MeV. This result is in fundamental contradiction with the statistical theory at different assumptions of the level density law of the residual nucleus. In going over to higher γ-ray energies ($E_{\gamma m} = 28$ MeV and 30.5 MeV) a change in the shape of the spectrum at its upper limit is likewise observed, as seen from Fig. 9, where the spectra of fast protons from copper are represented in a logarithmic plot.

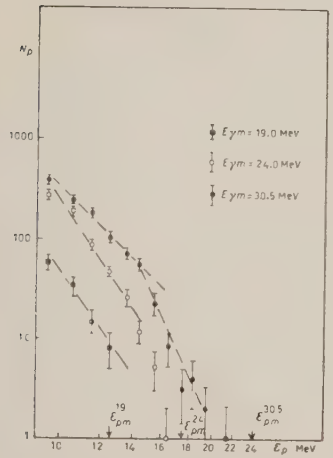

Fig. 9. – Energy spectrum of fast protons from copper in the logarithmic plot. Arrows indicate the maximum possible energy values from the given energy $E_{\gamma m}$.

The energy distribution for nickel was compared with data obtained on the statistical theory at $E_{\gamma m} = 25.5$ MeV. Data on the dependence of the cross-section of the (γ, n) reaction on E_γ required for calculations are taken from [17]. In the case of nickel the basic contribution to the energy distribution of evaporation protons comes from the lighter isotope ^{58}Ni. The value of binding energy E_{p^0} for ^{58}Ni=12.0 MeV [20]. The binding energy of the proton, as obtained from β-decay data [21], is 9.5 MeV. Two level densities were used: ω_1 and ω_2. The excess of high energy protons as compared with copper is somewhat higher. The dependence of the fast protons fraction p% on $E_{\gamma m}$ is shown in Fig. 10: the absence of the sharp rise observed in case of copper should be noted (*).

The study of angular distribution for photoprotons likewise reveales a number of peculiarities.

The angular distribution of $\varepsilon_p \geqslant 3$ MeV photoprotons from copper shows a marked departure from spherical symmetry at $E_{\gamma m} = 19$ MeV and 24 MeV. At $E_{\gamma m} = 30.5$ MeV the anisotropy is notably decreased. These peculiarities are most sharply marked for $\varepsilon_p \geqslant 10$ MeV protons. As seen from Fig. 4, the angular distribution of fast protons at $E_{\gamma m} = 19.0$ MeV and 24.0 MeV is described by a $\sin^2\theta$ law and at $E\gamma_m = 30.5$ MeV by a $a + b\sin^2\theta$ law, where $b/a \simeq 0.8$. The statistical theory does not seem able to account for this high anisotropy and particularly for its sharp decrease with an $E_{\gamma m}$ rise of only a few

(*) The comparison of data obtained for copper and nickel with those for cobalt [24] at $E_{\gamma m} = 24.0$ MeV, revealed a near similarity in the energy distribution of the three elements. It must be noted, that in the theoretical spectrum for Co the upper limit is appreciably shifted towards higher energies. This appears somewhat strange as the parameters used for calculation in the three cases are fairly similar.

MeV. Within the limits of experimental error no forward shift in the angular distribution of protons from copper was observed [25]. The angular distributions from nickel at $\varepsilon_p \geqslant 3$ MeV and $\varepsilon_p \geqslant 10$ MeV and $E_{\gamma m} = 21.0$ and 25.0 MeV in Fig. 7, are nearly isotropic (*), which contrasts with data obtained for copper at similar values of $E_{\gamma m}$. Deviations from statistical theory in case of nickel does not seem to be bound with a preferential proton emission in any direction (with the exception of certain forward shift) for fast protons.

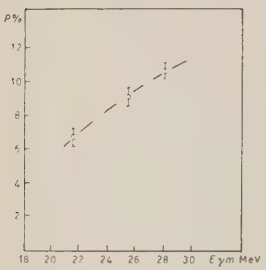

Fig. 10. – Dependence of the fast photoproton fraction (p%) from nickel on $E_{\gamma m}$.

The study of the dependence of photoproton yields from copper on $E_{\gamma m}$ (Fig. 5) also revealed marked discrepancies with the statistical theory. In our calculations we used the level density of the residual nucleus ω_1, all other data are those already used in the calculation of the energy distribution, postulating an isotropic emission of evaporation protons. Consequently the theoretical yield at $E_{\gamma m} = 24.0$ MeV is taken to equal the yield corresponding to the isotropic portion in the proton angular distribution.

Thus in the present work besides some previously noted deviations from the statistical theory (excess of fast protons in the case of copper and nickel, angular anisotropy for copper protons), some new data have been obtained which cannot be reconciled with the concept of a compound nucleus. As an example, we may cite the sharp increase of the fast photoproton fraction and the change in their angular distribution in going over from $E_{\gamma m} = 24.0$ MeV to $E_{\gamma m} = 28.0$ and 30.5 MeV.

As already pointed out above, the discrepancy from statistical theory seems to be due to a direct interaction between γ-rays and individual protons in the nucleus. According to Fig. 5 the contribution of this mechanism in case of copper may be evaluated to $\sim 40\,\%$ at $E_{\gamma m} = 24.0$ MeV.

It may be shown, that most of the experimental facts might be successfully accounted for qualitatively on the assumption that in the direct photoeffect the shell structure of the nucleus manifests itself. Such a point of view seems natural since in the absorption of a γ-ray by an individual nucleon the process must depend on the state of the nucleon within the nucleus. According to the accepted scheme of filling of the states in the shell model [26] the copper nucleus corresponds to the proton configuration $(1s_{\frac{1}{2}})^2 \ldots (4f_{7/2})^2(3p_{\frac{3}{2}})^1$. The close analogy of the energy and angular distribution of fast protons from copper at $E_{\gamma m} = 19.0$ MeV and 24.0 MeV may be considered as evidence for these

(*) A similar result has been obtained for cobalt in [24].

protons being ejected from the $3p_{\frac{3}{2}}$ level by γ-rays. At higher $E_{\gamma m}$, the number of fast protons must include also particles from the lower level $4f_{7/2}$, which is occupied by 8 protons. This seems to account for the experimental « jump » in the yield of fast particles, as well as for the sharp change in their angular distribution. The decrease of anisotropy may be considered as evidence of the high angular momentum of particle [7] occupying the lower level, in agreement with the above mentioned scheme of level order in the copper nucleus [26]. The spacings between the upper level in the potential well may be roughly evaluated from values of $E_{\gamma m}$ at which the « jump » in proton characteristics is observed to be equal to $6 \div 8$ MeV. A very near value of ΔE is obtained from considerations of the energy spectrum of fast photoprotons from copper (Fig. 9). In case of nickel the level $4f_{7/2}$ lies at the top of distribution in the well, which seems to account for the near similarity of results obtained for nickel at all values of $E_{\gamma m}$ and those for copper at $E_{\gamma m}=28.0$ MeV and 30.5 MeV. It is interesting to note the similarity in the angular distribution of fast photoprotons from nickel and cobalt [24], in agreement with the suggested interpretation, since both nuclei have the same top level.

The absence of sharp variations in the characteristics of fast proton with increase of $E_{\gamma m}$, observed in the case of nickel, may be tentatively ascribed to the fact that the transition to a next level in this case is not accompanied by such a considerable increase in the number of protons as is the case of copper.

It must be noted, however, that the interpretation of experimental facts on the basis of the nuclear shell model is not free from certain difficulties. Thus, the angular distribution of fast photoprotons from copper at $E_{\gamma m} = 19.0$ MeV and 24.0 MeV by the $\sin^2\theta$ law does not correspond, according to [7], to the photoeffect from the $3p_{\frac{3}{2}}$ level. The absence of the isotropic component in the above mentioned distributions might be interpreted as evidence of a greater transparency of the nucleus for $10 \div 20$ MeV protons, or else for the formation of fast photoprotons on the surface of the nucleus.

The observations reported in this paper appear to support the view that the study of (γ, p) reactions may in some instances enable us to obtain some information on nucleons occupying different levels even by means of the continuous γ-ray spectrum, provided the experiments are carried out at various values of the upper limit.

* * *

The authors are very grateful to prof. V. I. Veksler for many fruitful discussions on the results of this work. They express also their thanks to R. Polukarova and Z. Koroleva for assistance in the scanning of photographic plates, as well as to the synchrotron group.

REFERENCES

[1] A. B. MIGDAL: *Žu. Éksper. Teor. Fiz. SSSR*, **15**, 81 (1945).
[2] M. GOLDAHBER and E. TELLER: *Phys. Rev.*, **74**, 1046 (1948).
[3] H. STEINWEDEL and J. H. D. JENSEN: *Zeits. f. Naturforsch.*, 5a, 413 (1950).
[4] R. V. HOHLOV: *Dokl. Akad. Nauk SSSR*, **97**, 239 (1954).
[5] J. S. LEVINGER and D. C. KENT: *Phys. Rev.*, **95**, 418 (1954).
[6] O. HIRZEL and H. WÄFFLER: *Helv. Phys. Acta*, **20**, 373 (1947).
[7] E. D. COURANT: *Phys. Rev.*, **82**, 703 (1951)l
[8] B. C. DIVEN and G. M. ALMY: *Phys. Rev.*, **80**, 407 (1950).
[9] P. R. BYERLY and W. E. STEPHENS: *Phys. Rev.*, **83**, 54 (1953).
[10] M. E. TOMS and W. E. STEPHENS: *Phys. Rev.*, **92**, 362 (1953).
[11] H. MCMANUS and W. T. SHARP: *Phys. Rev.*, **87**, 188 (1952).
[12] E. M. LEJKIN, R. M. OSOKINA and B. S. RATNER: *Dokl. Akad. Nauk SSSR*, **102**, 245 (1955).
[13] E. M. LEJKIN, R. M. OSOKINA and B. S. RATNER: *Dokl. Akad. Nauk SSSR*, **102**, 493 (1955).
[14] M. LAX: *Phys. Rev.*, **72**, 61 (1947).
[15] J. ROTBLAT: *Nature*, **167**, 550 (1951).
[16] E. SEGRÈ: *Experimental Nuclear Physics*, vol. I (New York, 1953).
[17] L. KATZ and A. G. W. CAMERON: *Can. Journ. Phys.*, **29**, 518 (1951).
[18] J. HALPERN and A. K. MANN: *Phys. Rev.*, **83**, 370 (1951).
[19] V. F. WEISSKOPF: *Lecture Series in Nuclear Physics* (1948).
[20] R. SHER, J. HALPERN and A. K. MANN: *Phys. Rev.*, **84**, 387 (1951).
[21] J. M. HOLLANDER, I. PERLMAN and G. F. SEABORG: *Rev. Mod. Phys*, **25**, 469 (1953).
[22] J. M. BLATT and V. F. WEISSKOPF: *Theoretical Nuclear Physics* (New York, 1952).
[23] R. MONTALBETTI, L. KATZ and J. GOLDENBERG: *Phys. Rev.*, **91**, 659 (1953).
[24] M. E. TOMS and W. E. STEPHENS: *Phys. Rev.*, **95**, 1209 (1954).
[25] A. K. MANN, J. HALPERN and M. ROTHMAN: *Phys. Rev.*, **87**, 146 (1952).
[26] P. F. A. KLINKENBERG: *Rev. Mod. Phys.*, **24**, 63 (1952).
[27] L. I. SCHIFF: *Phys. Rev.*, **83**, 252 (1951).

SUPPLEMENTO AL VOLUME III, SERIE X
DEL NUOVO CIMENTO

N. 1, 1956
1° Semestre

Investigation of the Proton-Proton Interaction at High Energies (*).

M. G. MEŠČERJAKOV, N. P. BOGAČEV and B. S. NEGANOV

Institute of Nuclear Problems, Academy of Sciences of the USSR - Moscow

CONTENTS. — 1. **Introduction.** – 2. **Experimental method.** 1. Proton beam. 2. The method of conjugated telescopes. 3. Targets. – 3. **Elastic proton-proton scattering.** 1. (p-p) scattering at 460 MeV. 2. (p-p) scattering at 657 MeV. 3. Determination of differential (p-p) scattering cross-sections in the region of 460-657 MeV. 4. Discussion of results of the experiments on (p-p) scattering. – 4. **Meson production in** (p-p) **collisions.** 1. The $p + p \to d + \pi^+$ reaction at 460 MeV. 2. The $p + p \to d + \pi^+$ reaction in the Region of 510-657 MeV. 3. Remarks on the relation between elastic scattering and meson production in (p-p) collisions.

1. – Introduction.

In the present paper are presented some results of the investigation of the proton-proton collisions in the energy region from 460 to 660 MeV.

In this region the (p-p) interaction includes elastic scattering and meson production:

(I) $$p + p \to d + \pi^+$$

(II) $$p + p \to p + n + \pi^+$$

(III) $$p + p \to p + p + \pi^0 .$$

In addition to these processes, beginning from 600 MeV the production of two π-mesons becomes energetically possible in single (p-p) collisions.

(*) Reported at a meeting of the Academy of Sciences of the USSR, Moscow, on December 17th, 1954.

The experiments described below were carried out in 1951-1953 on the synchrocyclotron of the Institute of Nuclear Problems of the Academy of Sciences of the USSR [1-5].

2. – Experimental Method.

2·1. *Proton Beam.* – An unpolarised proton beam from the synchrocyclotron was collimated to the required size by passage through a hole in a steel block 3.6 meters in length placed in a 4 meter shield wall of reinforced concrete.

In the majority of experiments, the diameter of the beam near the target was approximately 2 cm. The energy of the primary protons was determined from the angle of emission of Čerenkov radiation. In the experiments of 1951-1952, the corresponding value was 460.0 ± 0.9 MeV, in the 1953-1954 experiments 657 ± 2 MeV. The momentum spread of the primary protons did not exceed 1%.

The mean proton flux density of the beam was 10^6 protons per cm^2 s. The beam intensity was monitored by an ionization chamber filled with argon; the chamber was calibrated by determining the absolute charge collected by a massive electrode exposed to the protons. Account was taken of the charge loss from the collector due to escape of secondary particles ($\sim 2\%$ correction).

Observation of proton tracks in photographic plates sensitive to particles of minimum ionization, made it possible to evaluate the increase of the chamber current due to particles entering the beam as a result of multiple scattering in the walls of the collimator; the magnitude of this correction did not exceed 1%.

2·2. *The Method of Conjugated Telescopes.* – Elastic (p-p) scattering and reaction (I) were separated from other accompanying processes by registration of both secondary particles by conjugated telescopes, each of which consisted of three scintillation counters (Fig. 1). For protection against the stray magnetic field of the synchrocyclotron, the photomultipliers and the tolane or anthracene crystals were placed in a steel case. Secondary particles were registered in the solid angle subtended by the crystal of the defining telescope which was nearest to the target.

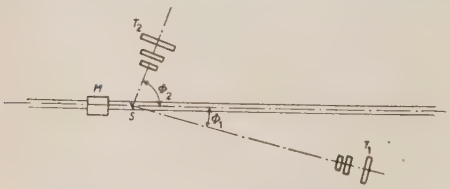

Fig. 1. – Experimental Arrangement. T_1: defining telescope. T_2: conjugated telescope. M: monitor; S: target.

In both telescopes, the distance between the first and second crystals was

6 cm, and between the second and third 18 cm. In order to reduce the effect of multiple scattering, the crystals, which usually had a thickness of 1 cm, were so selected that their dimensions increased with the distance from the entrance aperture of the telescope. Care was taken to secure uniform particle sensitivity of the crystal surface.

The electronic circuits permitted simultaneous counting of coincidences between the telescopes, as well of triple or double (in any desired combination) coincidences of the telescope counters. The triple coincidence resolution time in each telescope was $3 \cdot 10^{-8}$ s; the resolution time of the circuit recording coincidences between the telescopes was $5 \cdot 10^{-8}$ s. The curve representing the dependence of the triple coincidence rate on the voltage applied to the photomultipliers had a plateau of about 300 V. The proton counting efficiency of the telescope system on the plateau amounted to 0.94 ± 0.02 in the energy range from 50 to 615 MeV. The telescopes were mounted on a goniometer and the angles between the optical axes of the telescopes and the direction of the beam could be measured with an accuracy up to 0.1°. In setting up the apparatus, special care was taken to guarantee coplanarity of the telescope axes and the axes of the proton beam.

Particle identification was based on range measurements in filters placed in front of the last crystals of the telescopes and on pulse size measurements. Nuclear processes, consisting of the emission of two charged particles, were identified by measuring the corresponding angles of emission.

As a matter of fact the method amounts to measuring the dependence of the coincidence rate on the angle between the telescopes.

In the case of (p-p) scattering at 460 MeV, the results of such measurements, which are shown in Fig. 2, were obtained in conditions when one telescope was placed at an angle of 42° to the beam, and the second could be moved on the opposite side of the beam within the limits of 36° to 48°. Calculations show that under the conditions of this experiment, the relativistic deviation from an angle of 90° between the directions of the scattered proton and the recoil proton should be 6.26° whereas the experimental value was found to equal $6.2° \pm 0.2°$. Such quantitative

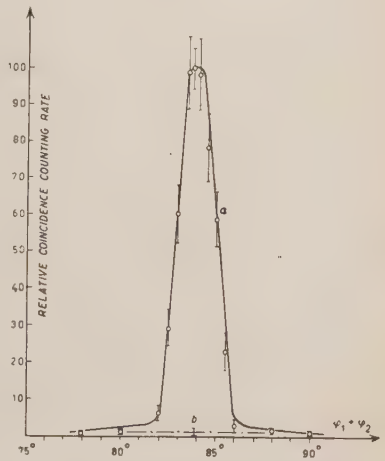

Fig. 2. – Dependence of coincidence counting rate on scattering angle. *a*, effect from hydrogen; *b*, background from carbon.

agreement signifies that at 460 MeV proton-proton collisions not connected with meson production is a strictly elastic process. Observations at 657 MeV lead to a similar conclusion.

As can be seen from Fig. 2, the coincidence counting rate was zero at divergence angles greater than 86°. This was proof that the primary beam contained no low-energy proton contaminant. When a filter entirely stopping elastically scattered protons was placed in one of the telescopes, there were no coincidences. When the paraffin target was substituted for a graphite target, the coincidence counting rate was reduced approximately 40 times.

2·3. *Targets.* – The yield of elastically scattered protons and π^+-mesons in (p-p) collisions was determined from the difference of the counting rates obtained by alternately employing paraffin ($CH_{2.083}$) and graphite targets possessing an equal number of carbon atoms per surface unit. The thicknesses of the targets were usually between 500 and 900 mg/cm². Within experimental error the measured cross-sections were found to be dependent upon the target thicknesses.

3. – Elastic Proton-Proton Scattering.

3·1. (p-p) *Scattering at* 460 MeV. – In the center of mass system, elastic (p-p) scattering was observed by the conjugated telescope method within an angle range of $55° \leqslant \theta \leqslant 90°$. Scattered protons were also recorded by a single telescope in the angle range $20° \leqslant \theta \leqslant 90°$. Corrections were introduced to account for accidental coincidences, counting losses, and also for absorption and multiple scattering of the protons in the target and scintillation crystals. The effect due to π^+-meson contamination among the secondary protons was taken into account in the measurements carried out with a single telescope. Control experiments also showed that the passage of an elastically scattered proton through the telescope defining the solid angle ω, within which (p-p) scattering was observed, was always accompanied by the pas-

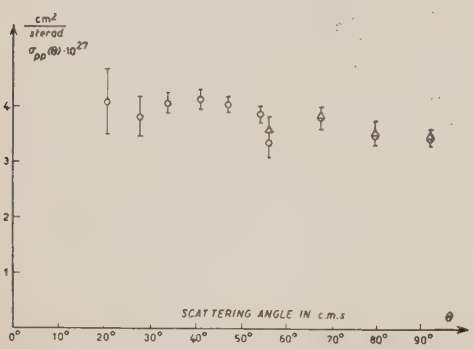

Fig. 3. - Differential p-p scattering cross-section at proton energy 460 MeV.

sage of a recoil through the conjugated telescope. Under typical experimental conditions ω was equal to $(1.01 \pm 0.01) \cdot 10^{-3}$ steradian.

Fig. 3 shows the values found for $d\sigma/d\omega$; circles show the results obtained by means of the single telescope; method data, represented by triangles, were obtained by conjugated telescope method. Indicated errors are statistical standard deviations. An account of all other sources of errors shows that the accuracy of the absolute values of $d\sigma/d\omega$ amounts to about 10%.

As can be seen from Fig. 3, at 460 MeV the values of $d\sigma/d\omega$ increases weakly with decreasing angle. Further indication of a departure from isotropy of (p-p) scattering was obtained in experiments, in which the relative yields of protons scattered at angles of 90° and 30° was measured with the aid of a single telescope. It was thus found that the ratio

$$\left(\frac{d\sigma}{d\omega}\right)_{30°} \Big/ \left(\frac{d\sigma}{d\omega}\right)_{90°} = 1.14 \pm 0.06 \ (*) .$$

For the scattering angle 90°, $d\sigma/d\omega = (3.50 \pm 0.20) \cdot 10^{-27}$ cm/sterad. Linear extrapolation of $d\sigma/d\omega$ to the region of small angles gives a value of $(22 \pm 2) \cdot 10^{-27}$ cm² for the total elastic (p-p) scattering cross-section.

3·2. (p-p) *Scattering at* 657 MeV. – The (p-p) scattering differential cross-section was measured by the conjugated telescope method in the angle range from 90° to 30°. Results of the measurement and statistical errors are given in Fig. 4, from which it can be seen that at 657 MeV the value of $d\sigma/d\omega$ rises sharply as the angle decreases. The ratio of the differential cross-sections at angles of 30° and 90° is $(d\sigma/d\omega)_{30°}/(d\sigma/d\omega)_{90°} = 2.7 \pm 0.2$. For a scattering angle of 90°, $d\sigma/d\omega = (2.1 \pm 0.2) \cdot 10^{-27}$ cm²/sterad. The total elastic (p-p) scattering cross-section at 657 MeV, found by means of linear extrapolation of $d\sigma/d\omega$ to small angles, is $(23 \pm 2) \cdot 10^{-27}$ cm².

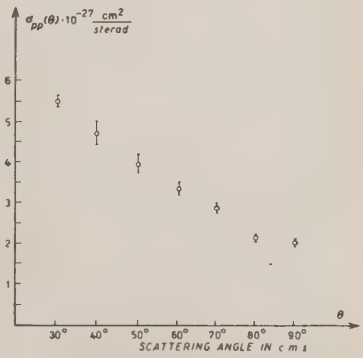

Fig. 4. – Differential (p-p) scattering cross-section at 657 MeV.

(*) This result was obtained in 1952 [1]. At that time data on (p-p) scattering were known up to 340 MeV [6]. These data showed that within experimental error (10÷15%) large-angle-scattering does not depend on the energy or angle. An increase of the scattering cross-section of approximately 20% with decreasing angle was observed recently at 435 and 428 MeV [7, 8].

3·3. *Determination of Differential* (p-p) *Scattering Cross-Sections in the Region of* 460-657 MeV. – The results of the two previous experiments lead to the conclusion that as the energy rises from 460 to 657 MeV, there is a sharp rise in departure from isotropy of (p-p) scattering. The next step in determining the properties of (p-p) scattering in the stated energy region were experiments, in which the dependence on energy of the differential cross-sections for angles of 30° and 90° in the center of mass system was determined by conjugated telescope method. Protons of intermediate energies were obtained by placing paraffin absorbers of suitable thickness in the beam path in front of the collimator. Throughout the whole energy region all differential cross-section measurements were carried out in strictly identical conditions with the sole exception that with variation of energy of the primary protons, angles φ_1 and φ_2 at which the telescopes were positioned on opposite sides of the beam, had to be changed slightly. These angles were found from the relation $\operatorname{ctg}\varphi_1 \cdot \operatorname{ctg}\varphi_2 = 1 + (E/2Mc^2)$. The statistical probable error at 90° did not exceed 3%.

A consideration of all other sources of error showed that the absolute values of $d\sigma/d\omega$ had been determined with an accuracy of about 5% at 90° and of about 8% at 30°.

The results of the present experiments are shown in Fig. 5. Results obtained in [1, 6, 7, 9, 10] for a scattering angle of 90° and for energies lying between 75 and 437 MeV are presented in the same figure. It can be seen that the value of $(d\sigma/d\omega)_{90°}$ remains approximately constant as the energy changes from 140 to 460 MeV, and then begins to decrease slightly as the energy increases from 460 to 560 MeV. As the energy rises further, the value of $(d\sigma/d\omega)_{90°}$ decreases more and more sharply. Thus, as the energy changes from 610 to 657 MeV, $(d\sigma/d\omega)_{90°}$ decreases from $(2.63 \pm 0.10)\cdot 10^{-27}$ cm²/sterad to $(2.05 \pm 0.07)\cdot 10^{-27}$ cm²/sterad.

The differential cross section $(d\sigma/d\omega)_{30°}$ increases approximately 1.6 times as the energy increases from 460 to 657 MeV. The value of the ratio $(d\sigma/d\omega)_{30°}/(d\sigma/d\omega)_{90°}$ given in Table I, also testifies to the fact that departure from the isotropy of (p-p) scattering is most rapid in the region of 560–657 MeV.

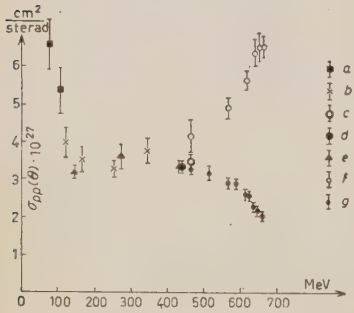

Fig. 5. – Dependence of differential cross-section on the energy of the incident protons for scattering angles 30° and 90°. *a* [9] — 90°; *b* [6] — 90°; *c* [1] — 90°; *d* [7] — 90°; *e* [10] — 90°; *f* [4] — 90°; *g* [4] — 30°.

TABLE I.

Values of $(d\sigma/d\omega)_{30°}/(d\sigma/d\omega)_{90°}$ *for* (p-p) *scattering in the energy range* 460÷657 MeV.

Energy in MeV	460	562	610	634	645	657
$\left(\frac{d\sigma}{d\omega}\right)_{30°} \Big/ \left(\frac{d\sigma}{d\omega}\right)_{90°}$	1.26±0.15	1.67±0.15	2.16±0.15	2.77±0.20	2.97±0.25	3.20±0.20

It should be noted that the values of $(d\sigma/d\omega)_{90°}$ and the magnitude of the ratio $(d\sigma/d\omega)_{30°}/(d\sigma/d\omega)_{90°}$ found in the experiment, are in satisfactory agreement with the corresponding results of the two previous experiments.

3·4. *Discussion of Results of the Experiments on* (p-p) *Scattering.* – When identical nucleons collide, only $^1S_0$ and $^3P_0$ states can give isotropic scattering. The maximum contribution of these states to the cross-section is $2\lambda\!\!\!^{-2}$ cm²/sterad ($\lambda\!\!\!^{-}$ is the nucleon wave length in the center of mass system). The value of $2\lambda\!\!\!^{-2}$ for 460 MeV is $\approx 3.5 \cdot 10^{-27}$ cm²/sterad. Thus, the experimental value of the (p-p) scattering differential cross-section for large angles may be explained qualitatively if we assume that scattering is mostly due to interaction in $^1S_0$ and $^3P_0$ states and the phase shift of the respective waves differ only slightly from 90°.

One thus introduces the assumption that there is an appreciable difference between the phase shift of the $^3P_0$ wave and the phase shifts of the $^3P_1$ and $^3P_2$ waves and this is equivalent to assuming the presence of strong spin-orbit coupling. The purpose of the further analysis of the properties of (p-p) interaction must be a quantitative explanation of such effects observed in the present experiments as the departure from isotropy of (p-p) scattering and the appearance of proton polarization in (p-p) collisions [11]. Both of these effects definitely testify that in the energy region under consideration, not only $^1S_0$ and $^3P_0$ states contribute to (p-p) scattering but also other states which give a certain asymmetric addition to the cross-section.

The results obtained at 657 MeV point to a strong dependence of the differential cross-section on the scattering angle.

Obviously, in this case, in addition to those states that give an isotropic contribution to the cross-section, there are other states which play a considerable role in (p-p) scattering and which are characterized by a non vanishing total angular momentum. A notable feature of the phenomenon under consideration consists in the fact that in the transition from 460 to 657 MeV the weakening of scattering at large angles is approximately compensated by an increase in scattering at angles $\theta < 50°$, so that the total elastic (p-p) scattering cross-section, within experimental errors, remains constant and its value is of approximately $23 \cdot 10^{-27}$ cm².

As inelastic processes are always accompanied by elastic forward scattering, one may attempt to explain qualitatively the rise of (p-p) scattering at small angles by assuming that in the energy region under consideration the cross sections of reactions (I-III) sharply increase. Indeed, it will be shown below that the contribution of inelastic processes to the total (p-p) interaction cross-section increases from $\sim 18\%$ at 460 MeV to 45% at 657 MeV (see 4·3).

Only a theory accounting for both nucleon-nucleon elastic scattering and meson production in nucleon collisions will enable one to judge the validity of the proposed explanation of the fact that a rapid increase of the meson production cross-section is accompanied by highly asymmetric (p-p) scattering. Here, it will be sufficient to note that repeated attempts to describe nucleon interaction at high energies with the aid of various potentials have proved unsuccessful.

It is especially noteworthy that the character of (p-p) scattering begins to change most rapidly precisely when the energy of the incident protons is in the vicinity of 560-660 MeV i.e. at available energies in the center-of-mass system of about 260-300 MeV. It is well known that at these energies the cross-sections for π-meson-nucleon scattering and photoproduction of mesons grow rapidly and pass through a maximum of resonance type. The similarity of these three processes is undoubtedly a reflection of the properties of the interaction of nucleon and meson fields.

As is well known, one of the possible explanations of the non-monotonic variation with energy of the cross-sections for scattering processes and photoproduction of mesons is based on the assumption that nucleons possess an excited state with isotopic spin $\frac{3}{2}$ and excitation energy of about 300 MeV. From this viewpoint it would appear natural that in nucleon-nucleon collisions the particles are first excited and then disintegrate into a meson and a nucleon.

According to this picture, the rapid change in the properties of (p-p) scattering in the region of 560-660 MeV may be an indication that the first stage of (p-p) interaction is the excitation of protons.

4. – Meson Production in (p-p) Collisions.

4·1. *The* $p + p \to d + \pi^+$ *Reaction at* 460 MeV. – Reaction (I) was identified by registration (by two conjugated telescopes) of the coincidences between a π-meson and a deuteron. π-meson yield was measured in the range from 17° to 50° to the direction of a narrow collimated proton beam. Under the conditions of this experiment, the pulse height due to deuterons exceeded more than twice the pulse height from the primary protons. In order to lower the accidental coincidence rate due to overloading of the deuteron telescope by

protons experiencing diffraction scattering on carbon nuclei in the target, the deuteron pulses were separated from the elastically scattered proton pulses by a discriminator. In control experiments it was found that: 1) the effect due to process (I) always disappeared when a filter completely stopping the deuterons was interposed between the deuteron telescope crystals and: 2) when the angular setting of the two telescopes did not correspond to the kinematics of reaction (I), coincidences between the two telescopes were not observed.

In this same series of experiments it was established that reaction (II) does not contribute to the observed effect. Taking into consideration the efficiency of the apparatus employed for recording triple coincidences between the telescope scintillation counters and double coincidences between the telescopes, and also making allowance for absorption and scattering of π-mesons and deuterons in the target and scintillation crystals, as well as for the decay in-flight of π-mesons, it may be shown that in the present experiments the efficiency of registration of the elementary acts of reaction (I) amounted to 0.73 ± 0.04.

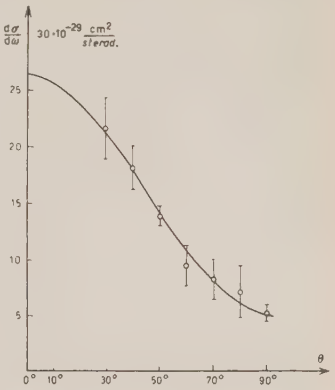

Fig. 6. – Angular distribution of π^+-mesons from reaction $p+p \rightarrow d+\pi^+$ at 460 MeV.

The results of measurements of the angular distribution of π-mesons from reaction (I) are represented in Fig. 6. The dependence of values of the differential cross-section of reaction (I) on the π-meson ejection angle in center of mass system is given by the following expression:

$$\frac{d\sigma}{d\omega} = (2.13 \pm 020)[(0.24 \pm 0.03) + \cos^2\theta] \cdot 10^{-28} \text{ cm}^2/\text{sterad.}$$

The numerical coefficients of this expression were determined by the least squares method. Assuming that the same expression also describes the angular distribution of π-mesons in the region of small angles, and integrating $d\sigma/d\omega$ over solid angle, we obtain the total cross-section of reaction (I):

$$\sigma(\text{I}) = (15.4 \pm 1.6) \cdot 10^{-28} \text{ cm}^2 .$$

The ratio of differential cross-sections at angles of 0° and 90° in this case proves to be $(d\sigma/d\omega)_{0°}/(d\sigma/d\omega)_{90°} = 5.1 \pm 0.8$.

In the case when pseudoscalar π^+-mesons are produced in (p-p) collisions only in S and P states, transitions to the $^3S_1$ state of the final (p-p) system

are allowed from $^1S_0$, $^3P_1$, $^1D_2$ states of the initial (p-p) system; the $^1S_0 \to {}^3S_1$ and $^3P \to {}^3S_1$ transitions lead to an isotropic distribution of mesons, whereas the transition $^1D_2 \to {}^3S_1$ leads to a distribution of the type $\frac{1}{3} + \cos^2\theta$.

Since near the meson production threshold, the amplitudes of transitions $^1S_0 \to {}^3S_1$ and $^1D_2 \to {}^3S_1$ corresponding to the emission of mesons in the p-state, must be proportional to the meson momentum, and the amplitude of transition $^3P_1 \to {}^3S_1$ connected with the emission of mesons in the s-state, is in this case constant, it may be expected that only at sufficiently small meson energies the emission of mesons in the s-state will appreciably contribute to the cross-section of reaction (I).

The angular distribution obtained in this paper corresponds to meson production chiefly, if not entirely, in the p-state. If meson production does take place at 460 MeV in the d-state, then the contribution to the cross-section from the respective transitions does not in any case exceed 10%.

The departure of the observed angular distribution from the $\frac{1}{3} + \cos^2\theta$ law is apparently due to interference of transitions from $^1S_0$ and $^1D_2$ states of the (p-p) system. In this case, as was calculated in [12, 13], the meson angular distribution $F(\theta)$ may be represented as follows:

$$F(\theta) \sim \frac{1 + (\varepsilon^2/2) + \sqrt{2}\,\varepsilon\cos\sigma}{3\left((\varepsilon^2/2) - \sqrt{2}\,\varepsilon\cos\sigma\right)} + \cos^2\theta\,,$$

where $\eta = \varepsilon e^{i\sigma}$ is a parameter, included in the linear combination of spherical vector functions, corresponding to transitions $^1S_0 \to {}^3S_1$ and $^1D_2 \to {}^3S_1$, in the wave function of the final state. The relative contribution of the above-mentioned transitions to the partial cross-section of meson production in the P-state is determined by the value of the parameter ε^2. In the general case, the ratio between the intensities of the transitions $^1S_0 \to {}^3S_1$ and $^1D_2 \to {}^3S_1$ cannot be uniquely determined from the form of the meson angular distribution curve without additional experimental data, such as data on deuteron polarisation in reaction (I).

For the angular distribution found in the present experiment, permissible (although not the only) values of ε and σ are those for which ε^2 lies between 280 and 7, when the σ phase changes from 0° to 72° (or from 180° to 108°). If we assume this choice of values of ε and σ to be correct, then we may arrive at the conclusion that at 460 MeV, meson production in reaction (I) is mostly due to $^1D_2 \to {}^3S_1$ transitions which correspond to a noncentral interaction in the (p-p) system. But this signifies that mesons are produced in reaction (I) and, correspondingly, are absorbed in reaction (IV) $\pi^- + d \to p + p$, chiefly in a state when their orbital moments are parallel to the spins of the deuterons. Thus, the meson angular distribution of reaction (I) at 460 MeV is compatible with the assumption that meson-nucleon interaction is great for states with an angular moment of $\frac{3}{2}$.

4·2. *The* $p + p \rightarrow d + \pi^+$ *Reaction in the Region of* 510-657 MeV. – Methods for observing reaction (I) in the stated energy range were the same as in the preceeding experiment, with the sole exception that for deuteron counting a telescope consisting of five scintillation counters was used. Double coincidences from the last two counters were connected in anticoincidence with the first three counters. A filter placed in front of the last two counters was sufficient to stop the deuterons, but transmitted protons, elastically scattered by carbon nuclei in the target. In this way deuterons emitted at small angles to the primary beam could be counted at a considerably lower accidental coincidence background rate, while the efficiency of detection of meson production in process (I) remained unchanged. A correction determined experimentally was applied too, in order to account for the contribution of reaction (II) to the coincidence counting rate between π-mesons and deuterons. The necessity of such a correction is that in the energy region under consideration, reaction (II) is more intense than reaction (I).

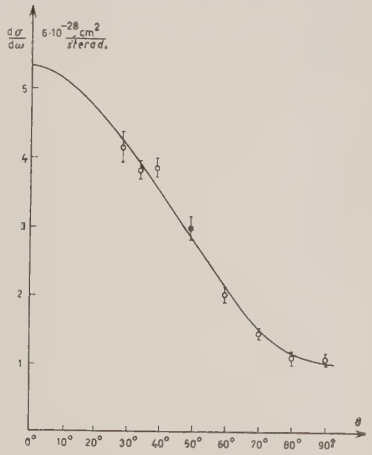

Fig. 7. – Angular distribution of π^+-mesons from reaction $p+p \rightarrow d+\pi^+$ at 657 MeV.

Results of the measurements of the angular distribution of mesons from reaction (I) at 657 MeV are given in Fig. 7. The dependence of differential cross-section of reaction (I) upon the emission angle of the π-mesons is

$$\frac{d\sigma}{d\omega} = (4.35 \pm 0.25)[(0.23 \pm 0.03) + \cos^2\theta] \cdot 10^{-28} \text{ cm}^2/\text{sterad}.$$

Extrapolation of this dependence to small angles and integration over the solid angle gives for the total cross-section of reaction (I) the value

$$\sigma(\text{I}) = (3.1 \pm 0.2) \cdot 10^{-27} \text{ cm}^2.$$

Taking advantage of the circumstance that as the proton energy rises from 460 to 657 MeV the center of mass angular distribution of mesons from reaction (I) in the region of large angles changes but slightly, it was possible to determine the total cross-section σ(I) for intermediate energies from the values of the differential cross-sections found at some single angle.

Observations of mesons at 50° in the center of mass system proved most convenient.

The values of $\sigma(I)$ which were found in a similar way, together with the result of the preceeding experiment are represented as a function of the π-meson energy in Fig. 8. The results obtained at lower energies [14-18] are given in the same figure.

As can be seen from Fig. 8, in overlapping energy regions the results of this work satisfactorily agree with the data of other papers. It should be noted that for energies of 25, 40, 53, 76 and 94 MeV the total cross-sections of reaction (I) were obtained by means of the principle of detailed balance from observations on the reverse reaction (IV), the assumption being made that the π-meson spin is zero.

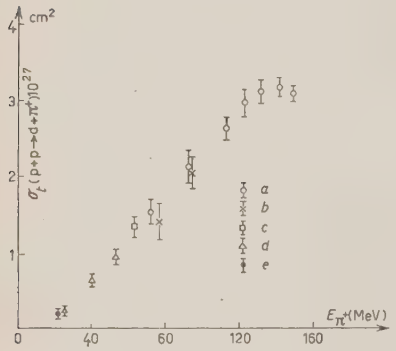

Fig. 8. – Dependence of total cross-section of reaction $p+p \rightarrow d+\pi^+$ on the π^+-meson energy. *a* [5, 2]; *b* [14]; *c*[15]; *d* [16]; *e*, averaged result [17, 18].

The results of these experiments show that the total cross-section of reaction (I) grows rapidly with energy up to ~ 600 MeV, and then remains approximately constant. Beginning at 657 MeV, a tendency towards reduction of the cross-section of reaction (I) can be noticed.

The excitation curve of the reaction (IV) was found by using the relation $\sigma(IV) = \frac{2}{3}(k^2/\eta^2)\sigma(I)$, where η and k are the momenta of the meson and of the proton in the center of mass system. It turns out that the cross-section of reaction (IV) has a maximum at a center of mass energy of ~ 130 MeV. At about the same meson energy in the center-of-mass system the cross-sections for meson-nucleon scattering and photomeson production reach also their maximum value. The fact that the cross-section of reaction (IV) does not vary monotonically with the meson energy, just as the cross-sections for meson-nucleon scattering and photoproduction of mesons suggests that all these three processes are caused by the same mechanism of meson-nucleon interaction, probably related to the existence of an excited state of the nucleon.

At 657 MeV, just as at 460 MeV, the measured angular distribution corresponds to emission of mesons chiefly in the p-state. A comparison of this result with the fact that meson-nucleon interaction (as it apparently follows from experiments of meson scattering in hydrogen) proves to be strongest for states with a total isotopic spin of $\frac{3}{2}$ and angular momentum of $\frac{3}{2}$, leads one to the conclusion that throughout the energy range under consideration

the $^1D_2$ state of the (p-p) system gives the basic contribution to the cross-section of reaction (I), this cross-section being a nonmonotonic function of energy.

Further conclusions concerning the properties of reaction (I) may be made after conducting measurements of the total cross-section at still higher energies and after determining the angular distribution of mesons at angles less than 30°, where one may hope to notice an effect from mesons produced in the *d*-state.

4·3. *Remarks on the Relation Between Elastic Scattering and Meson Production in* (p-p) *Collisions.* – Data obtained in the present experiments concerning the total cross-sections for elastic (p-p) scattering and the production of mesons in reaction (I) for energies of 460 and 657 MeV are given in Table II. For the same energies, the total cross-sections of (p-p) interaction were evaluated by interpolation of data obtained for energies 410, 535, 615, 830 MeV in reference [19]. The total cross-sections of reaction (III) were measured by KOZODAEV *et al.* [20] for energies of 480 and 670 MeV. In passing from these energies to 400 and 657 MeV it was assumed that, near 500 MeV, $\sigma(\mathrm{III}) \sim \eta^6$; whereas, in the region 600-680 MeV, $\sigma(\mathrm{III}) \sim \eta^{4.5}$ (η is the maximum π-meson momentum in the center of mass system).

TABLE II. – (p-p) *Cross-Sections.*

Energy in MeV	Total Cross-Section in 10^{-27} cm^2					
	Total (p-p) interaction	Elastic (p-p) interaction	Inelastic processes	$p+p \to d+\pi^+$	$p+p \to p+p+\pi^0$	$p+p \to p+n+\pi^+$
460	28 ± 2	22 ± 2	~ 6	1.5 ± 0.2	0.4 ± 0.2	~ 4
657	41 ± 2	23 ± 2	~ 18	3.1 ± 0.2	3.4 ± 0.7	~ 11.5

In the energy range under consideration, the most striking peculiarity of proton-proton collisions consists in the constancy of the total elastic scattering cross-section and in the rapid growth with energy of the meson production cross-sections. As a result of this, the contribution at 657 MeV of inelastic processes to the total (p-p) interaction cross-section proves to be only slightly less than the contribution from elastic scattering. At the same energy, reaction (I) makes only a relatively small contribution to the total π-meson production cross-section. The rapid growth of the cross-section of reaction (II) with energy may be due to the increase in the intensity of the above mentioned transitions $^1D_2 \to {}^3S_1$ and $^1S_0 \to {}^3S_1$ which are not accompanied by formation of deuterons, as well as to the increasing role of other transitions and first of all of transitions from the odd triplet states of the (p-p) system. In this connection it should be noted that the strong departure from the isotropy of

(p-p) scattering when the energy increases from 460 to 657 MeV also points to the appearance in (p-p) interactions of states possessing nonvanishing values of the total angular momentum.

The estimate of the cross-section of reaction (III) given here for 657 MeV was obtained on the assumption that pair production of mesons in single (p-p) collisions gives a relatively small contribution to the total interaction cross-section. At present there are no direct data on the magnitude of the cross section of this process near the threshold.

REFERENCES

[1] M. G. Meščerjakov, N. P. Bogačev, B. S. Neganov and E. V. Piskarev: *Report of the Institute of Nuclear Problems, Academy of Sciences, USSR* (1954); B. S. Neganov: *Report of the Institute of Nuclear Problems, Academy of Sciences, USSR* (1954); *Dokl. Akad. Nauk SSSR*, **99**, 955 (1954).

[2] M. G. Meščerjakov, B. S. Neganov, N. P. Bogačev and V. M. Sidorov: *Report of the Institute of Nuclear Problems, Academy of Sciences, USSR* (1952); *Dokl. Akad. Nauk SSSR*, **100**, 673 (1955).

[3] N. P. Bogačev, I. K. Vzorov: *Report of the Institute of Nuclear Problems, Academy of Sciences, USSR* (April 1954); *Dokl. Akad. Nauk SSSR*, **99**, 931 (1954).

[4] M. G. Meščerjakov, B. S. Neganov, L. M. Soroko and I. K. Vzorov: *Dokl. Akad. Nauk SSSR*, **99**, 959 (1954).

[5] M. G. Meščerjakov and B. S. Neganov: *Dokl. Akad. Nauk SSSR*, **100**, 677 (1955).

[6] O. Chamberlain, E. Segrè and C. Wiegand: *Phys. Rev.*, **85**, 923 (1951).

[7] W. E. Mott, R. B. Sutton, J. G. Fox and J. A. Kane: *Phys. Rev.*, **90**, 712 (1953).

[8] A. J. Hartzler and R. T. Siegel: *Phys. Rev.*, **95**, 185 (1954).

[9] R. Birge, V. Cruse and N. Ramsay: *Phys. Rev.*, **83**, 274 (1951).

[10] J. Marshall, L. Marshall and V. Nedzel: *Phys. Rev.*, **92**, 834 (1953).

[11] H. G. de Carvalho, E. Heiberg, J. Marshall and L. Marshall: *Phys. Rev.*, **94**, 1796 (1954).

[12] K. Watson and C. Richman: *Phys. Rev.*, **83**, 1256 (1951).

[13] V. B. Beresteckij: *Dokl. Akad. Nauk SSSR*, **94**, 421 (1954).

[14] H. L. Stadler: *Phys. Rev.*, **96**, 496 (1954).

[15] T. H. Fields, J. G. Fox, J. A. Kane, R. A. Stallwood and R. B. Sutton: *Phys. Rev.*, **95**, 638 (1954).

[16] R. Durbin, H. Loar and J. Steinberger: *Phys. Rev.*, **84**, 581 (1951).

[17] V. Peterson, E. Iloff and D. Sherman: *Phys. Rev.*, **84**, 372 (1951).

[18] M. Whitehead and C. Richman: *Phys. Rev.*, **83**, 855 (1951).

[19] A. M. Shapiro, C. P. Leavitt and F. F. Chen: *Bull. Am. Phys. Soc.*, **29**, No. 4, 75 (1954).

[20] A. A. Tjapkin, M. S. Kozodaev and Ju. D. Prokoškin: *Dokl. Akad. Nauk SSSR*, **100**, 689 (1955).

ABSTRACT

of the International System of Transliteration of Cyrillic Characters

(2nd Draft I S O Recommendation N. 9)

advised by the Editorial Board of *Il Nuovo Cimento*
for the Compilation of the Reviews
of Physics Papers published in Slavonic Languages

Cyrillic Character		Transliteration from :					Examples & Remarks
		Bulgarian	Russian	Ukrainian	White Russ.	Serbian	
1.	А, а	a	a	a	a	a	Адрес = Adres
2.	Б, б	b	b	b	b	b	Ваба = Baba
3.	В, в	v	v	v	v	v	Вы = Vy
4.	Г, г	g	ɡ	ɡ	g	g	Глава = Glava = Golova
5.	Ґ, ґ			ġ [1]	ġ [1]		Ґреци = Ġreci
6.	Д, д	d	d	d	d	d	Да = Da
7.	Ђ, ђ					đ	Croat dj and gj changed to đ in alphabetized headings
[2] 8.	Е,е (ё)	e	e(ё)	e	e(ё)	e	Еще = Ešče
9.	Є, є			je			Твоє = Tvoje
10.	Ж, ж	ž	ž	ž	ž	ž	Журнал = Žurnal
11.	З, з	z	z	z	z	z	Звезда = Zvezda
12.	S, s						(not used)
13.	И, и	i	i	y	i		Или = Ili
14.	І, і		i [3]	i	i	i	Ьілий = Bilyi
15.	Ї, ї			ji			Їзда = Izda
16.	J, j					j	Јован = Jovan
17.	Й, й	j	j	j	j	j	-ый, -ий, -ой =-yj,-ij,-oj
18	К, к	k	k	k	k	k	Как = Kak
19.	Л, л	l	l	l	l	l	Любить = Ljubit'
20.	Љ, љ					lj	Љубав = Ljubav
21.	М, м	m	m	m	m	m	Муж = Muž
22.	Н, н	n	n	n	n	n	Нижний = Nižnij
23.	Њ, њ					nj	Њива = Njva
24.	О, о	o	o	o	o	o	Общество = Obščestvo

(1) The character no. 5 is no longer used in Ukrainian and White Russian.
(2) Cyrillic ё to be transliterated by ë only when diacritical appears in the original.
(3) The character no. 14 is no longer used in Russian.

Cyrillic Character		Transliteration from :					Examples & Remarks
		Bulgarian	Russian	Ukrainian	White Russ.	Serbian	
25.	П, п	p	p	p	p	p	Первый = Pervyj
26.	Р, р	r	r	r	r	r	Рыба = Ryba
27.	С, с	s	s	s	s	s	Сестра = Sestra
28.	Т, т	t	t	t	t	t	Товарищ = Tovariščˇ
29	Ћ, ћ					ć	Кућа = Kuća
30.	У, у	u	u	u	u	u	Утро = Utro
31.	Ф, ф	f	f	f	f	f	Физика = Fizika
32.	Х, х [4]	h	h	h	h	h	Химческий = Himičeskij
33.	Ц, ц	c	c	c	c	c	Центральный = Central'nyj
34.	Ч, ч	č	č	č	č	č	Часы = Časy
35	Џ, џ					dž	Џамија = Džamija
36.	Ш, ш	š	š	š	š	š	Школа = Škola
37.	Щ, щ	št	šč	šč	šč		Щека = Ščeka
38	(medial) Ъ, ъ (final)	ă ŭ	"or" Not transliterated	"or"	"or"		In modern Russian, where' replaces medial ъ, transliteration is still".
39.	Ы, ы	y	y		y		Был = Byl
40.	Ь, ь	'or'	'or'	'or'	'or'		Маленький = Malen'kij
41.	Ѣ, ѣ	ě	ě [5]	ě [5]	ě [5]		Ѣсть = Ěst'
42.	Э, э		ė		ė		Это = Ėto
43.	Ю, ю	ju	ju	ju	ju		Южный = Južnyj
44.	Я, я	ja	ja	ja	ja		Яйцо = Jajco

[4] Countries with a firmly established tradition in favour of ch or kh may use whichever of these two is the more appropriate, provided that, in catalogues, indexes etc. containing the variant, permanent cross-references are made to and from the h.
[5] The character no. 41 is no longer used in Russian, Ukrainiam and White Russian.

Added by the Editorial Board of *Il Nuovo Cimento*

In the Reviews published in *Il Nuovo Cimento*, x is transliterated into h. Place names commonly transcribed into another language (*e.g.* Moscow in English) can be retained in their traditional form.

PROPRIETÀ LETTERARIA RISERVATA

Direttore responsabile: G. POLVANI Tipografia Compositori - Bologna
Questo fascicolo del *Supplemento* è stato licenziato dai torchi il 2-II-1956